The University Of Sheffield.

Reducing stomatal density in *Hordeum vulgare* improves drought tolerance and water use efficiency

By: Jonathan David Hughes

Department of Molecular Biology and Biotechnology

A thesis submitted for the degree of Doctor of Philosophy

Submission Date: June 2017

Acknowledgements

I am deeply grateful to my supervisor, Professor Julie Gray, and the rest of the lab for their assistance and support with various aspects of this project.

I would like to thank the support services of the University of Sheffield for their assistance throughout my bouts of ill health, without which this thesis would not have been possible.

Thanks to my parents and brother, who alone helped carry me through the lowest points and who motivated me to return to finish this work.

Finally, I would like to thank the Gatsby Charitable Foundation for the funding and the opportunity to experience all the wonderful possibilities plant science has to offer.

Table of Contents

Abstract

Manipulation of the expression of the epidermal patterning factor (EPF) family of secreted signalling peptides in order to regulate stomatal density has previously been demonstrated to improve water use efficiency in *Arabidopsis thaliana* (Franks et al., 2015). Following the sequencing of the barley genome an ortholog of EPF2 was identified and overexpressed. HvEPFL1 overexpression limits both entry into, and progression through, the stomatal lineage. Lines overexpressing HvEPFL1 showed significant increases over controls in terms of both water use efficiency and drought tolerance, without a detrimental effect on grain yield. This suggests that the manipulation of stomatal density could be utilised in order to futureproof crops against future climate change.

Chapter 1 – Introduction

Over the course of the current century we collectively face a number of environmental and social crises that have collectively been described as the "perfect storm" (Beddington, 2008). The major concern is meeting the increased demand for food due to a growing population, particularly given the potential negative impacts on agricultural productivity as a result of global climate change (Godfray et al., 2010; Joshi et al., 2016).

1.1 Food Security

Current international policy is geared towards ensuring food security. Food security is defined as being "when all people, at all times, have physical and economic access to sufficient, safe and nutritious food to meet their dietary needs and food preferences for an active and healthy life" (FAO, 1996). Currently 52 countries have serious or alarming rates of hunger, according to the global hunger index, with the issue particularly acute in sub Saharan Africa (IFPRI, 2015). It has been estimated that 795 million people were undernourished globally in 2015 (FAO, 2015). The current population projections estimate that the global population will rise from 7.4 billion in 2015 to 9.7 billion in 2050, reaching 11.2 billion by the end of the century (UNPD, 2015) including significant population rises in areas that already exhibit significant food insecurity, such as Africa where the population is expected to double (UNPD, 2007). The burgeoning population will significantly increase the demand for food, with an estimated requirement for global food production to increase by 70-100% by 2050 to meet food security standards (Defra, 2009, FAO, 2009), with a predicted rise in world cereals demand of 50% by 2030

(World Bank, 2008). Whilst there has been significant improvement in crop development over the last 50 years, with food crop yield per unit area doubling (Balmford et al., 2005), the rate of increase in agricultural productivity is projected to decline from 2.2% per annum in 2007 to 0.8% per annum by 2050 (Alexandratos and Bruinsma, 2012). This decline is largely due limitations in the supply of land for agriculture, since the 1960's total area under cultivation has increased by only 11% (Pretty, 2008) and agricultural land is being lost due to urbanisation, desertification, salinization and soil erosion (Godfray et al., 2010). The deterioration of agricultural land is likely to increase in the coming years as consequence of climate change which will increase heat, drought and salinity stress on crops, reducing yields and rendering some previously arable land unusable (IPCC, 2007). There will also be increasing demand for land on which to grow biofuels and restrictions on increasing cultivated area in order to protect biodiversity (Balmford et al., 2005).

1.2 Climate Change

1.2.1- Global CO_2 concentration projections

Climate change as a consequence of increased atmospheric CO2 is a significant challenge to ensuring food security. (IPCC, 2007). The IPCC has modelled the projected change in CO2 under different sets of assumptions about human activity, the representative concentration pathways (RCP). These models all predict a rise in global CO2 concentration over this century. The least severe of the models, RCP2.6, predicts that the global CO2 concentration will rise from 379ppm in 2000 to 400ppm by 2100. The most severe projection, RCP8.5, predicts a staggering increase of atmospheric CO2 to over 900ppm over the same time period (Van Vuuren et al., 2011; IPCC, 2014).

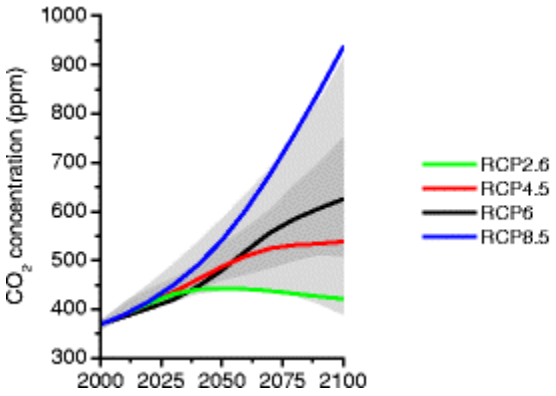

Figure 1.1 - The changes in atmospheric CO2 concentrations predicted by 4 different RCPs over this century. (Taken from Van Vuuren et al., 2011)

1.2.2 Projected changes to water availability in the future

Climate change will have numerous effects on crop production, most notably the increased prevalence of drought as a consequence of more frequent water shortages. (IPCC, 2007)

Agriculture is the most water intensive of all human activities, accounting for 70-90% of all freshwater utilised by humans, mostly for crop production (FAO, 2007; Morison et al., 2008). Global water supply is expected to be constrained by climate change, with an increase in water stress of between 62.0 and 75.8% of total river basin area by 2050 (Alcamo et al., 2007)

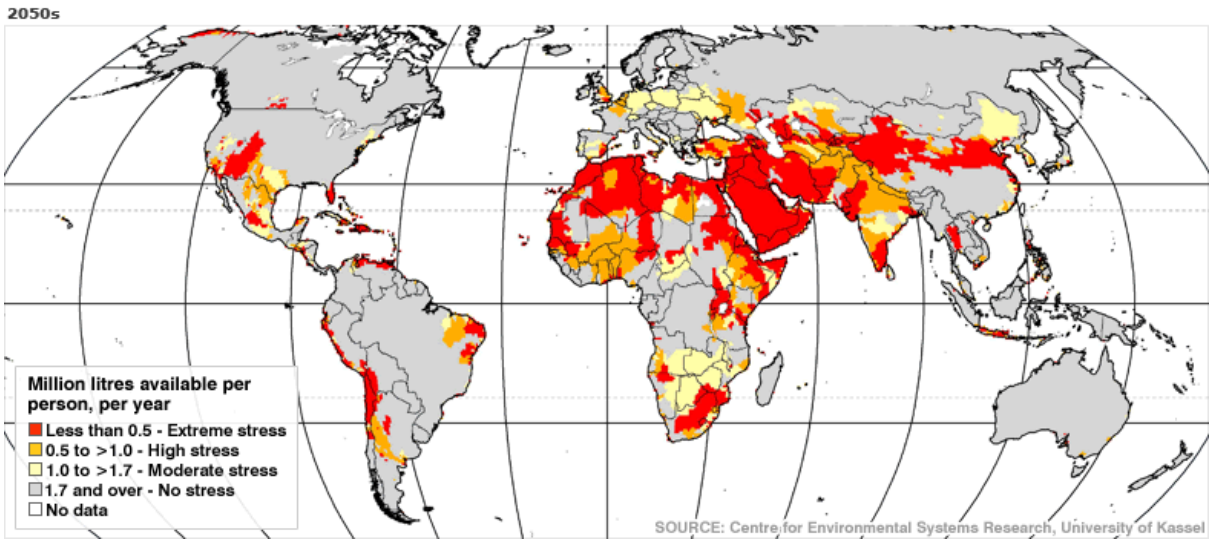

Figure 1.2- prediction the prevalence of water stress in the 2050s. Figure adapted by the BBC (http://news.bbc.co.uk/1/hi/sci/tech/7821082.stm) from Alcamo et al 2007.

However water demand is expected to rise by 40-60% between 2000 and 2025 (Shen, 2008, figure 3) with 1.2 billion people already living in areas where water is scarce (IWMI, 2007). As a consequence of increased water scarcity (figure 1.4) as a consequence of climate change as much as 66% of the global population will experience water stress (Wallace and Gregory, 2002). Decreased water availability is particularly problematic for irrigated agriculture, which accounts for just under 20% of total farmed land and provides 40-45% of global food (Doll and Siebert, 2002).

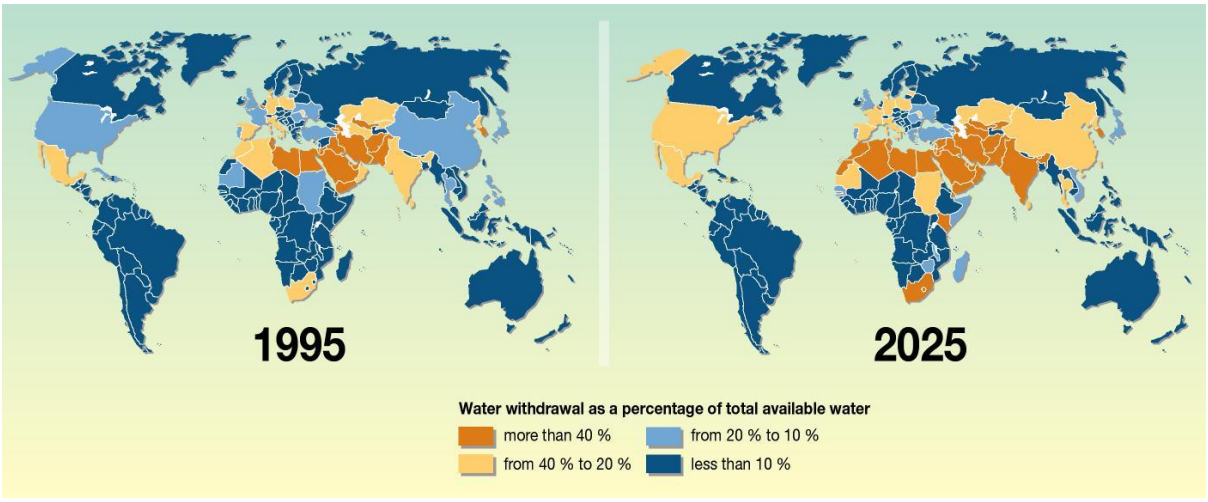

Figure 1.3 – Increase in water withdrawal as a percentage of total available water between 1995 and 2025. (obtained from UNEP vital water graphics, 2008)

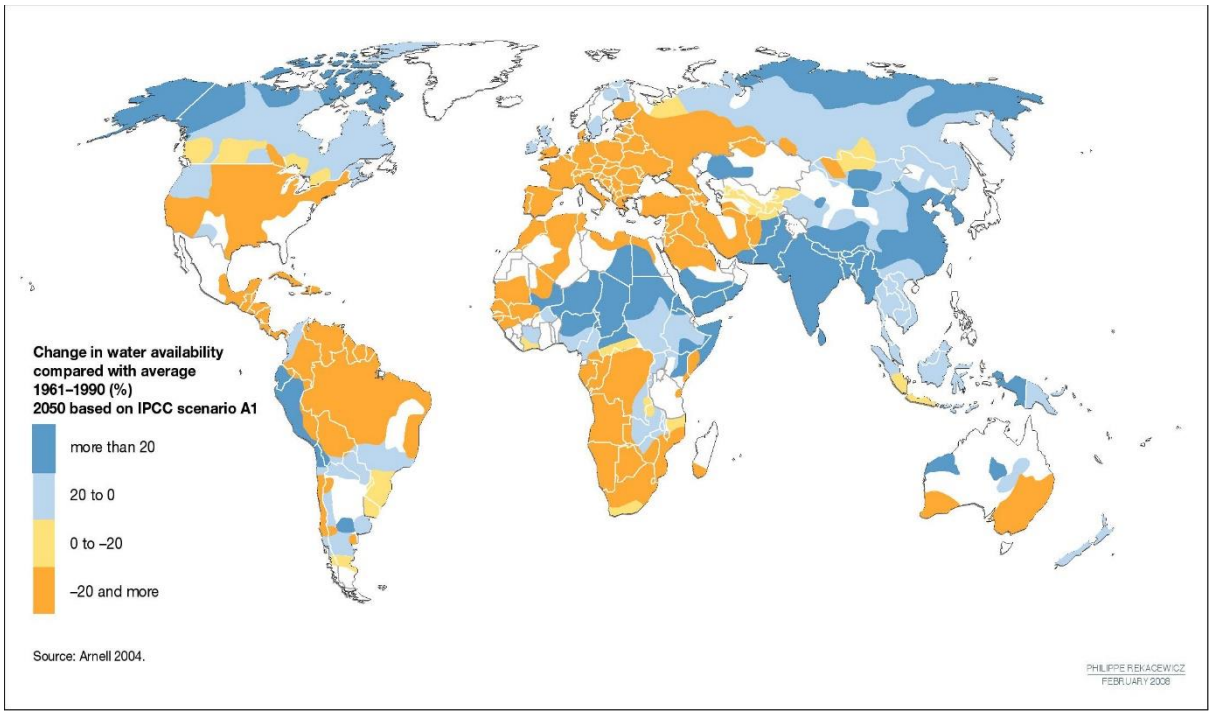

Figure 1.4- Map of changes to global water availability between the average from the period 1961-1990 and the predicted availability in 2050. (Obtained from UNEP vital water graphics, 2008)

Drought has a significantly limiting effect on crop yield, more so than most other stresses (Boyer 1982). The increase in heat and drought stress as a consequence of climate change could severely reduce yields (IPCC 2007; Prasad et al., 2008). In response to this it is

apparent that we need to adapt our agricultural methods to reduced water availability and produce crops with increased productivity per unit of water, “more crop per drop”. (The Royal Society, 2009; UN, 2000)

1.3- Ensuring more crop per drop: drought tolerance and water use efficiency

The efficiency with which plants utilise water and their ability to withstand periods of drought has long been an area of active study due to the obvious agricultural implications of reduced water availability, particularly in light of the global shifts in water availability (see figure 1.4).

1.3.1- Defining drought tolerance

Drought tolerance is the ability for plants to survive, grow and reproduce in a satisfactory manner when water is limited either in the long term or periodically (Turner, 1979; Fleury et al., 2010). Drought resistance adaptations to drought fall into two broad categories; dehydration avoidance and dehydration tolerance (Levitt, 1972).

Dehydration avoidance is where the plant maintains high water status despite drought, thus avoiding or reducing tissue dehydration and the resultant stress on biological functions (Blum, 2005). Methods for avoiding dehydration include reducing water loss and enhancing uptake of soil water moisture (Blum, 2005). Crop plants bred for increased drought tolerance often exhibit reduced leaf area, reduced tillering and fewer leaves whilst flowering earlier (Blum, 2004).

Dehydration tolerance is where the plant maintains its functions despite it being in a dehydrated state. Such adaptations are rare in crop plants. (Blum, 2004)

1.3.2- Defining Water Use Efficiency

There are several ways of measuring and defining plant water use efficiency (WUE). These different methods vary in both the duration of time over which they measure (from minutes to whole plant life time) and also the scale at which analyse WUE (from single leaves to whole canopies and biomes) (Gago et al., 2014). Here individual plant and leaf measures of WUE will be considered.

At the whole plant level it is the ratio of biomass accumulated to water used that provides a measure of WUE (Monteith, 1993). This integrated WUE can either be total biomass accumulated (WUE_B) or yield (WUE_Y) per unit of water used (Yoo et al., 2009). As whole biomass or yield and total water used is required, this measure supplies an average WUE approximation across the entire plant life time.

At the leaf level it is possible to measure WUE over a period of minutes or hours, using an infra-red gas analyser. It is therefore possible to obtain values of WUE throughout a plant's life cycle. This allows the effects of environmental stimuli, and subsequent physiological and biochemical responses, on plant WUE to be gauged.

The two commonly reported WUE measures collected from gas exchange measurements are instantaneous WUE and intrinsic WUE.

Instantaneous WUE is defined as A/E where A is the rate of carbon assimilation and E is the rate of evapotranspiration (Penman and Schofield, 1951; Farquhar and Sharkey, 1982; Yoo et al., 2009; Morison et al.,2008). Instantaneous WUE is sometimes described as the assimilation transpiration rate (ATR) (Morison et al.,2008). Hence WUE can be improved either by increasing the rate of assimilation relative to transpiration or reducing transpiration relative to assimilation.

Intrinsic WUE is defined as A/Gs where Gs is the stomatal conductance (Morison et al., 2008). This is a more conservative measure of WUE as it removes some of the influence

and hence variability introduced by the environment. E takes into account both the environmental changes, such as the effect of leaf temperature and humidity on gas properties, and Gs. By just using Gs in the calculation of the WUE, most of the environmental variation is cut out, although the environment still influences WUE through effects on Gs as a result of plant environmental responses (reviewed later) (Morison et al., 2008).

Finally, carbon isotope discrimination, specifically an increase in C13 incorporation (Δ), can be used as a proxy for WUE in C3 plants (Farqhuar et al., 1982; Farquhar and Richards, 1984). Carbon discrimination doesn't show the relative contribution of assimilation versus stomatal conductance to WUE, but this can be determined by looking at oxygen 18 discrimination (Farqhuar and Richards, 1984; Barbour et al., 2004).

1.3.3- The effect of altering Water Use Efficiency

As a general rule higher WUE correlates with reduced stomatal conductance, slower growth rate and lower assimilation (Flexas et al., 2004; Lawson and Blatt, 2014). As a general rule selection for higher WUE is often selection for low water use rather than improved assimilation and plant production, consequently selection for high WUE has often lead to the generation of small varieties with low yields (Condon et al., 2004, Blum, 2005). However it is theoretically possible to improve WUE without significant assimilation penalties (Yoo et al., 2009).

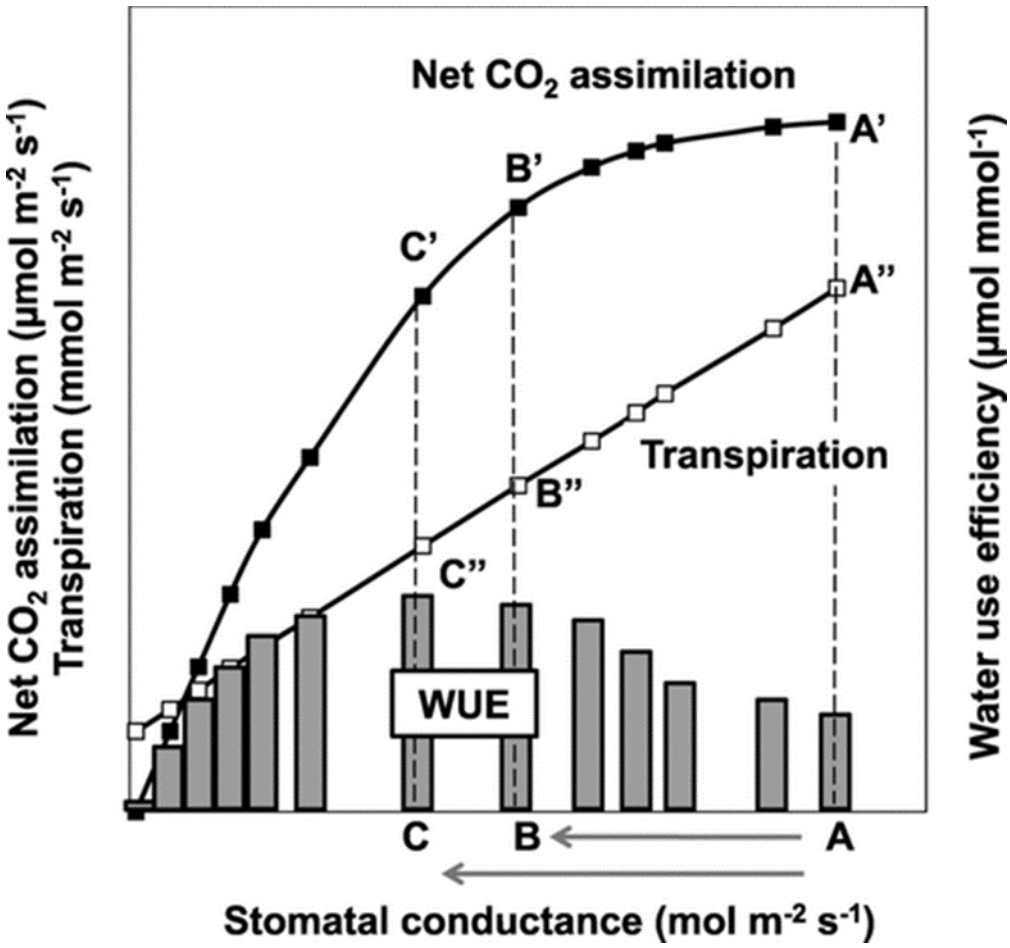

Figure 1.5- Graph demonstrating how A, E and instantaneous WUE vary with stomatal conductance. The differential responses to changes in stomatal conductance of A (linear increase followed by saturation at high stomatal conductance) and E (linear increase with no saturation at high stomatal conductance) means that a reduction in stomatal conductance from A to B will improve instantaneous WUE. This is because E is reduced from A" to B", whilst the reduction in A is negligible, as between A' and B' the rate of assimilation is at or near saturation. The line with closed squares shows how A varies with Gs, the line with open squares shows how E varies with G_s and the grey bars are the instantaneous WUE at a given Gs. (Taken from Yoo et al., 2009)

As figure 1.5 shows the two components of instantaneous WUE (assimilation/transpiration) differ in their response to increasing stomatal conductance. Transpiration increases in a linear manner whereas assimilation initially increases in a linear manner before saturating at higher conductance values when CO_2 availability is no

longer the limiting factor in photosynthesis. Consequently, any drop in stomatal conductance within the range where assimilation is saturated (such as from point A to B in figure 5) will yield significant WUE improvements without assimilation dropping significantly (Yoo et al., 2009).

This suggests the possibility that reducing water use through reduction of stomatal conductance, for example by altering stomatal density, could be used to improve WUE, potentially without significant yield penalties if stomatal conductance remains sufficiently high to allow adequate CO_2 uptake (Yoo et al., 2009). Indeed some studies have provided evidence to support this assertion in crop species. In *Hordeum Vulgare* (Miskin et al.,1972) a correlation was found between stomatal density and the rate of evapotranspiration across a range of seven barley populations, but not between the rate of photosynthesis and stomatal density, i.e. reducing density could reduce water loss without negatively affecting assimilation. In poplar stomatal density was positively correlated with Δ, which is, as outlined above, negatively correlated with WUE, whilst there was no correlation between Δ and productivity (Farqhuar et al., 1982; Rae et al., 2004; Monclus et al., 2006).

Moreover, in natural populations of both *Oryza Sativa* (Impa et al., 2005) and *Triticum Aestivum* (Van Boogaard et al., 1997) WUE is negatively correlated with the rate of evapotranspiration but not correlated with assimilation across the range of natural variation, i.e. assimilation is not necessarily effected by improved WUE, with changes in stomatal conductance accounting for the variation.

It should be stressed however that early investigations demonstrated that assimilation correlated with stomatal conductance when other factors were not limiting photosynthesis (Wong et al., 1979) and under well-irrigated conditions Gs and Δ have been found to be positively correlated with higher yields in *Triticum Aestivum* (Fischer et al., 1998). Potential explanations for the latter, positive correlation include the possibility of decreased stomatal sensitivity to vapour pressure deficit, the potential for minor water

stress events between irrigation events, extra evaporative cooling particularly at warmer temperatures (the study was carried out in Mexico), or increased sink strength (Fischer et al., 1998; Richards, 2000).

1.4 – Stomata, a basic outline

Stomata are microscopic pores in the epidermis of plants that provide a passageway between the external environment and the internal air spaces where gas exchange can occur between the air and the mesophyll tissue of the internal leaf, which lacks the epidermal tissue's impermeable cuticle and provides a large surface area for gas exchange. (Hetherington and Woodward, 2003)

Individual stoma at their most basic consist of a pair of kidney shaped guard cells surrounding an aperture although more complex structures are found in some plant lineages, notably grasses (see section 3.2).(Stebbins and Jain, 1960; Sack, 1994; Hetherington and Woodward, 2003; Serna, 2011).

Stomata respond to and integrate various environmental cues (for more details see section 1.7) and modulate gas exchange accordingly. Stomata regulate this gas exchange in both the short and the long term.

In the short-term stomata alter the turgor of the guard cells to alter the size of the stomatal apertures. This enables stomata to actively respond to everyday fluctuations in conditions to optimise gas exchange and water use efficiency (Daszkowska-Golec and Szarejko, 2013).

In the long term the stomatal density of the developing leaf can be modified. Plants, as sessile organisms, need to adapt their body plans to the conditions prevailing in the environment in which they are growing, requiring close, indeterminate, plastic control of their developmental processes. Like other traits stomatal density (and size) are modified

to better adjust the plant to the growth conditions found at the time and location where the plant is developing (Casson and Hetherington, 2010).

1.5- How stomata function

The role of stomata in regulating gas exchange in photosynthetically active tissues of higher plants, via the closure response under conditions where water use efficiency is low i.e. low carbon assimilation with high water loss, is well elucidated. In response to a myriad of environmental signals including CO_2 levels, light and temperature, as well as under drought conditions, the stomata close (Hetherington and Woodward, 2003; Casson and Hetherington, 2010; Chater et al., 2014). Under drought the plant shoots, roots and guard cells produce a phytohormone, abscisic acid (ABA), which passes to the leaves via the phloem where it induces stomatal closure (Merilo et al., 2015; Bauer et al., 2013). In brief ABA binds to a group of 14 START proteins known as the PYROBACTIN RESISTANCE (PYR) or REGULATORY COMPONENT OF ABA RECEPTOR (RCAR) proteins (Park et al., 2009). Upon binding ABA, the PYR/RCAR proteins can interact with a subset of protein phosphotases of the PP2C group, notably ABA INSENSITIVE 1 (ABI1) (Ma et al.,2009), preventing it from dephosphorylating and hence inactivating a group of SNF-related kinase2 protein family members, including OPEN STOMATA 1 (OST1) (Merlot et al., 2002; Mustilli et al., 2002; Cutler et al., 2010) . OST1 triggers a truly byzantine network of interactions between various membrane bound ion channels and transporters with resultant shifts in membrane potentials activating further channels in both the plasma membrane and vacuolar membrane. The net effect is ion efflux triggering the net movement of water out of the guard cells. These consequently lose turgor and cause the stomatal aperture to close, preventing further gas exchange between the internal and

external environments, reducing water loss. (Reviewed in Sirichandra et al., 2009; Kim et al., 2010; Cutler et al., 2010).

1.6 -Stomatal Development in the model organism Arabidopsis Thaliana

Stomatal development in Arabidopsis consists of a series of transitions through various cell fates commenced by a specialised subgroup of protodermal cells. The formation of the stomatal lineage is indeterminate, providing the flexibility for the modification of stomatal density in response to prevailing environmental conditions (see section 1.7) (Hetherington and Woodward, 2003)

1.6.1- An overview of cell fate progression in the stomata lineage

Leaf development consists of cell division at the base followed by cell expansion and differentiation towards the tip. The initial protodermal cells can differentiate into three main cell types; trichromes, epidermal pavement cells and stomatal lineage cells. Adrian et al., 2015 analysed the transcriptome of the various stages of Arabidopsis stomatal development and found enrichment of known trichrome patterning genes such as *ENHANCER OF TRIPTYCON AND CAPRICE (ETC)2* and *ETC3*. This finding suggests that stomata and trichromes share a common pool of pluripotent progenitor cells, with a subsequent bifurcation down different developmental pathways.

The subset of the protodermal cells that enter the stomatal lineage do so by taking on meristemoid mother cell (MMC) fate, the first stage of stomatal development, with downstream events in the lineage's development controlling the density and distribution of stomata (Lau and Bergmann., 2012). MMCs undergo the first of the series of asymmetric divisions that typify the development of the stomatal lineage. This initial division, referred to as the entry division, forms a large stomatal lineage ground cell (SLGC)

and a smaller, triangular shaped cell called a meristemoid. Meristemoids have stem cell-like characteristics, being capable of division with self-renewal (Nadeau and Sack, 2002; Bergmann and Sack, 2007).

The meristemoid can undergo 1 to 3 further asymmetric divisions. These amplifying divisions conserve the meristemoid whilst generating additional SLGC sister cells that expand and further separate neighbouring stomata (Robinson et al., 2011).

The young SLGCs can either terminally differentiate into epidermal pavement cells or re-establish MMC identity and divide asymmetrically to produce a secondary (or satellite) meristemoid. These secondary meristemoids never form adjacent to the original meristemoid, hence these divisions are also referred to as the spacing divisions. This is the so called one cell spacing rule, which ensures stomata do not form immediately adjacent to one another, which would interfere with the closure response. The one cell spacing is important in order to optimise stomatal conductance and enable efficient response to environmental signals (Dow et al., 2013). There are a number of mutants in which the one cell spacing rule is broken (see figure 1.6).

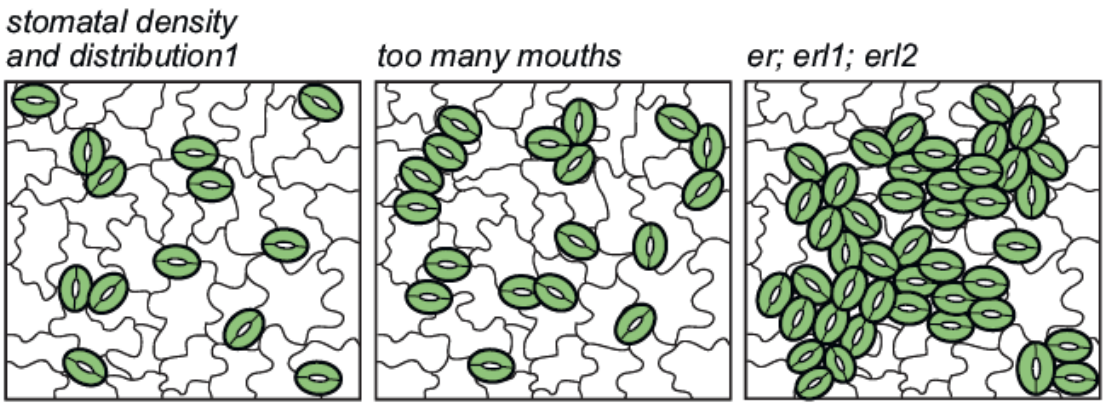

Figure 1.6- Stomatal mutants in which one cell spacing rule is broken.
Mutations in the *SDD1* signalling peptidase, *TMM* leucine rich repeat receptor-like protein and *ERECTA* family leucine rich repeat receptor like kinases cause the breakdown of the one cell spacing rule. The function of *SDD1* Is discussed in section 1.6.10 whilst *TMM* and *ERECTA* are discussed in section 1.6.4 From Bergmann and Sack, 2007.

It is the ability to significantly vary meristemoid number that provides the developmental plasticity to adapt to variable conditions. (Nadeau and Sack, 2002; Gray, 2007; Lau and Bergmann, 2012; Pillitteri and Torii, 2012)

Meristemoids mature into guard mother cells (GMCs), round shaped cells that undergo a single symmetrical division to form the guard cells of the mature stomatal complex (Gray, 2007; Lau and Bergmann, 2012; Pillitteri and Torii, 2012). The transitions and divisions of stomatal development are summarised in figure 1.7.

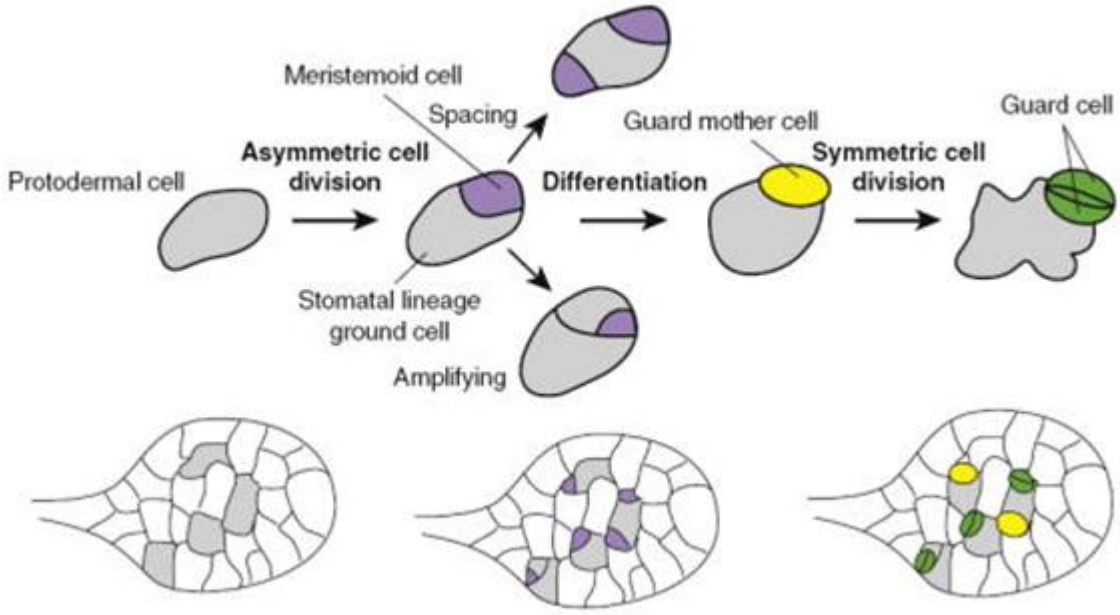

Figure 1.7- Model of stomatal development in Arabidopsis. Scheme showing the stages through which the stomatal lineage progresses in both an isolated cell (top) and in the context of a developing leaf (bottom) in Arabidopsis. A protodermal cell undergoes an asymmetric entry division to produce a SLGC and a meristemoid (purple). The meristemoid can undergo additional asymmetric amplifying divisions that produce additional SLGCs whilst the SLGC can undergo an asymmetric spacing division that produces a secondary meristemoid distal to the original meristemoid. The meristemoid differentiates into a GMC (yellow) which divides symmetrically to produce the mature stoma (green). Bottom shows the scattered distribution of the subset of protodermal cells that enter the lineage and how meristemoids are spaced so that stomata don't form adjacent to one another From Katsir et al., 2011.

1.6.2-Overview of the genetic components of the core stomatal development pathway

The core components of the stomatal development pathway in Arabidopsis are now well elucidated. This section will first provide a brief overview of the core stomatal development pathway, each of which will be further described in later sections.

Stomatal development is regulated by a peptide signalling pathway. Signalling peptides are small, secreted proteins that bind leucine rich repeat receptor like kinases (LRR-RLKs) in order to induce a signalling cascade. LRR-RLKs are a large family of receptors with over 200 members in Arabidopsis, several of which have been identified as binding to signalling ligands, notably the CLAVATA3 (CLV3)/ENDOSPERM SURROUNDING REGION (CLE) peptides involved in meristem size regulation and the EPIDERMAL PATTERNING FACTOR LIKE (EPFL) family (Katsir et al., 2011). Some members of the *EPFL* family regulate stomatal density and patterning.

The receptor complex for the EPF peptides consists of the TOO MANY MOUTHS (TMM) receptor-like protein (RLP) and members of the ERECTA family of LRR-RLKs. Upon the binding of the members of the EPFL family that negatively regulate stomatal density, the TMM-ERECTA complex activates a mitogen activated protein kinase (MAPK) cascade which transduces the EPFL signal and inhibits stomatal fate, via suppression of a transcription factor, SPEECHLESS (SPCH).

The transition between cell fates in Arabidopsis is controlled via sequential expression of a series of 3 basic helix-loop-helix (bHLH) transcription factors; *SPCH, MUTE* and *FAMA* (MacAlister et al., 2007; Ohashi-ito and Bergmann.2006; Pillitteri et al., 2007 see figure 1.8). SPCH, MUTE and FAMA heterodimerise with a second set of bHLH factors, INDUCER OF CBF EXPRESSION 1/SCREAM (ICE1/SCRM) and SCRM2 that are expressed

throughout the stomatal lineage and which are functionally redundant (Kanoaka et al.,2008).

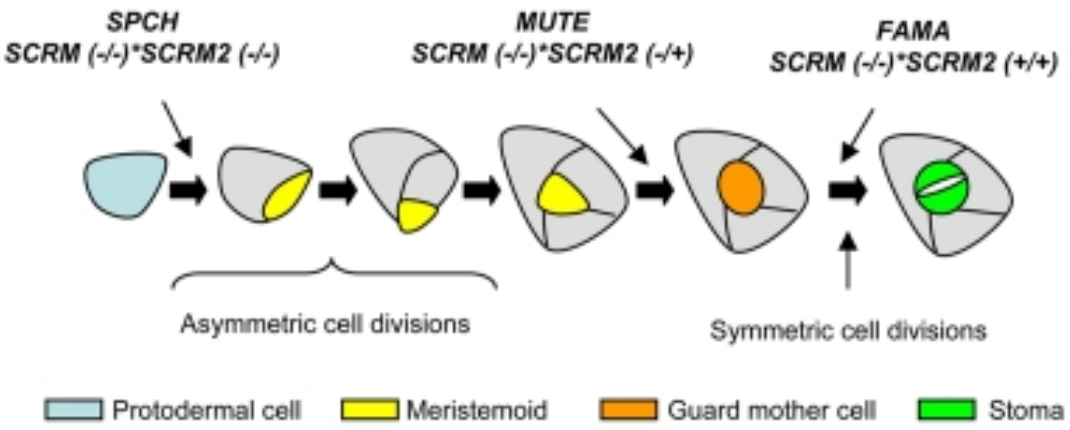

Figure 1.8- The role of bHLH transcription factors in stomatal development. SPCH, MUTE and FAMA promote asymmetric divisions, meristemoid to GMC transitions and GMC to mature stoma transitions respectively. SCRM/SCRM2 heterodimerise with the other factors and are required for SPCH MUTE and FAMA function. from Serna, 2009

1.6.3-The EPFL family of signalling peptides regulate of stomatal development

The EPFL family consists of 11 cysteine rich signalling peptides, only some of which are directly involved in stomatal development. These include two primary negative regulators, EPF1 and EPF2, as well as one positive regulator, EPFL9/STOMAGEN (Hara et al., 2007; Hunt and Gray, 2009; Hara et al., 2009; Hunt et al.,2010; Kondo et al.,2010; Sugano et al., 2010). The negative *EPFL*s are both expressed by stomatal lineage cells only (Hara et al., 2007; Hunt and Gray, 2009; Hara et al., 2009) whilst *STOMAGEN* is expressed by the cells that will go on to form the photosynthetic mesophyll tissue and diffuses to the L1 layer where the STOMAGEN peptide competes with EPF2 for the ER receptor (Kondo et al.,2010; Sugano et al., 2010; Lee et al.,2015).

EPF1 negatively regulates stomatal density and enforces the one cell spacing rule. The *epf1* mutant exhibits a stomatal clustering phenotype as well as increased stomatal density, whilst overexpressing *EPF1* reduces stomatal density and increases the prevalence of arrested stomatal precursors (Hara et al., 2007; Hara et al., 2009). *EPF1* is expressed later on in the developmental series, by the late meristemoids, GMCs and guard cells (Hara et al., 2007). It represses meristemoid formation and in particular effects the asymmetric spacing divisions of SLGCs that re-enter the stomatal lineage, ensuring that when they divide they do not form the secondary meristemoid adjacent to the stomatal lineage cell expressing *EPF1*, hence enforcing the one cell spacing rule (Hara et al., 2007).

EPF2 is a negative regulator of stomatal density as well but possesses no clustering phenotype in the loss-of-function mutant, which exhibits increased stomatal and pavement cell density only. Similarly the overexpressor reduces stomatal density, consistent with EPF2 possessing a negative regulatory role. (Hunt and Gray, 2009; Hara et al., 2009). *EPF2* is expressed in MMCs and early on in meristemoids and inhibits the formation of stomata. This inhibition is achieved by repressing MMC fate via both repressing entry divisions by protodermal cells that form the initial population of MMCs and by preventing the reacquisition of MMC fate by SLGCs, consequently repressing the formation of secondary stomata (Hara et al., 2009). It also represses the amplifying divisions, hence the high pavement cell density found in the *epf2* mutant (Hara et al., 2009; Han and Torii, 2016). The *EPF2* promoter has been found to be hypermethylated and consequently inactivated in *ros1* mutants, leading to an accumulation of small, arrested stomatal precursors such as those seen in the *epf2* mutant (Yamamuro et al., 2014). *EPF2* expression can be restored in *ros1* mutants by mutations in the RNA-directed DNA methylation pathway, leading to the suppression of the small cells phenotype (Yamamuro et al., 2014). Whether alterations in the methylation state of the *EPF2* promoter is used to

regulate stomatal density in adaptive response to environmental signals is unclear (Han and Torii, 2016).

The *epf1epf2* double mutant has an additive phenotype, demonstrating that their negative regulatory roles are independent of one another. (Hunt and Gray, 2009; Hara et al., 2009)

These negative regulators are secreted from the stomatal lineage cells and diffuse over the surrounding area, suppressing stomatal development in the epidermal cells located adjacent and nearby. (Hara et al, 2007; Hunt and Gray, 2009; Hara et al., 2009)

The positive regulator of stomatal density, STOMAGEN has a similar peptide sequence to EPF1 and EPF2 but has a reduced number of cysteine residues (Hunt et al.,2010; Kondo et al.,2010; Sugano et al., 2010). Overexpression of *STOMAGEN* increases stomatal density and produces clustered stomata whilst antisense transgenics possess a reduced stomatal density phenotype (Hunt et al., 2010; Sugano et al., 2010).

The structure of the EPFLs have been determined utilising NMR (Okhi et al., 2011, shown in figure 1.9). The EPFLs possess a distinctive knot structure scaffold that is formed as a result of 3 disulphide bonds between a set of conserved cysteine residues. EPF1 and EPF2 contain an additional pair of cysteines and form an additional disulphide bond. The EPFL structure also contains a loop of residues (yellow coloured residues in figure 1.9 B). Swapping the EPF2 loop domain into the STOMAGEN scaffold is sufficient to produce a negative regulator of stomatal development whilst the reciprocal swap is sufficient to produce a positive regulator. This suggests that the loop structure confers specificity in the EPFLs. Meanwhile disrupting the disulphide bonds of the scaffold leads to inactivation of the peptides. The similarities in the structure between EPF2 and STOMAGEN provided early support for the competition for receptors theory for explaining

how the antagonism between STOMAGEN and EPF2 is resolved (Ohki et al., 2011; Lau and Bergmann, 2012).

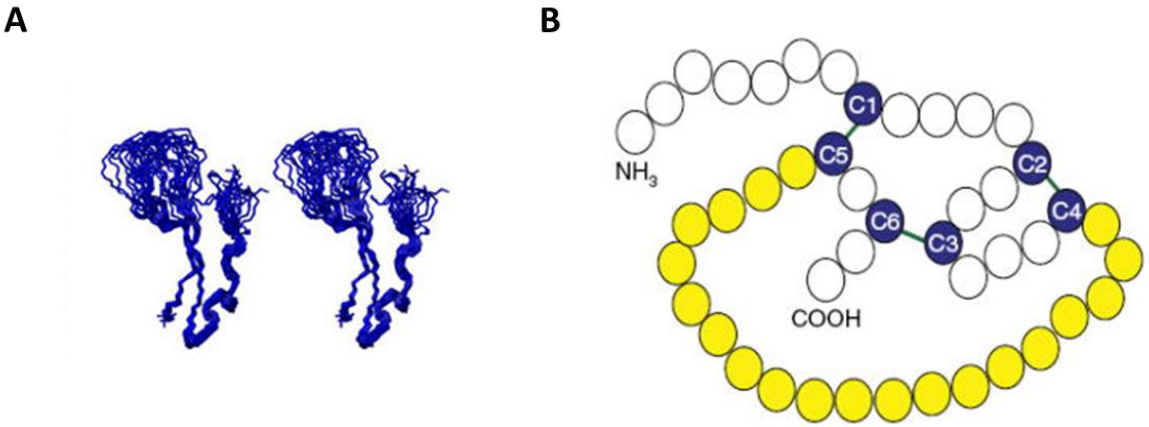

Figure 1.9- the structure of STOMAGEN. (A) A stereoview of 20 NMR structures from STOMAGEN. Only the backbones are depicted. From Okhi et al., 2011 (B) simplified, experimentally derived structure of stomagen showing conserved cysteine residues (blue) linked by disulphide bonds. The variable loop demain residues are shown in yellow. From Katsir et al., 2010

1.6.4-The ERECTA family of LRR-RLKs are the receptors of the EPFL peptides and their stomatal roles are specified by the receptor-like protein TOO MANY MOUTHS

TOO MANY MOUTHS (TMM) is a receptor-like protein (RLP) possessing a leucine-rich repeat (LRR) receptor domain but lacking a C-terminal kinase domain necessary for the subsequent transmission of signalling (Torii, 2004). As with other RLPs it forms associations with LRR-receptor like kinases (LRR-RLKs) in order to bring about signal transduction (Torii, 2004; Lee et al., 2012). The ERECTA family of LRR-RLKs, consisting of ERECTA, ERECTA LIKE1 (ERL1) and ERL2, are the partners of TMM in stomatal development transduction. These ERECTA receptors act as inhibitors of the transition to stomatal lineage fate and are partially redundant. (Shpak et al., 2005) They do however show some separation of

function (Shpak et al., 2005; Lee et al., 2012). The ERECTA receptors also possess a wide variety of roles in regulating cell proliferation and the development of plant organs (Shpak et al., 2003, Shpak et al., 2004, van Zanten et al., 2009).

ERECTA is expressed in protodermal cells where, in response to EPF2, it represses entry divisions (Shpak et al., 2005; Lee et al., 2012). STOMAGEN competes with EPF2 for the ERECTA receptor (Lee et al., 2015). Both peptides bind to ER with similar affinities but only EPF2 activates downstream signalling and consequently inhibits stomatal development (Lee et al., 2015). It seems likely that this competition provides the means by which stomatal patterning is fine-tuned to prevailing requirements (see figure 1.10).

ERL1 and *ERL2* are expressed later in the stomatal lineage (Shpak et al., 2005). The *erl1* mutant possesses a stomatal clustering phenotype which, in conjunction with a coimmunoprecipitation study suggesting ERL1 is paired with EPF1, suggests ERL1 enforces the one cell spacing rule via orientating cell divisions. ERL1 also restricts meristemoid differentiation (Shpak et al., 2005; Lee et al., 2012).

The *tmm* mutant, the first stomatal phenotype mutant identified, possesses an increased number of stomata on leaves and abolishes the formation of stomata on stems (Yang and Sack, 1995). The orientation of spacing divisions is also affected, resulting in clustering (Geisler et al., 2000). TMM functions to specify stomatal signalling. Whilst the ERECTA family is a widely expressed set of receptors with diverse functions in growth and development, TMM is stomatal lineage specific (Nadeau and Sack, 2002) and is required for the perception of stomatal interacting EPFLs (Hara et al., 2007; Hara et al., 2009; Hunt and Gray, 2009; Kondo et al., 2010; Sugano et al., 2010). However, TMM inhibits the interactions between the ERECTA receptors and other EPFLs involved in growth in other, internal tissues, such as EPFLs 4-6, known as the CHALLAH family ligands (Abrash and Bergmann, 2010; Abrash et al., 2011). These ligands are not expressed in the leaves and EPFL4 and EPFL6 have been identified as functioning in ERECTA-mediated

signalling pathways that determine aspects of inflorescence architecture (Uchida et al., 2012). The CHALLAH ligands interact with ERECTA receptors to effect growth in the stems of plants but TMM prevents these ligands interfering with stomatal development in the stem epidermis, isolating the two distinct ERECTA functions (Abrash and Bergmann, 2010; Abrash et al., 2011). CHALLAH ligands freely interact with the ERECTA receptors in the absence of TMM, negatively regulating stomatal differentiation in the manner of EPF2, i.e. the mutant lacks the ability to discriminate between the different EPFL groups (Abrash et al., 2011). This is why *tmm* mutants lack stem stomata (Yang and Sack, 1995, Geisler et al., 1998) Exogenous application of EPFL5 causes meristemoids to arrest and *MUTE* transcript levels to drop, i.e. produces a similar phenotype to EPF1 (Niwa et al., 2013).

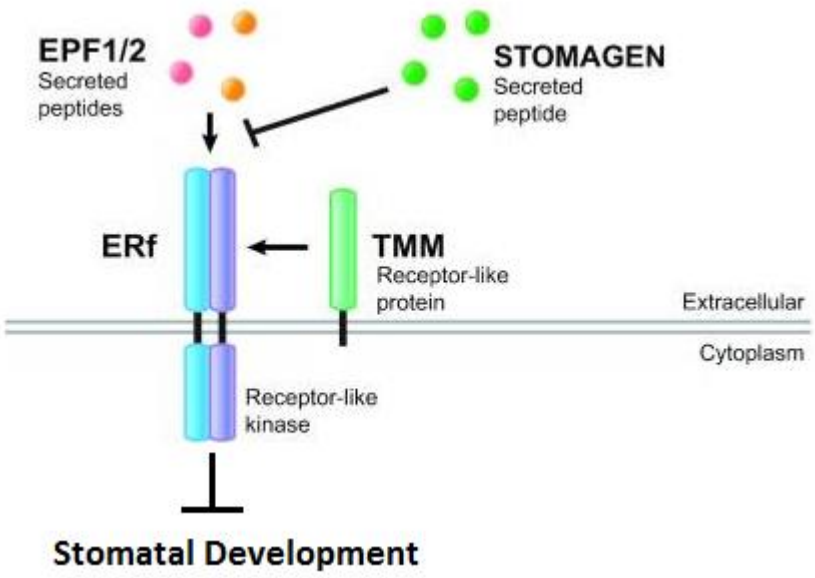

Figure 1.10- the EPF/TMM/ERECTA signalling module. ERECTA receptors perceive EPF signals in the presence of TMM. STOMAGEN competes with the EPFs for the receptor. Upon receipt of the EPF signal stomatal development is repressed (Lau and Bergmann 2012)

1.6.5-Signal transduction occurs via a MAPK cascade

Once the EPF signal is perceived by the ERECTA/TMM complex it is transmitted by the YDA, MKK4/5 and MPK3/6 signalling cascade (Wang et al., 2007). Loss of function MKK4/5 and MPK3/6 results in disruption of cell fate specification leading to stomatal clustering whilst overexpression results in a lack of stomatal differentiation consistent with the role of the MAPK cascade in regulating SPCH (Wang et al., 2007; Lampard et al., 2008, see section 1.6.6). Similarly, *yda* mutants produce excess stomata whilst constitutive YDA expression abolishes stomatal formation entirely (Bergmann et al., 2004). This is consistent with the MAPK cascade transducing an inhibitory signal of stomatal development (Bergmann et al., 2004; Wang et al., 2007; Han and Torii, 2016).

Overexpression of *AP2C3*, a MAPK phosphatase expressed in stomatal lineage cells, leads to an epidermis that is solely composed of stomata (Umbrasaite et al., 2010). This suggests it could function as a promoter of stomatal formation through disruption of stomatal signalling via dephosphorylation of the cascade components transducing the signal triggered by the EPFs, which are negative regulators of stomatal development (Umbrasaite et al., 2010; Hara et al.,2007; Hunt and Gray, 2009; Hara et al., 2009).

1.6.6-SPCH regulates the initiation and proliferation of stomata

SPCH is the first of the bHLH transcription factors in the series. Most of the *spch* mutants utilised in the original study (MacAlister et al., 2007) lack stomata entirely due to an absence of entry divisions, resulting in an epidermis formed entirely of pavement cells. However in the *spch-2* mutant some MMCs undergo entry divisions, albeit at a reduced rate compared to wildtype. *spch-2* mutants also produce fewer secondary meristemoids and fewer SLGC sister cells than wildtype, indicative of a reduction in the asymmetric

spacing and amplifying divisions respectively. The meristemoids also prematurely differentiate into GMCs. Although the number of spacing divisions is reduced, the one cell spacing rule is still in effect. (MacAlister et al., 2007). Conversely, constitutive overexpression of *SPCH* results in increased asymmetric divisions in pavement cells and additional stomatal lineage cells (MacAlister et al., 2007; Pillitteri et al., 2007).

SPCH expression is also required for the maintenance of meristemoid stem cell-like character, with SLGCs that regain *SPCH* expression also regaining the ability to undergo self-renewing divisions following an initial asymmetric division, i.e. forming new meristemoids (Robinson et al., 2011).

Taken together this evidence demonstrates that the role of SPCH is to promote the asymmetric divisions within the stomatal lineage. SPCH induces the initial entry division and maintains the self-renewing character of the meristemoid as it undergoes amplifying divisions. Disrupting *SPCH* expression results in fewer protodermal cells entering the stomatal lineage and early loss of meristemoid character, resulting in a reduction in the number of SLGCs formed (MacAlister et al., 2007; Robinson et al., 2011).

As might be expected, given its role in specifying the earliest events in the stomatal development pathway, SPCH is an important node in density regulation. SPCH is the primary target of the MAPK cascade induced by EPF2 signalling, and is targeted for degradation once phosphorylated by MPK3/6 (Lampard et al., 2008).

SPCH expression and consequently the stomata are specific to L1 layer, i.e. found on the epidermis. Interestingly, ectopic overexpression of the L1 layer specific homeobox transcription factors MERISTEM LAYER 1 (ATML1) and HOMEODOMAIN GLABOROUS 2 (HDG2) induces *SPCH* expression and subsequent stomatal formation in non-epidermal tissues such as the mesophyll (Takada et al., 2013; Peterson et al., 2013).

SPCH has been found to bind directly to the promoters of various genes involved in the stomatal lineage including both its heterodimeric partners (*SCRM* and *SCRM2), TMM,*

EPF2, ERL1, MUTE, BASL and *POLAR* (see respective sections for details on these genes' functions) (Lau et al., 2014).

SPCH can also be regulated via epigenetic mechanisms. In low humidity conditions *SPCH* is transcriptionally repressed via de novo cytosine methylation in Arabidopsis, which leads to a reduction in stomatal density (Tricker et al., 2012; Tricker et al., 2013). Plants with loss of function mutations in DNA methylation enzymes do not exhibit a reduction in stomatal density in low humidity (Tricker et al., 2012; Tricker et al., 2013).

1.6.7- MUTE terminates the asymmetric division phase of the lineage and promotes meristemoid differentiation

MUTE expression is required for the loss of stem cell-like character in meristemoids and the transition between meristemoid and guard mother cell fate. In the loss-of-function *mute* phenotype SPCH activity continues for an extended period leading to additional asymmetric cell divisions (Pillitteri et al., 2007). The meristemoid then aborts, failing to transition to a GMC and as a result no stomata are formed (Pillitteri et al., 2007).

Ectopic overexpression of *MUTE* produces an epidermis composed solely of stomata and induces stomatal cell fate in cell types that do not normally enter the stomatal lineage, demonstrating that MUTE is sufficient to induce stomatal fate in pavement cells (Pillitteri et al., 2007; Pillitteri et al., 2008).

MUTE expression appears in late stage meristemoids, coinciding with the decline in *SPCH* expression (Davies and Bergmann, 2014). A 175bp region of the MUTE promoter is necessary and sufficient for meristemoid-specific expression (Mahoney et al., 2016).

1.6.8- FAMA promotes guard cell fate and restricts stomatal lineage symmetric divisions

FAMA regulates the final stage of stomatal development, the transition from GMC to the mature stoma via a single symmetric division (Ohashi-Ito and Bergmann, 2006). Loss of function mutants undergo additional symmetric divisions to produce collections of narrow epidermal cells in place of stomata, i.e. additional guard cell-like cells (Ohashi-Ito and Bergmann, 2006). FAMA alone is sufficient to induce guard cell fate with ectopic overexpression leading to an epidermis solely comprised of unpaired, kidney-shaped guard cells (Ohashi-Ito and Bergmann, 2006).

More recent studies have demonstrated that FAMA has a role in guard cell identity stability. Notably FAMA maintains guard cell identity via the RETINOBLASTOMA-RELATED PROTEIN (RBR) dependent epigenetic repression of stomatal development genes. In transgenic lines that disrupt the ability of RBR to bind to FAMA, such as a *fama* mutant that lacks the RBR binding LxCxE motif, stomatal lineage genes such as *SPCH* are not repressed, leading to new entry divisions in guard cells. This leads to stomata forming within previously formed stomata (Lee et al., 2014; Matos et al., 2014).

FAMA can be regulated via epigenetic mechanisms. Like *SPCH, FAMA* is transcriptionally repressed in low humidity conditions via DNA methylation (Tricker et al., 2013).

1.6.9- Two additional bHLH transcription factors are required for SPCH, MUTE and FAMA activity

In order to function SPCH, MUTE and FAMA require the presence of 2 paralogs that are widely expressed within the stomatal lineage, SCRM and SCRM2, with which they form heterodimers (Kanoaka et al., 2008). Progressive loss of these two

paralogs results in *spch*, *mute* and *fama* phenotypes, whilst the gain of function scrm-D mutant produces a stomata only epidermis such as that seen when MUTE is ectopically overexpressed (Kanoaka et al., 2008).

SCRM and SPCH act together in the early protoderm to control the initiation of the stomatal lineage. Whilst both the *SCRM* and *SPCH* promoters are active to a similar degree across the protoderm, SPCH and SCRM protein accumulation is restricted to those protodermal cells that eventually give rise to the stomatal lineage. *SCRM* expression is upregulated by a positive feedback loop, wherein SCRM upregulates its own expression in the presence of SPCH. SPCH-SCRM also upregulates EPF2 and TMM which acts as a negative feedback loop, with secreted EPF2 inducing SPCH breakdown via phosphorylation (Lampard et al., 2008) and consequently causing *SCRM* expression to fall in neighbouring protodermal cells, causing them to not enter the stomatal lineage. These feedback loops are represented in figure 1.11. The net result is that the population of protodermal cells that become MMCs is restricted (Horst et al., 2015). The roles of the EPF/TMM/ERECTA signalling module, MAPK cascade and bHLH transcription factors are summarised in figure 1.11.

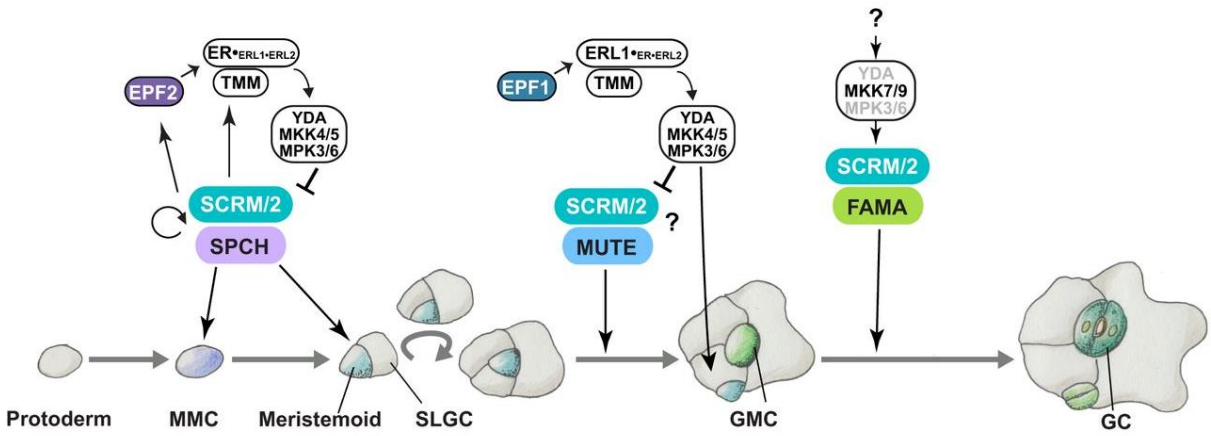

Figure 1.11- Stomatal development in Arabidopsis. For description of lineage transitions see figure 1.8. SPCH, MUTE and FAMA, in conjunction with SCRM/SCRM2, mediate the lineage transitions. They are antagonised by the MAPK cascade triggered when EPF2 or EPF1 signalling peptides are perceived by the ERECTA/TMM receptor complex. EPF1 and EPF2 are perceived by different members of the ERECTA family.

1.6.10- STOMATA DENSITY AND DISTRIBUTION 1 (SDD1)

SDD1 encodes a subtilisin-like Ser protease that is expressed strongly in meristemoids and guard mother cells (Von Groll et al., 2002). The *sdd1-1* mutant possesses clustered stomata and 2- to 4-fold increases in stomatal density (Berger and Altmann, 2000) whilst the *SDD1* overexpressor exhibits stomatal density reductions of around 2- 3-fold whilst also producing arrested stomatal precursors (meristemoids/GMC) (Von Groll et al., 2002). GFP fusions also demonstrated that the mature SDD1 peptide is exported to the apoplast and associated with the plasma membrane (Von Groll et al., 2002). Surprisingly, despite a likely role in the processing of signalling peptides, the known regulators of stomatal development EPF1, EPF2 and STOMAGEN are not substrates for proteolysis by SDD1 (Hara et al., 2007, Hara et al., 2009, Hunt and Gray, 2009, Hunt et al., 2010). Indeed, the substrate remains unknown. (Hunt et al., 2010)

The transcriptional regulator GT-2 LIKE 1 (GTL1) binds to the GT3 box of the *SDD1* promotor, repressing *SDD1* and so increasing stomatal density in water replete conditions. (Yoo et al., 2010) In contrast *gtl1* mutant plants have lower stomatal densities and reduced transpiration relative to wild type individuals. (Yoo et al., 2010)

1.6.11- BASL and POLAR

A notable feature of stomatal development is the series of asymmetric divisions that occur to produce SLGCs and satellite meristemoids via amplifying and spacing divisions respectively (Bergmann and Sack, 2007; Lau and Bergmann, 2012). The principle intrinsic regulator of asymmetric cell division in Arabidopsis that has been identified is BREAKING OF ASYMMETRY IN THE STOMATAL LINEAGE (BASL) (Dong et al., 2009). *BASL* encodes a novel protein and was identified from the *basl* mutant which exhibits a high proportion of MMCs which divide symmetrically. BASL is notable for its distinctive, asymmetric distribution in MMCs prior to mitosis (Dong et al., 2009). It localises to both the nucleus and to a band of the cell cortex located opposite the future division plane, where it induces cell expansion. The cell then divides asymmetrically with the cortex BASL band being contained within the larger daughter cell, the SLGC (Dong et al., 2009). If the daughter meristemoid only possesses nuclear BASL it will differentiate into a GMC, if a new BASL cortex band is formed it will continue to divide asymmetrically, i.e. amplifying divisions will occur (Dong et al., 2009; Han and Torii, 2016). Similarly the fate of the SLGC is dependent upon whether nuclear and/or cortical localisation of BASL continues. If only cortical BASL is retained the cell terminally differentiates into an epidermal pavement cell. If both cortical and nuclear BASL is retained the SLGC transitions to MMC fate and undergoes a spacing division (Dong et al., 2009). Interestingly this process sees the reorientation of the cortical band, which reforms adjacent to the sister meristemoid and therefore distal to the future

division plane, ensuring the satellite meristemoid forms away from the primary stomatal lineage cell, enforcing the one cell spacing rule (Nadeau and Sack, 2002; Dong et al., 2009).

BASL functions as a scaffold for MAPK signaling, with BASL being able to directly bind YDA (Zhang et al., 2015). As a result YDA is spatially concentrated at the cortex BASL band that is then segregated into the SLGC following the asymmetric division (Zhang et al., 2015). This leads to increased repression of SPCH in the SLGC via phosphorylation from the MAPK cascade, inhibiting stomatal lineage identity (Zhang et al., 2015, Zhang et al., 2016). MAPK6 directly phosphorylates BASL in vitro and phosphorylation is necessary for BASL polarisation, suggesting the possibility of a positive feedback loop wherein phosphorylated BASL is asymmetrically distributed, taking the components of the MAPK cascade with it to the cell cortex where MAPK activity ramps up BASL polarity whilst promoting cell expansion and repressing stomatal cell fate (Zhang et al., 2015; Zhang et al., 2016; Han and Torii., 2016).

POLAR is a coiled-coil protein that, like BASL, exhibits a polarised distribution prior to asymmetric division in meristemoids (Pillitteri et al., 2011). POLAR is distributed evenly in the meristemoid (when BASL is located only in the nucleus) until prior to asymmetric cell division when it relocalises to the distal end of the cell cortex, coinciding with the formation of the cortical BASL band there (Pillitteri et al., 2011). Indeed BASL is required for asymmetric POLAR localisation, suggesting POLAR functions downstream in a BASL-dependent pathway (Pillitteri et al., 2011).

1.7- Stomata and the environment

As stated in section 1.4, stomata respond to and integrate various environmental cues including light quantity and quality, vapour pressure deficit, soil water content, and

CO_2 concentration (Chater et al., 2014). It response to these cues with both short-term and long-term responses. In the short term the stomata close in response to unfavourable conditions whilst in the long-term mature leaves detect these environmental cues and relay the information to developing leaves which adapt their development accordingly by, for example, modifying stomatal density (Lake et al., 2001; Lake and Woodward, 2008; Casson and Hetherington, 2010; Chater et al., 2014).

Stomatal density changes under varying CO_2 concentration and vapour pressure deficit correlate with the concentration of the phytohormone ABA whilst mutants in the ABA biosynthesis pathway exhibit reduced concentrations of ABA and increases in stomatal density (Lake et al., 2002; Tanaka et al.,2013). As a consequence of this evidence ABA has been proposed as the core regulator of environmental influence on stomatal development (Chater et al., 2014). In this section a brief overview is provided of the response of plants to different environmental stimuli, focusing primarily on stomatal development.

1.7.1- Response to water stress

In the short term, stomata respond to water stress by closing, whether as a consequence of ABA signalling or hydropassive closure (Chater et al., 2014; MacAdam and Brodribb, 2011), to conserve water and increase water use efficiency (Daszkowska-Golec & Szarejko, 2013).

In the long term both drought and osmotic stress do possess the capability to influence stomatal development, likely acting though ABA (Tanaka et al., 2013; Han and Torii., 2016), in order to improve WUE.

It is possible for plants to respond to drought by reducing stomatal density, for example the reduction in stomatal density observed in wheat under drought (Quarrie and Jones, 1977) and the reduction in stomatal differentiation, potentially due to the

downregulation of a putative homologue of *STOMAGEN*, under drought conditions in Poplar (Hamanishi et al., 2012).

However, this is not necessarily a universal concept. There have been studies in which stomatal density has been positively correlated with WUE and has increased in response to drought (Elias, 1995; Fraser et al., 2009) or has increased or decreased under drought, dependent on drought severity (Xu and Zhou, 2008). One suggested explanation is that under moderate drought stomatal density, and hence transpiration, may be increased in order to improve nutrient uptake, demonstrated in *Vigna sinesis* where stomatal density reduction under drought only occurs in phosphorous rich conditions (Sekiya and Yano, 2008; Yoo et al., 2009). These studies indicate that the potential for modifying stomatal density as a means of crop improvement, but highlights that the degree and indeed the direction of change in the trait that is beneficial is highly context dependent.

1.7.2- Response to light

As light intensity increases stomatal density on developing leaves increases and the stomatal index (the ratio of the number of stomata divided the number of stomata and other epidermal cells in a given area) increases (Casson and Hetherington, 2010). Stomatal index was found to increase in higher intensity monochromatic red light relative to low red light conditions whilst exposure to far-red light at the end of the photoperiod was found to reduce stomatal index, suggesting that the receptor responsible for perceiving the change in light was a phytochrome, a red/far red light receptor (Casson et al., 2009; Boccalandro et al., 2009; Casson and Hetherington, 2010). Phytochrome B (phyB) was identified as the primary photoreceptor promoting stomatal differentiation in response to increased light, with *phyB* mutants showing reduced stomatal density and index relative to wild type (Casson et al., 2009; Boccalandro et al., 2009). PhyB, as a consequence of increasing the

stomatal density, reduces the water use efficiency of the plants (Boccalandro et al., 2009) but may increase drought tolerance due to it upregulating ABA signalling pathway components and increasing ABA sensitivity (González *et al*., 2012). The increase in stomatal density may also help mitigate the consequences of high light stress (González *et al*., 2012).

The bHLH transcription factor phytochrome-interacting factor 4 (PIF4) was found to be involved in modulating stomatal density in a phyB dependent manner, with *pif4* mutants grown at high irradiances showing significantly reduced stomatal index and stomatal density relative to Col-0 (Casson et al., 2009).

Whilst phyB modulates stomatal development in response to red light, cryptochrome (CRY) 1 and CRY2 modulates stomatal differentiation under blue light (Kang et al., 2009). Mutants in these photoreceptors all show reduced stomatal density and increases in arrest of immature stomatal lineage cells, suggesting a role for light signalling in regulating all aspects of stomatal development from the entry divisions to the final symmetric division (Kang et al., 2009) These photoreceptors are believed to act by stopping the negative regulation of stomatal development by CONSTITUTIVE PHOTOMORPHOGENIC 1 (COP1) (Kang et al., 2009). It is theorised that COP1 interacts with and activates the YDA/MAPK signalling cascade, leading to the inhibition of stomatal development (Kang et al., 2009; Han and Torii, 2016).

The EPF peptide STOMAGEN is also upregulated in high light, again contributing to the increase in stomatal differentiation in high light (Hronkova et al., 2015).

1.7.3- Response to CO_2

Growth at elevated CO_2 concentrations is commonly associated with reduced stomatal conductance and stomatal density (Woodward, 1987; Woodward and Kelly, 1995) albeit with some exceptions where stomatal conductance reduces but stomatal density does not (Woodward and Kelly, 1995; Ainsworth and Rogers, 2007). When CO_2

concentration varies the stomatal conductance changes to reflect this, with stomata opening more in response to low CO_2 concentrations and closing more in response to elevated CO_2 (Casson and Gray, 2008; Casson and Hetherington, 2010). This reduces transpiration in mature leaves which in turn influences stomatal development in developing leaves, for example causing a reduction in stomatal density in plants grown at elevated CO_2 (Miyazawa et al., 2006; Lake and Woodward, 2008; Chater et al., 2014).

There are two known molecular mechanisms which influence stomatal density in response to altered CO_2 concentration.

Firstly, *high carbon dioxide* (*HIC*), which encodes a 3-keto acyl coenzyme A synthase involved in long chain fatty acid biosynthesis, acts as a negative regulator of stomatal density when CO_2 is elevated (Gray et al., 2000). The *hic* mutants exhibited a 42% increase in stomatal density when CO_2 concentrations were doubled (Gray et al., 2000).

More recently two carbonic β-anhydrase genes, *CA1* and *CA4*, have been shown to repress stomatal development in response to high CO_2 (Engineer et al., 2014).The *ca1 ca4* double mutant exhibits increased stomatal development at elevated CO_2 concentrations, i.e. demonstrates an inverse response to wildtype (Engineer et al., 2014). *EPF2* expression is induced in response to high CO_2 and is required for the CO_2 response. The expression of CO_2 RESPONSIVE SECRETED PROTEASE (CRSP), a subtilase that cleaves the EPF2, but not EPF1, pro-peptide to form the mature EPF2 signalling peptide is also upregulated, generating a positive feedback loop that represses stomatal development (Engineer et al., 2014).

Both the short term aperture closure and long term density reduction stomatal responses to increased CO_2 require the presence of ABA, suggesting that ABA is the point of integration between the CO_2 and ABA signalling pathways (Chater et al., 2015).

1.8- The Evolution of Stomata

1.8.1 The ancient origins of stomata

Plants colonised the terrestrial environment from an aquatic origin around 450MYA (Peterson et al., 2010). This shift from aquatic to terrestrial habit presented a significant problem in terms of plant water relations, namely the dry atmosphere, and subsequent problems due to desiccation, inherent in life on the land (Kendrick and Crane, 1997; Peterson et al., 2010). This led to the evolution of the waxy cuticle of the above ground organs that acts as an impermeable barrier to the passage of water (Kendrick and Crane, 1997; Peterson et al., 2010). However photosynthesis and respiration present a requirement for the ready exchange of gases between plant tissues and the environment, to which the cuticle also acts as a barrier (Kendrick and Crane, 1997; Peterson et al., 2010). The solution to this problem came about with the evolution of stomata, which provide a means of allowing gas exchange across an otherwise impermeable leaf epidermis but which can close to seal off the plant's permeable exchange surfaces in the internal leaf spaces from the surrounding environment, preventing water loss in unfavourable conditions (Peterson et al., 2010).

Stomata evolved over 420 MYA (Edwards et al., 1998; Berry et al., 2010) with Silurian and Devonian fossils of plants such as *Cooksonia* and *Aglaophyton* possessing recognisable stomatal structures (Edwards et al., 1998). Indeed the stomata observed are very similar in appearance to the stomata seen in extant fern and moss plant lineages (Edwards et al., 1998). The distribution of these stomata is evenly spread out on the epidermis and stomatal clustering has not been observed, suggesting the presence of a stomatal patterning system and ancient origin for the one cell spacing rule (Edwards et al., 1998; Caine et al., 2016).

Stomata in mosses are restricted to a band around the base of the sporophyte spore capsule, leading to suggestions that early stomata evolved to allow for tissue drying as part of capsule dehiscence prior to been coopted for their canonical role in gas exchange after plants developed vasculature and started to grow vertically away from the damp soil surfaces favored by basal land plants (Duckett et al., 2009; Peterson et al., 2010).

1.8.2 The deep conservation of the EPF/TMM/ERECTA signalling pathway

A series of studies, primarily using the model moss *Physcomitrella patens*, has revealed deep conservation of the components of the stomatal development pathway that has been reviewed earlier in this chapter.

Firstly two *Physcomitrella patens* orthologues of the *Arabidopsis thaliana* bHLH 1A subgroup, which includes *SPCH, MUTE* and *FAMA* were identified and used to attempt to complement *Arabidospsis thaliana spch*, *mute* and *fama* mutants (MacAlister and Bergmann, 2011). These transcription factors, PpSMF1 and PpSMF2, have a high degree of sequence similarity to SPCH, MUTE and FAMA relative to the other members of the Arabidopsis bHLH transcription factors (MacAlister and Bergmann, 2011). *PpSMF1* and *PpSMF2* could not rescue *spch* mutants but partially rescued *mute* and *fama* mutants, suggesting that the role of the 1A subgroup in the regulation of stomatal development is ancient and conserved (MacAlister and Bergmann, 2011). This was then demonstrated conclusively in the native *Physcomitrella patens* background (Chater et al., 2016). In *Physcomitrella patens*, *PpSMF1* knockout mutants lack stomata as do *PpSCRM1* knockout mutants, showing that these othologues possess roles similar to those of the bHLH transcription factors controlling stomatal development in Arabidopsis (Chater et al., 2016). Moreover, PpSMF1 and PpSCRM1 were found to directly interact suggesting that the heterodimerisation between the SCRM-like and SPCH-like bHLH transcription factors,

which is also required for Arabidopsis stomatal development, is highly conserved amongst land plants and is ancient (Kanoaka et al., 2008; Chater et al., 2016).

Another recent study demonstrated further conservation of the molecular mechanisms of stomatal development between *Physcomitrella patens* and *Arabidopsis thaliana*. Single homologues of the *EPFLs* and *TMM* were found in *Physcomitrella patens* and named *PpEPF1* and *PpTMM* respectively (Caine et al., 2016). Knockout mutants of these genes produce sporophytes with dysfunctional stomatal development, the knockouts of *PpEPF1* possessing elevated stomatal density whilst *PpTMM* knockouts showed both an increase in stomatal numbers and a stomatal clustering phenotype (Caine et al., 2016). Furthermore, overexpression of *PpEPF1* significantly reduced the number of stomata per sporophyte capsule (Caine et al., 2016). These findings demonstrate conservation of the role of EPFls and TMM in the negative regulation of stomatal density between the basal land plants and dicots (Caine et al., 2016). PpERECTA1 was also found to affect stomatal development, suggesting that the EPF/TMM/ERECTA signalling module is a highly conserved, universal aspect of stomatal development (Caine et al., 2016).

The conservation of known components of stomatal development in grasses is discussed in detail in chapter 3 section 2.

1.8.3- Conservation of stomatal functional control

Further to the evidence of the conservation of key stomatal development components, there is evidence that genes involved in stomatal aperture response are similarly conserved. Stomata were found to respond to ABA in both *Physcomitrella patens* and *Selaginella unicata* (Chater et al., 2011; Ruzsala et al., 2011). PpOST1 has been found to mediate ABA and CO_2 response in *Physcomitrella patens* in a dosage dependent manner, with stomatal closure impaired in knock outs (Chater et al., 2011; Chater et al., 2014). Furthermore, complementation of the Arabidopsis thaliana *ost1* mutant with both *PpOST1*

and the *OST1* homologue of the lycophyte *Selaginella moellendorffii* resulted in the rescue of stomatal aperture response to ABA (Chater et al., 2011; Ruzsala et al., 2011). However there is significant debate in the literature as to when active stomatal response to ABA and environmental cues evolved with some studies suggesting that stomatal closure in basal land plants, lycophytes and ferns occurs primarily via hydropassive mechanisms, with the lycophyte and fern species investigated not showing any response to ABA application (Brodribb and MacAdam, 2011; MacAdam and Brodribb, 2012). Moreover a study of several extant moss and hornwort species found no stomatal aperture or stomatal development response to changes in CO_2 concentration (Field et al., 2015). These studies would suggest that active stomatal aperture control evolved after the divergence of ferns 360 MYA (Brodribb and MacAdam, 2011; MacAdam and Brodribb, 2012; Chater et al., 2014; Field et al., 2015). However given the high conservation of molecular components and their ability to affect both stomatal aperture control and development it seems likely that either active control is an ancestral, monophyletic trait to the extant stomata bearing plants or, significantly less likely, that the same molecular components have been co-opted for the same/similar roles in regulating stomatal environmental responses through multiple origins of active control in different lineages (Chater et al., 2014).

1.8.4- Response of stomatal development to CO_2 over evolutionary time

Over evolutionary time the atmospheric CO_2 concentration has varied significantly. Studies of fossils have found that the stomatal density of plants tracks the predicted global CO_2 concentration, with relatively high stomatal densities at times of low global CO_2 and relatively low stomatal densities at times of high global CO_2 (Beerling and Woodward, 1997; Hetherington and Woodward 2003; Franks and Beerling, 2009).

This would suggest that the adaptation of stomatal characteristics to global CO_2 is beneficial and that futureproofing crops by lowering stomatal density in anticipation of higher CO_2 levels as a consequence of climate change has some merit.

Stomatal size varies inversely with stomatal density and changes in stomatal size are also seen in the fossil record. Small stomata have shorter diffusion path lengths, facilitating CO_2 uptake in low CO_2 conditions (Franks and Beerling, 2009) and close faster in response to environmental cues, protecting against high water potential gradients (Drake et al., 2013; Raven, 2014). As a consequence of this inverse relationship the density and size phenotypes partially compensate on another, e.g. at low stomatal densities the stomatal aperture of individual stoma is larger (Büssis et al., 2006).

1.9- The concept- modifying stomatal density to improve water use efficiency and/or drought tolerance

The aim of the experiments contained within this thesis was to investigate two key ideas, the first being whether the role of EPFLs in the negative regulation of stomatal density was conserved between monocots and dicots. The second was whether reducing stomatal density in a crop plant could potentially be used to futureproof crops against the predicted rise in drought conditions due to climate change by improvements to water use efficiency and/or drought tolerance.

Significant evidence exists to indicate that the conservation of the role of the EPFLs in stomatal regulation is likely. The evolutionary conservation of stomatal development components and aperture responses in both basal land plants and monocots, reviewed in sections 1.8 and chapter 3 respectfully, suggests that the EPF/TMM/ERECTA signalling module predates the divergence between monocots and dicots by a significant margin

(Chater et al., 2014; Caine et al., 2016), with the bHLH transcription factors retaining their role in guiding stomatal development progression in the monocots (Liu et al., 2009; Raissig et al., 2016).

There is also significant evidence suggesting that reducing stomatal density can achieve significant improvements in WUE and drought tolerance. Examples of natural reductions in stomatal density leading to improvements in water use efficiency in barley and poplar are discussed in section 1.3.3. More recent transgenic work has added further evidence to the benefits to water relations of reducing stomatal density. Overexpressing *EPF2* in Arabidopsis increased both instantaneous and long-term water use efficiency in Arabidopsis (Franks et al., 2015) whilst the reduction in stomatal density in *Arabidopsis thaliana gtl1* mutants was also associated with increased water use efficiency and drought tolerance (Yoo et al., 2010; Yoo et al., 2011). Overexpressing *PdEPF2* in *Arabidopsis thaliana* also lead to improved drought tolerance (Liu et al., 2016) whilst overexpressing *ZmSDD1* in maize lead to reduced stomatal density and improved drought tolerance and water use efficiency (Liu et al., 2015).

That plants naturally lowered stomatal density in geological time periods of high global CO_2 concentration also supports the idea that lower stomatal densities could be beneficial in future crops under the elevated global CO_2 concentration caused by climate change (Beerling and Woodward, 1997; Hetherington and Woodward 2003; Franks and Beerling, 2009).

Following the publication of the barley genome (Mayer et al., 2012) we set out to investigate the role of EPFs in monocot stomatal development by overexpressing a putative barley homologue of *EPF1* and *EPF2* in both *Arabidopsis thaliana* and *Hordeum vulgare* backgrounds. Following an initial screen of the transgenic barley lines we analysed two single insert *HvEPFL1* barley lines to ascertain the effect of this barley EPFL on stomatal development, gas exchange, water use efficiency and drought tolerance.

Chapter 2 – Materials and Methods

2.1- General chemical reagents

Unless otherwise specified, all chemicals and reagents utilised were obtained from New England Biolabs, Sigma-Aldrich, Thermo Fisher Scientific or Bio Rad.

2.2-Plant material

2.2.1- Hordeum vulgare

The barley *HvEPFL1* overexpressor construct was generated by Dr Lee Hunt. They were placed into the PBRACT214 gateway vector by LR recombination and transformed into the barley cultivar "Golden Promise" by the James Hutton Institute using a previously described method (Harwood et al., 2009). Empty vector lines, i.e. lines transformed with only the hygromicin resistance cassette, were also generated to act as controls. T0 plants were initially grown on selective medium and successful transformants were confirmed by PCR. T1 seed of the successfully transformed EPFL and empty vector lines was then sent to the University of Sheffield for analysis. Initial phenotype screens and copy number determination (section 2.17) were carried out in T1 generation plants, the rest of the experiments utilised one empty vector and two single insert transgenic lines (A and B) in the T2 generation. All transformants were confirmed by genotyping (see section 2.5). In all instances below a barley leaf is considered fully expanded when the ligule has formed.

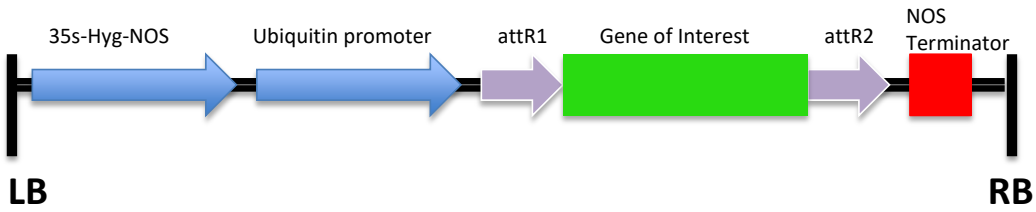

Figure 2.1- Diagram of the construct insert. Gene of interest is *HvEPFL1*

2.2.2-Arabidopsis thaliana

The *epf2* mutant has been described previously (Hunt and Gray., 2009). The HvEPFL2 OE was generated by Dr Lee Hunt. The predicted coding region of HvEPFL1 was amplified (see section 2.5) using primers that introduced flanking AscI and NotI restriction sites to the desired insert. Restriction digests of the amplified gene and the pENTR/dTOPO gateway entry vector were carried out using AscI and NotI restriction enzymes in CutSmart buffer (NEB). The cut products were run out on a 1% agarose gel (see section 2.6) and the relevant bands excised and purified using the PCR and Gel kit (Bioline). Then the insert was ligated into the pENTR/dTOPO backbone to generate an entry vector. This was transformed by freeze-thaw method into E.coli and grown up at 37^{o}C for 2 days with selection (kanamycin 50mg/ml). The entry plasmid was then extracted and the insert recombined into cTapi destination vectors (Rohila et al., 2004). The overexpressor utilised the standard cTapi vector where the gene of interest was placed under the control of the constitutive CaMv 35S promoter whilst for the pEPF2 complementation vector a modified cTAPi vector was used where the 35s promoter had been replaced with the Arabidopsis pEPF2 native promoter. The destination vectors were transformed via freeze-thaw into agrobacterium strain C58, and Arabidopsis was then transformed using the floral dip method (Clough and Bent, 1998). Collected seeds were stratified and germinated as described in section 2.3.3 and then transformants selected by treatment with Basta herbicide (Liberty; Agrevo,Cambridge, UK). T2 plants were used in the experiments

detailed in this thesis, following confirmation of transgene presence by PCR (see section 2.5).

2.3- Growth conditions

2.3.1- Hordeum vulgare

All barley growth and gas exchange experiments were carried out in a greenhouse. Conditions were set to a 20°C, 12 hour duration day and a 16°C, 12 hour duration night. CO_2 and humidity were at ambient levels and supplementary lighting was utilised so the PAR did not fall beneath 180 $\mu molm^{-2}s^{-1}$ at bench level. The consequences for experimental design of these conditions are discussed in detail in section 2.8.3.

Barley seeds were germinated on M3 compost in petri dishes sealed with micropore tape (3M). Successful germination was considered to have occurred if Zadoks stage 07 was achieved (see figure 2.2 for full details of the Zadoks growth scale). Once germinated, plants were transferred to pots containing M3 compost (Levington) and perlite in a ratio of 4:1. For the initial phenotypic screen and drought tolerance experiments (see section 2.12) plants were grown in 13cm diameter pots. For the plant initial growth experiment (see section 2.11) and for the plants used for gas exchange and yield (sections 2.8 and 2.10 respectively), 1 litre pots were used. Each of these pots was supplemented with 5g of Osmocote controlled release fertiliser (The Scotts Company, Marysville, OH).

2.3.2- Soil water content specification

For the experiments requiring soil water content to be controlled the following protocol was carried out. Firstly M3 Compost, Perlite and Osmocote in the required ratio and quantities for the experiment (see section 2.3.1) were mixed until homogeneous prior to being divided equally amongst individual pots.

Five pots were subsequently watered to saturation to obtain the weight of 100% soil water content. The soil from a further five pots was transferred into five separate A4 manilla envelopes and dried in an oven at 80°C for two days at which point their measured weight ceased to change. This weight was taken as the value for 0% soil water content. The 60% and 25% values were then calculated utilising the following formula:

$$\text{Soil Water Content}(\%) = \frac{\text{x} - \text{ Dry Weight}}{\text{Saturated Weight} - \text{ Dry Weight}} * 100$$

where x equals the soil weight at a given soil water content %. Once the soil weights for 25% and 60% soil water content were calculated, the remaining pots were maintained at the required weights, being watered to either 25% or 60% soil water content level every 2 days.

2.3.3- Arabidopsis thaliana

Arabidopsis seeds were stratified on wet M3 compost contained within 13cm diameter pots at 4°C in dark for 72 hours to synchronise germination. Seed pots were covered with cling film and transferred to a growth chamber (Conviron model MTPS120) set to ambient CO_2 with a 22°C, 9 hour duration day and a 16°C, 15 hour duration night. Day time irradiance was set at 200 $\mu molm^{-2}s^{-1}$. After germination and the formation of the cotyledons, plants were transferred to standard seed trays divided into 24 cells (dimensions 50x48x52mm), an individual plant being placed into each cell. Then the trays were covered with a propagator for an initial two weeks, following which the propagator was removed and the plants grown to maturity.

2.4- Extraction of nucleic acids and cDNA synthesis

2.4.1- Tissue collection

For nucleic acid extraction, tissue was collected from an individual leaf from each relevant plant. Young expanding leaves were selected and excised. Barley leaf tissue was collected at Zadoks stage 12.2. For barley samples collected for RNA extraction particular care was taken to ensure that the base of the leaf, located within the protection of the leaf sheath, was sampled. This was due to the fact that stomatal lineage progression primarily occurs at the base (Liu et al., 2009) and a rice homologue of EPF2 had previously been identified as been expressed in the early stages of leaf development (van Campen et al., 2016). Once excised the leaf samples were placed into individual 1.5ml Eppendorf tubes and frozen in liquid nitrogen. The collected samples were stored at -80°C until such time as they could be processed (circa 1 week). For each sample the collected tissue was ground in liquid nitrogen with a pre-chilled micropestle until it was reduced to a fine powder prior to DNA (section 2.4.2) or RNA (section 2.4.3) extraction.

2.4.2- DNA extraction

In order to extract DNA 750µl of DNA extraction buffer (100mM tris-HCl pH8, 50mM EDTA pH8, 500mM NaCl, 10mM β-mrecaptoethanol) was added to the Eppendorf tube containing powdered tissue and the contents vortexed for 30 seconds. 50µl of 20% (w/v) sodium dodecyl sulphate (SDS) was then added and the sample incubated at 65°C for 10 minutes, with the tube contents being regularly mixed, again by inversion. 250µl of chilled, 5M potassium acetate pH4.8 was subsequently added, the tube mixed by inversion and the sample then incubated on ice for 20 minutes. The sample was then spun down in a microcentrifuge (12,000 rpm, 20 minutes) and the supernatant transferred to a second tube containing 0.6 vol of isopropanol. Following sufficient mixing by inversion the sample was incubated overnight at -20°C. The DNA was then pelleted using a microcentrifuge

(12,000 rpm, 10 minutes) and the supernatant carefully decanted. The DNA pellet was washed twice with 70% (v/v) ethanol with further centrifugation (12,000 rpm, 10 minutes) followed by the removal of the ethanol utilising a pipette. Any remaining fluid was removed by evaporation under a vacuum and the pellet was resuspended in sterile, deionised water.

2.4.3- RNA extraction and cDNA synthesis

RNA was extracted from the ground tissue using the Spectrum Plant total RNA kit (Sigma-Aldrich) in accordance with manufacturer's instructions. Any DNA contamination was removed from the eluted RNA using the Ambion DNA-*free*™ DNA removal kit (Thermo Fisher Scientific). The purified RNA was then used to produce cDNA using Maxima H minus Reverse Transcriptase (Thermo Fisher Scientific), again in accordance with manufacturer's instructions. RNA was stored at -80°C and cDNA was stored at -20°C for short term use and at -80°C for long term storage.

2.5 PCR

PCR amplification was used in order to genotype plants, carry out expression analysis and in generating construct inserts. 2X Biomix™ Red Taq polymerase reaction mix (Bioline) was used for both genotyping and expression analysis. Each individual PCR reaction typically consisted of the following components:

5µl Biomix™ Red

2µl Primer F (0.5µM)

2µl Primer R (0.5µM)

1µl Template (DNA, plasmid or cDNA)

Thermal cycling commenced with an initialisation step of 95°C for 5 minutes. 30-40 cycles (dependent on template concentration) were then carried out to amplify the

specified target. Each cycle consisted of a denaturation step of 95°C for 15 seconds, followed by an annealing step of 57-63°C (dependent upon primers used) for 30 seconds which was in turn followed with an elongation step of 30-90 seconds (dependent upon product length) at 72°C. Once cycling was complete a final extension step at 72°C for 5 minutes was applied.

Construct inserts were amplified using KOD polymerase (Novagen) in accordance with manufacturer's instructions.

2.6 Agarose gel electrophoresis

DNA fragments were separated using agarose gel electrophoresis. 50mg of agarose was added to 1X TAE buffer in a 250ml conical flask. The 1X TAE buffer was prepared from 50X stock solution (2M Tris base ,1M glacial acetic acid, 50mM EDTA pH8). The flask contents were heated in a microwave for 75 seconds to dissolve the agarose. The flask was then left to cool to a temperature at which it could be held but the contents still be in a molten state. 5µl of ethidium bromide (10mg/ml) was added and the conical flask swirled to mix. The contents of the flask was then poured into a gel tank, with combs inserted to form the wells. The agarose gel was left to set for at least 30 minutes. Once set the gel was transferred into an electrophoresis cell (BioRad) and submerged in 1XTAE running buffer. The combs were removed and the wells loaded. Hyperladder1 (Bioline) was used to aid fragment size determination. Biomix Red prepared PCR products were loaded directly into the wells (the reaction mix is of sufficient density to sink to the bottom of the well) whilst other DNA products were mixed with 6X bromophenol blue loading dye (4g sucrose, 25mg bromophenol blue, dH_2O to 10ml) prior to being loaded into wells. The gels were run at 100V for 30 minutes and imaged on a UVitech transilluminator with attached digital camera.

2.7- Phenotyping

2.7.1- Creating dental resin impressions

In order to screen large numbers of barley and *Arabidopsis* transformants and to confirm phenotype presence prior to subsequent experiments where leaf removal was undesirable, a relatively high throughput, non-destructive phenotyping method was utilised. This involved applying dental resin (Coltene Whaledent) to the abaxial surface of fully expanded, still attached leaves. In the case of Arabidopsis the resin was applied to the whole leaf surface whilst in barley it was applied to the full width of a 3-5cm strip midway along the proximodistal axis of the leaf. The resin, once it had set and been peeled away from the leaf tissue, provided an impression of the leaf epidermis. A coat of clear nail varnish was applied to these impressions, allowed to dry for 3-4 minutes and then transferred to a microscope slide using clear adhesive tape. Barley impressions were placed on the microscope slide in such a manner that the stomatal files ran parallel to the microscope slide, aiding counting (see section 2.7.4.2).

2.7.2- Leaf clearing

More detailed analysis of barley epidermal patterning was carried out on cleared leaves. At Zadoks stage 1.2 the second leaf was excised and a 3-5cm strip midway along the proximodistal axis of the leaf was cut out. These leaf samples were then submerged in Clarke's solution (a 3:1 ratio of ethanol to glacial acetic acid, also referred to as Carnoy's 1 solution). Following 1 hour of vacuum infiltration the samples were left in Clarke's solution for 24 hours for fixation. Once fixed the samples were transferred into 100% ethanol for long term storage at 4^{o}C (circa 2 weeks). Prior to imaging the leaf samples were cleared in 50% bleach solution overnight. The midrib of each sample was excised and the remaining leaf sections mounted in deionised water on microscope slides for imaging.

2.7.3- Microscopy

The microscope slides produced by methods 2.7.1 and 2.7.2 were imaged on an Olympus BX51 microscope utilising the differential interference contrast functionality.

2.7.4- Analysing stomata

2.7.4.1- Arabidopsis thaliana

Stomatal counts in *Arabidopsis* were taken from the widest point of the abaxial surface of the leaf, avoiding the midrib and the edges of the leaf. The stomatal density of three leaves each from five plants was counted for each genotype. 5 fields of view (FOV) were counted per leaf and averaged to provide plant stomatal density averages.

2.7.4.2- Hordeum vulgare

Stomatal and arrested precursor counts in barley were taken from the abaxial surface of the leaf, avoiding the midrib and the edges of the leaf. The FOV was positioned such that the uppermost stomatal file aligned with the top edge of the FOV. The stomatal and arrested precursor density of one leaf (five FOV averaged) from 4-5 plants was counted for each genotype per treatment. Only one leaf was used as stomatal density differs on a leaf by leaf basis with stomatal density increasing as you go up the plant. Unless otherwise stated the leaf utilised for phenotyping the barley was the first leaf formed (Zadoks stage 11) with the leaves for clearing being excised (or the dental resin impressions being produced) when the plants developed beyond Zadoks stage 12.

2.7.4.3- Stomatal size

Guard cell length in barley was measured using ImageJ. 30 stomata were measured on one cleared leaf apiece from at least four different individual plants per genotype. Stomatal size (S) was then calculated as the guard cell length (L) multiplied by the width of the guard cell pair, which was estimated as being L/8 (Franks and Beerling, 2009).

2.7.4.4- Stomatal index

Stomatal index (SI) of a given FOV was calculated utilising the following equation:

$$\text{Stomatal index } (\%) = \frac{\text{Number of stomata}}{\text{Number of stomata} + \text{Number of non} - \text{stomatal epidermal cells}} * 100$$

2.8- Gas Exchange

2.8.1- Introduction

The gas exchange characteristics and stomatal conductance of control and transgenic barley plants were measured using an infra-red gas exchange analyser (IRGA) system, a Licor li6400 with a li6400-40 leaf chamber fluorimeter sensor head attached (Licor, Licoln, NE). For each reading a single, fully expanded and still attached leaf was clamped into the chamber (see section 2.8.2). For each experiment the leaf selected was standardised in terms of age and position to ensure a fair test.

With a li6400 CO_2 is scrubbed from the external air and reintroduced from a pure CO_2 cartridge (12g CO_2 cartridge, LISS) through an injector which allows for fine control of CO_2 levels within the chamber (to within 1 µmol mol^{-1}). PAR levels are altered by modifying the light intensity of light emitting diodes contained within the leaf chamber whilst temperature within the chamber is monitored with an inbuilt thermocouple and maintained at the desired temperature using inbuilt coolers.

For the experiments outlined in this section humidity within the chamber was maintained between 60% and 75% using a self-indicating desiccant (Drierite, Hammond

Drierite Company). Flow rate was set at 300 µmol s^{-1}. PAR, temperature and CO_2 levels were altered according to experimental design (see sections 2.8.4, 2.8.5 and 2.8.6).

2.8.2- Leaf chamber alignment

The default calculations of photosynthetic parameters assume that the leaf chamber, which has a circular cross-sectional area of $2cm^2$, is entirely filled by the clamped leaf but this is rarely the case with barley leaves. It is therefore necessary to measure the total area of the leaf contained within the chamber in order to correct outputs. This was achieved by measuring the width of the leaf at the position on the leaf to which the leaf chamber was to be attached then clamping the leaf so that the midrib directly bisected the circular area of the chamber. The leaf area could then be calculated and the values inputted into the li6400-generated excel results file in order to correct obtained values.

2.8.3- Ambient condition determination

The first requirement for gas exchange experimental design is to measure ambient conditions to ensure later experiments, in particular steady state measurements (section 2.8.4), accurately reflect the growth conditions in which the sample plants were grown. Ambient CO_2 in the greenhouse was measured at between 470ppm and 485ppm (elevated over the global average largely due to its location in the centre of a large city) so CO_2 was set to 500ppm for steady state gas exchange, light curves and the initial acclimation for A-Ci curves. Due to the measurements being made early in the year (March-April 2016) the plants were mostly grown under the supplementary lighting outlined in section 2.3.1. As a consequence of this light levels were around 210-260 µmol m^{-2} s^{-1} at plant canopy height. PAR intensity for the steady state measurements was consequently set at 200 µmol m^{-2} s^{-1}.

2.8.4- Steady state measurements

Steady state measurements were taken to determine gas exchange parameters and stomatal conductance in ambient conditions. The 6th leaf of the primary tiller (Zadoks stage 16) was used for these readings. CO_2 levels were set at 500ppm, PAR set at 200µmol m^{-2} s^{-1} and leaf temperature at 20°C. Plants were left to acclimate to leaf chamber conditions for 35-45 minutes. Once gas exchange was stabilised readings were taken every 20 seconds over 5 minutes and then averaged to provide reported results. The reference and sample IRGAs were matched at least every 15 minutes.

2.8.5- Light curves

Light curves were generated using the flag leaf of the primary tiller (Zadoks stage 39). The CO_2 level was set at 500ppm, PAR initially set at 1900µmol m^{-2} s^{-1} and leaf temperature at 23°C. Plants were left to acclimate to leaf chamber conditions for 45 minutes. Once gas exchange readings stabilised the initial reading was taken. Readings were taken at 1900, 1800, 1700, 1600, 1200, 800, 600, 400, 200, 100, 50 and 0µmol m^{-2} s^{-1}. After each reading PAR intensity was dropped to the next light level and left 2-4 minutes until pre-programmed stability criteria were met and the next reading taken. The reference and sample IRGAs were matched at least every 15 minutes during acclimation and after every reading during curve acquisition.

2.8.6 - A-Ci curves

A-Ci curves were also generated using the flag leaf of the primary tiller (Zadoks stage 39). The CO_2 level was initially set at 500ppm, PAR set at 1900µmol m^{-2} s^{-1} and leaf temperature at 23°C. Plants were left to acclimate to leaf chamber conditions for 45 minutes. The A-Ci curve was collected in two halves. For the first half readings were taken

at 500, 300, 200,100 and 50ppm before being returned to 500ppm. 2-3 minutes were left between readings until preprogramed stability criteria were met and the next reading taken. After being left to reacclimate at 500ppm for 15 minutes the second half of the A-Ci curve was collected. Readings were taken at 500, 800, 1000, 1200, 1400, 1600, 1800 and 2000ppm. 4-5 minutes were left between readings until preprogramed stability criteria were met and the next reading taken. The reference and sample IRGAs were matched at least every 15 minutes during acclimation and after every reading during curve acquisition.

2.9 - Zadoks growth scale

The Zadoks scale is a widely used cereal development scale and was used to as a means to standardise both the initiation of the withheld water experiment (section 2.12) and the gas exchange analysis (section 2.8). It is presented here for ease of reference.

Zadok Scale	**Description**
	Germination
00	Dry Seed
01	Start of imbibition
03	Imbibition complete
05	Radicle emerged from seed
07	Coleoptile emerged from seed
09	Leaf just at coleoptile tip
	Seedling Growth Count leaves on main stem only. Fully emerged = ligule visible.
10	First leaf through coleoptile
11	First leaf fully emerged
12	Two leaves fully emerged
13	Three leaves fully emerged
14	Four leaves fully emerged
15	Five leaves fully emerged
16	Six leaves fully emerged
17	Seven leaves fully emerged
18	Eight leaves fully emerged
19	Nine or more leaves fully emerged
	Tillering Count visible tillers on main stem.
20	Main stem only
21	Main stem and one tiller
22	Main stem and two tillers
23	Main stem and three tillers

24	Main stem and four tillers
25	Main stem and five tillers
26	Main stem and six tillers
27	Main stem and seven tillers
28	Main stem and eight tillers
29	Main stem and nine or more tillers
	Stem elongation
30	Pseudostem (youngest leaf sheath erection)
31	First node detectable
32	Second node detectable
33	Third node detectable
34	Fouth node detectable
35	Fifth node detectable
36	Sixth node detectable
37	Flag leaf just visible
39	Flag leaf ligule just visible
	Booting
41	Flag leaf sheath extending
43	Boots just visible swollen
45	Boots swollen
47	Flag leaf sheath opening
49	First awns visible
	Ear emergence from boot
51	Tip of ear just visible
53	Ear quarter emerged
55	Ear half emerged
57	Ear three quarters emerged
59	Ear emergence complete
	Anthesis
61	Beginning of anthesis (few anthers at middle of ear)
65	Anthesis half-way (anthers occurring half way to tip and base of ear)
69	Anthesis complete
	Milk development
71	Kernel water ripe (no starch)
73	Early milk
75	Medium milk
77	Late milk
	Dough development
83	Early dough
85	Soft dough
87	Hard dough
	Ripening
91	Grain hard, difficult to divide
92	Grain hard, not dented by thumbnail
93	Grain loosening in daytime
94	Over-ripe straw dead and collapsing
95	Seed dormant
96	Viable seed giving 50% germination

97	Seed not dormant
98	Secondary dormancy induced
99	Secondary dormancy lost

Figure 2.2- Table showing all stages in the Zadoks scale. Seedling growth can be subdivided by rating the emergence of the youngest leaf in tenths e.g. Zadoks scale 14.4 means 4 leaves are fully emerged whist the 5th is 40% emerged. Fully emerged means that the ligule is visible. Stage descriptions retrieved from the Department of Agriculture and Food, Government of Western Australia website (https://www.agric.wa.gov.au/grains/zadoks-growth-scale?page=0%2C0)

2.10- Harvesting

2.10.1- Introduction

Growth and yield under 60% and 25% watering regimes was assessed at the end of the lifecycle of control and transgenic barley plants. The plants used were the same individuals upon which gas exchange was carried out (section 2.8).

2.10.2 – Vegetative tissue

For each plant the total number of tillers and leaves were counted. The primary tiller height was measured from the root-shoot interface to the apex of the rachis. The number of spike-bearing tillers and prematurely senescing tillers was recorded. Ears were removed and the rest of the above ground tissue was sealed into an A4 manilla envelope, dried down at 80^{o}C for 2 days and weighed to obtain the dry weight of the shoots and leaves.

2.10.3- Assessing yield

The grains were counted and weighed per ear and the sum of the number and weight of grain on all the ears of individual plants recorded as the total grain number and the yield respectively. The average weight of individual seeds for each plant was then calculated as was the harvest index (the ratio of grain yield to total above ground biomass).

2.10.4- Δ C analysis

ΔC analysis correlates with long term WUE (Farqhuar et al., 1982; Farqhuar and Richards 1984) and was used here as an alternative measure of WUE to the intrinsic and instantaneous WUE values generated using infra-red gas exchange analysis (see sections 1.3 and 2.8.4). Flag leaves were excised from the plants analysed by gas exchange and dried at 80°C for 2 days. The samples were then ground finely and 3-4mg of each sample was sealed into individual foil cups. These were combusted at 1800°C, the components separated by gas chromatography and the isotopes of carbon ionised and separated by mass using an ANCA GSL 20-20 mass spectrometer (Sercon PDZ Europa).

2.11- Growth assessment

The time taken to germinate and the germination success rate were assessed with successful germination being recorded when the individual plant reached Zadoks stage 07 (N=40). Once the third leaf was fully expanded growth measurements were carried out every 3 days. This included counting the total number of fully expanded and expanding leaves as well as the total number of tillers and the height of the primary tiller.

2.12- Assessing drought tolerance

2.12.1- Introduction

In order to assess drought tolerance control and transgenic barley plants were grown until Zadoks stage 21. Half the plants of each line were then maintained at the initial watering level (60% soil water content) whilst water was withheld from the other half. The experiment continued for 19 days until the fluorescence levels measured reached 0 for all water withheld plants (see section 2.12.3). Drought tolerance was assessed by both monitoring the rate at which soil water was utilised to test for drought avoidance (see

section 2.12.2) and by monitoring plant stress using the light-adapted quantum yield of photosystem II (QY or Fv'/Fm') as a proxy (see section 2.12.3).

2.12.2- Measuring water consumption

Following the onset of the drought treatment the pots were weighed every day and used to calculate the percentage of initial soil water content remaining. Well-watered controls were maintained at 100% of the initial soil water content value (60% SWC) by daily watering.

2.12.3- Assessing drought stress

QY readings were taken each day from the most recent, fully expanded leaf of the primary tiller at day 1 of the drought treatment. The same leaf was monitored throughout the experiment. Readings were taken using a FluorPen FP100 (Photon Systems Instruments).

2.12.4- Relative water content (RWC)

Relative water content was measured on day 6 of the drought treatment. The second most recent, fully expanded leaf of the primary tiller was excised and a section 5cm long was cut out of the centre of the leaf. This was weighed to obtain the fresh weight. Samples were then placed into 20ml sample tubes containing 5ml of distilled water and left to hydrate overnight. The samples were then weighed to obtain the turgid weight of the leaf sections. Finally, the samples were dried at 80°C for two days and weighed to obtain the dry weight. RWC was then calculated using the equation:

$$\text{Relative Water Content}(\%) = \frac{\text{Fresh Weight} - \text{Dry Weight}}{\text{Turgid Weight} - \text{Dry Weight}} * 100$$

2.13- Graphing and data analysis

All data were graphed and statistically analysed using GraphPad Prism 7 software. Variation was considered significant when $p<0.05$.

2.14- Confocal microscopy

For the confocal microscopy samples were prepared as described in Wuyts et al., 2010 and viewed on an Olympus FV1000 confocal microscope using the 20x UPlan S-Apo N.A. 0.75 objective, 543nm laser, 555-655nm emission and Fluorview software. This work was carried out in collaboration with Dr Chris Hepworth.

2.15- Bioinformatics

Barley genomic and protein sequences used to produce primers and used in the alignment (section 3.4) respectively were obtained from Gramene (www.gramene.org) whilst *Arabidopsis thaliana* sequences were retrieved from TAIR (www.arabidopsis.org). The *HvEPFL1* gene is annotated as MLOC_67484.1 on Gramene. The putative HvEPFL1 protein sequence was identified using FGENESH (www.softberry.com).The sequence alignment between protein sequences and the subsequently generated phylogenetic tree were produced using MEGA7.

2.16- Primer design

Primers were designed using the PrimerQuest and OligoAnalyser tools supplied by Integrated

DNA Technologies (www.idtdna.com).

2.17- Sequencing

All produced constructs were sequenced to confirm that insert orientation and DNA sequence were correct. This service was carried out by the Core Genomic Facility (Faculty of Medicine, Dentistry and Health, University of Sheffield) using an M13 region reverse primer (CAGGAAACAGCTATGACC).

2.18- Copy number analysis

Single insert transgenic barley lines were identified by real time quantitative PCR carried out by iDNA Genetics (Norwich, UK) from leaf tissue samples collected from T1 transgenic lines (4 individuals sampled per line).

2.19- Stomatal patterning definitions and measurement

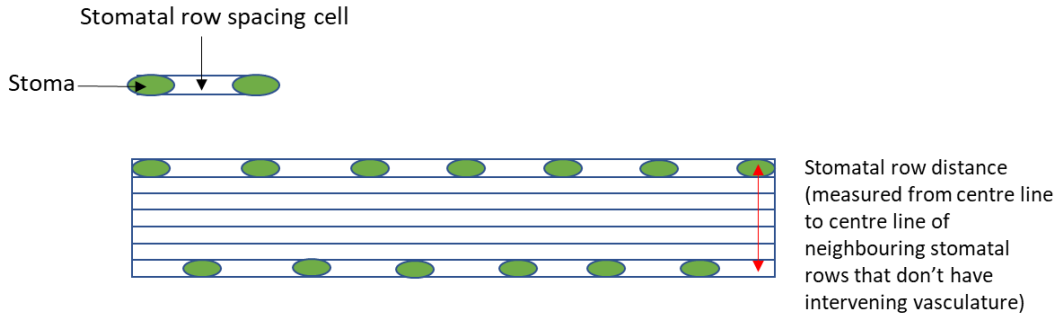

Figure 2.3- Illustrative diagram of the epidermis of *Hordeum vulgare*.

The length of spacing cells was measured (only when there was a single spacing cell present between consecutive stomata) in both transgenic and control lines and the results recorded in figure 3.21. The proportion of the spaces between consecutive stomata in rows that consisted of only a single intervening spacing cell was determined and recorded in figure 3.23. Finally, the distance between stomatal rows was determined as illustrated in figure 2.3 and recorded in figure 3.22.

Chapter 3- The effect of overexpressing *HVEPFL1* on epidermal development in *Hordeum vulgare*

3.1- Introduction

This chapter focuses on the effect overexpressing HvEPFL1 has on stomatal development. This includes analysis of the sequence conservation between and projected evolutionary relation of HvEPFL1 and the Arabidopsis thaliana EPFLs that have been demonstrated to influence stomatal development as reviewed in chapter 1. The changes in stomatal characteristics as a consequence of *HvEPFL1* overexpression in *Hordeum vulgare* are described and quantified, and the effects of *HvEPFL1* expression in Arabidopsis thaliana analysed. Together this data presents an insight into the signalling pathway governing stomatal development in *Hordeum vulgare* and provides additional reinforcement of the concept that the regulation pathways controlling stomatal patterning are conserved throughout the land plants (Liu et al., 2009; Chater et al., 2016; Caine et al.,2016; Raissig et al; 2016. Discussed in depth in sections 1.8 and 3.2).

3.2- The regulation of stomatal development in grasses

Stomatal patterning in grasses is a significant departure from the ancestral, dicot like stomatal pattern. In grasses stomata are organised into files of cells running parallel to the leaf veins (Serna, 2011; Raissig et al., 2016). Moreover, the stomata themselves differ in structure, with the guard cells possessing a dumbbell like shape rather than the kidney shape of Arabidopsis guard cells (Sack, 1994). These unique stomata are able to respond significantly faster to environmental cues than the ancestral state and so prove to be more efficient (Franks and Farqhuar, 2007; Chen et al., 2017). Grass stomata possess two subsidiary cells of specialised function, one on each side of the stomatal complex (Stebbins

and Jain, 1960; Stebbins and Shah, 1960). They are formed when grass GMCs induce adjoining epidermal cells in neighbouring cell files to develop subsidiary mother cell (SMC) fate and divide asymmetrically such that the smaller daughter cell of the SMC, the subsidiary cell, is adjacent to the GMC (Stebbins and Jain, 1960; Cartwright et al; 2009). The GMC then divides symmetrically to produce guard cells, forming the complete stomatal complex (Stebbins and Jain, 1960; Sack, 1994).

Unlike in Arabidopsis where stomatal development occurs at points scattered across the leaf, grasses demonstrate a base to tip gradient of stomatal differentiation with different zones of the developing leaf possessing stomatal lineage cells at different stages (Stebbins and Jain, 1960; Liu et al., 2009; Vaten and Bergmann, 2012). At the base stomatal rows are specified followed by asymmetric division within the stomatal rows to produce GMCs (Stebbins and Jain, 1960; Liu et al., 2009; Vaten and Bergmann, 2012). Further up the developing leaf subsidiary cells are seen to form whilst nearer the tip differentiated stomata are found (Stebbins and Jain, 1960; Liu et al., 2009; Vaten and Bergmann, 2012). The signalling involved in these asymmetric divisions to form subsidiary cells is one of the limited number of aspects of stomatal development regulation that is relatively well understood in grasses. Two LRR receptor like proteins called PANGLOSS 1 (PAN1) and PAN2 have been identified in maize which, in response to an unknown signalling peptide released by GMCs, induce pre-mitotic polarity and subsequent asymmetric division in SMCs (Cartwright et al., 2009, Zhang et al., 2012). Two Rho family GTPases (ROPs), ROP2 and ROP9, act in conjunction with PAN1 and PAN2 to induce SMC asymmetric divisions (Humphries et al., 2011). The polar localisation of PAN1 and PAN2 requires the SCAR/WAVE complex which activates the actin-nucleating ARP2/3 complex that likely means the formation of actin structures is responsible for PAN polarisation and subsequent asymmetric division (Facette et al., 2015). PAN1 and PAN2 have also been identified as

possessing broader roles in plant development, such as inducing cortical actin accumulation and cell expansion in diverse cell types (Sutimantanapi et al., 2014). Another interesting point to keep in mind when discussing asymmetric divisions in the stomatal lineage cells of grasses is the fact that grasses lack BASL and POLAR orthologues, as these arose after the divergence of monocots and dicots (see figure 3.1) (Vaten and Bergmann, 2012). This consequently means that induction of asymmetric divisions in the stomatal lineage of grasses must utilise a distinct mechanism (Vaten and Bergmann, 2012).

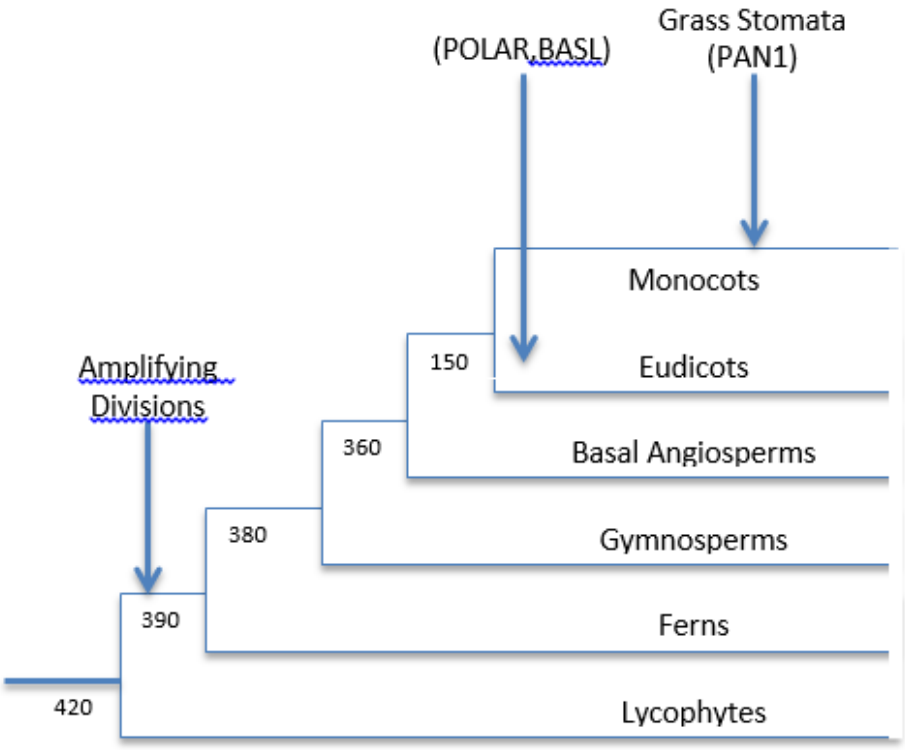

Figure 3.1- Divergence of major land plant lineages with the appearance of key factors in the asymmetric divisions of stomatal development labelled. Numbers are multiples of millions of years whilst brackets indicate that appearance has been predicted. Adapted from Vaten and Bergmann, 2012.

Our current knowledge on the specifics of the components regulating stomatal lineage progression in grasses is relatively limited, restricted to the functions of Orthologues of the bHLH transcription factors that control stomatal lineage progression in *Arabidopsis thaliana* (Liu et al., 2009; Raissig et al., 2016).

Liu et al., 2009 extensively profiled the orthologues of *SPCH*, *MUTE* and *FAMA* in rice (*Oryza sativa*) and the maize (*Zea mays*) *MUTE* orthologue. Maize and rice both possess one *FAMA* homologue each, the bHLH domains of which are highly similar to that of *Arabidopsis thaliana FAMA* (Liu et al., 2009). *OsFAMA* is expressed in the sheath and leaf blade expansion zones where the later stages of stomatal development occur in grasses i.e. consistent with *OsFAMA* having a role similar to *AtFAMA (*Liu et al., 2009). The *osfama-1* mutant sees guard cells forming in a box shape resembling the GMC rather than the canonical dumbbell shape suggesting *OsFAMA* is required for guard cell differentiation like it is in *Arabidopsis thaliana* (Ohashi-Ito and Bergmann, 2006; Liu et al., 2009). The extra symmetrical guard mother cell divisions seen in *Arabidopsis fama* mutants are absent in osfama-1 mutants however (Ohashi-Ito and Bergmann, 2006; Liu et al., 2009).

Overexpressing *OsFAMA* in *Arabidopsis* results in the proliferation of unpaired guard cells, just like *AtFAMA* overexpression, whilst complementation of the Arabidopsis *fama* mutant with *OsFAMA* results in phenotypic rescue (Ohashi-Ito and Bergmann, 2006; Liu et al., 2009). All in all, *FAMA* function appears to be highly conserved between grasses and *Arabidopsis*.

There are two orthologues of *SPCH* in maize and rice the expression patterns of which could not be determined (Liu et al., 2009). *OsSPCH2* is most similar to AtSPCH and the *osspch2-1* mutant does show a reduction in stomatal density consistent with a role in early stomatal development in rice (Liu et al., 2009). Overexpressing *OsSPCH2* in *Arabidopsis* does increase pavement cells divisions, however *OsSPCH2* cannot complement the

Arabidopsis spch mutant, suggesting a degree of diversification in *SPCH* activity between grasses and *Arabidopsis* (Liu et al., 2009).

OsMUTE is expressed earlier than *OsFAMA* suggesting that it has an earlier role in stomatal development consistent with lineage progression in *Arabidopsis* (Liu et al., 2009; Han and Torii, 2016). Unlike *Arabidopsis MUTE OsMUTE* expression is broad rather than restricted to the meristemoids, more closely resembling early *Arabidopsis SPCH* expression (Gray, 2007; Liu et al., 2009; Davies and Bergmann, 2014). It is also expressed earlier on in the formation of stomatal files than one would expect if it purely functioned in the same role as *Arabidopsis MUTE* (Liu et al., 2009). Overexpressing *OsMUTE* and *ZmMUTE* in *Arabidopsis* produces a phenotype resembling the *Arabidopsis MUTE* overexpression phenotype and *OsMUTE* partially rescues the Arabidopsis mute mutant (Pillitteri et al., 2007, Pillitteri et al., 2008; Liu et al., 2009). The *Brachypodium distachyon* otholog of *Arabidopsis* MUTE is necessary and sufficient to induce subsidiary cell formation (Raissig et al., 2017).

The main conclusion that can be drawn from Liu et al., 2009 is that whilst the same bHLH factors are involved in controlling stomatal lineage progression their exact roles have somewhat diverged with both *MUTE* and *SPCH* showing distinct differences in terms of expression pattern (*MUTE*) and function (both). One notable change is that OsMUTE and ZmMUTE both contain multiple MAPK cascade phosphorylation sites, more similar to *Arabidopsis* SPCH than Arabidopsis MUTE, which has not been identified as a target for phosphorylation in stomatal development (Lampard et al., 2008; Liu et al., 2009). Whether the differences in roles between grasses and *Arabidopsis* are due to such differences in protein composition or whether it is due to the distinct differences in the manner in which grass leaves develop is presently unclear (Liu et al., 2009).

More recent work in *Brachypodium distachyon* has demonstrated that the role played by *SPCH* and in initialling stomatal development is conserved between grasses and

Arabidopsis (Raissig et al., 2016). Like maize and rice*, Brachypodium distachyon* has two homologues of *SPCH* (Liu et al., 2009; Raissig et al., 2016). The *bdspch1* and *bdspch2* mutants show weak and strong reductions in stomatal density whilst in the *bdspch1 bdspch2* double mutant stomatal development is entirely abolished with no stomatal cells files initiating (Raissig et al., 2016). This stomataless phenotype is consistent with the phenotype of the *Arabidopsis spch* mutant, suggesting that the role of *SPCH* in initiating entry into the stomatal lineage is conserved (MacAlister et al., 2007, Raissig et al., 2016). Overexpression of *BdSPCH2* caused hair cell precursors to transition into stomata, resulting in ectopic stomatal cell fate (Raissig et al., 2016). This suggests that, unlike *SPCH* in *Arabidopsis*, *BdSPCH2* can act to determine cell fate, in a manner more akin to Arabidopsis *MUTE* (Raissig et al., 2016).

The same body of work also analysed a *Brachypodium distachyon* mutant called *stomataless* (stl) which completely lacks stomata like the *bdspch1 bdspch2* double mutant (Raissig et al., 2016). The mutation was tracked to the *BdICE1* gene, a homologue of *Arabidopsis ICE1/SCRM*, a known component of stomatal lineage progression (Kanoaka et al., 2008; Raissig et al., 2016). Like *SCRM*, *BdICE1* has a duplicated variant called *BdSCRM2*, although the *Arabidopsis* and *Brachypodium SCRM*s underwent duplication after the divergence of dicots, i.e. are products of distinct duplication events (Raissig et al., 2016). Unlike *Arabidopsis SCRM* and *SCRM2*, *BdICE1* and *BdSCRM2* are not functionally redundant (Kanoaka et al., 2008; Raissig et al., 2016). *BdSCRM2* is required only for late stage stomatal differentiation with guard cells failing to mature correctly in *bdscrm2* mutants (Raissig et al., 2016).

Raissig et al., 2016 shows that orthologues of the master regulators of stomatal lineage initiation in Arabidopsis are responsible for stomatal initiation in grasses, despite the significant change in the epidermal pattern of stomata in grasses, with only some divergence in the function and regulation of these bHLH transcription factors.

This conservation of the roles seen in the *SCRM* and *SPCH* orthologues of *Brachypodium distachyon* and *MUTE* and *FAMA* in rice and maize suggests that components of the *EPF/TMM/ERECTA* signalling pathway are likely to have conserved roles as well.

3.3- Methods summary

Prior to the author's involvement in the project *HvEPFL1* and *HvEPFL2* overexpression constructs were generated by Dr Lee Hunt and transformed into barley by the James Hutton Institute as described in chapter 2. The T1 seed of the resultant transgenic lines were germinated in 24 cell seed trays in a Conviron BDW growth chamber with conditions set to a 23°C, 12-hour day/ 16°C 12-hour night cycle with day time light intensity of 500µmol$m^{-2}s^{-1}$. Once the plants had grown to Zadox stage 1.2 dental resin impressions were made of the first, fully expanded leaf and these impressions were analysed to screen for stomatal density phenotypes. Plants were also genotyped and segregants were discarded.

Once transgenic lines with significantly reduced stomatal density were identified a subset were grown under greenhouse conditions (see section 2.3.1) and analysed to ascertain the copy number of inserts in order to guide generation of single copy, homozygous lines.

More detailed analysis of the stomatal patterning and characteristics was carried out on cleared leaves of T3 individuals using images obtained by DIC microscopy.

In the meantime, three Arabidopsis constructs, 35S::HvEPFL1, 35S::HvEPFL2 and pEPF2::HvEPFL1 were created and introduced into the Col-0 (35S constructs) and *epf2*(pEPF2) backgrounds.

3.4- Bioinformatic analysis of HvEPFL1

Following the sequencing of the barley genome 11 potential orthologues of Arabidopsis EPFL signalling peptides were identified. Of these one in particular showed close sequence homology to the negative regulators of stomatal development in

Arabidopsis, EPF1 and EPF2, and was consequently designated HvEPFL1. Figure 3.2 shows the alignment of the predicted amino acid sequence of HvEPFL1 against the mature peptide sequences of both EPF1 and EPF2. There is significant conservation of residues in this region and it is particularly important to note the conservation of the cysteine residues that have previously been reported as being vital for EPF function (Okhi et al., 2011). Not only does HvEPFL1 retain the 6 cysteines in the conserved positions found in all Arabidopsis EPFLs (marked by black arrows, figure 3.2) but it possesses the additional pair of cysteines found in EPF1 and EPF2 (marked by red arrows, figure 3.2), strongly suggesting that HvEPFL1 is likely to have a role in negatively regulating stomatal density, if function is conserved.

Figure 3.2- HvEPFL1 shows close protein sequence conservation to the *Arabidopsis Thaliana* negative regulators of stomatal density. Alignment of the protein sequence of HvEPFL1 against Arabidopsis EPF1 and EPF2. The putative mature signalling peptide sequences were used to generate the alignment. Black arrows mark cysteine residues conserved throughout the *Arabidopsis* EPFLs. Red arrows mark conserved cysteine residues unique to negative density regulators. The *Arabidopsis thaliana* protein sequences were retrieved from TAIR and the *Hordeum vulgare* sequence from Gramene. The alignment was generated with Multalin using default parameters.

That HvEPFL1 is a strong candidate for being a negative regulator of stomatal development is further supported by phylogenetic analysis based on the amino acid

sequences of HvEPFL1 and Arabidopsis EPFLs. HvEPFL1 groups with the negative regulators EPF1 and EPF2, not the CHALLAH or STOMAGEN groups which possess different roles in plant development as discussed in chapter 1.

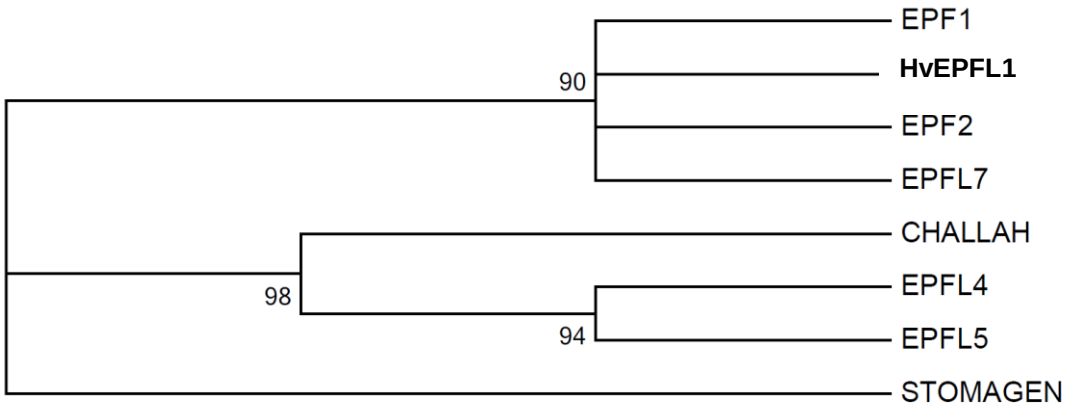

Figure 3.3- Phylogenetic analysis of the HvEPFL1 amino acid sequence groups it with known negative regulators of stomatal density. The amino acid sequence of the putative mature peptide of HvEPFL1 was aligned with the putative mature peptide sequences of the *Arabidopsis thaliana* negative regulators (EPF1, EPF2 and EPFL7), Challah group EPFLs (Challah, EPFL4 and EPFL5), and the positive regulator of stomatal density STOMAGEN, using MEGA7. The phylogenetic tree was generated using a maximum likelihood model. The numbers beneath the branches indicate bootstrap values. Branches with bootstrap values under 50%, i.e. poorly supported, were collapsed. Default MEGA7 values for model parameters were used when generating the tree with 1000 bootstrap replications run.

3.5 – Overexpression and mutant complementation using HvEPFL1 in *Arabidopsis thaliana*

3.5.1 – Introduction

In order to understand whether HvEPFL1 functions in a manner similar to those EPFs known to regulate stomatal development in the model plant *Arabidopsis thaliana*, it was first necessary to ascertain whether HvEPFL1 produced similar effects to those EPFs when introduced into the same genetic background in which those genes' functions were assayed.

To do this a construct was produced to ectopically overexpress *HvEPFL1* in Arabidopsis (schematic A, figure 3.4) and introduced into the Col-0 *Arabidopsis thaliana* ecotype as described in section 2.2.2. Two independent T2 lines were generated and their epidermal phenotype assessed (see section 3.5.2). The same process was carried out with a second putative barley EPFL orthologue, *HvEPFL2*.

To further assess the ability of *HvEPFL1* to play a role in regulating stomatal density in a manner similar to that of previously described EPFLs, a construct expressing *HvEPFL1* under the *Arabidopsis thaliana* native pEPF2 promoter was produced as described in section 2.2.2 and transformed into the Arabidopsis thaliana *epf2* mutant background. Owing to poor germination rates, high seedling mortality rates and very poor seed set, it was not possible to generate T2 lines. However, the results obtained from 3 independent T1 individuals have been pooled and reported in section 3.5.3 below which, whilst not ideal, provide some potential insight into *HvEPFL1* function.

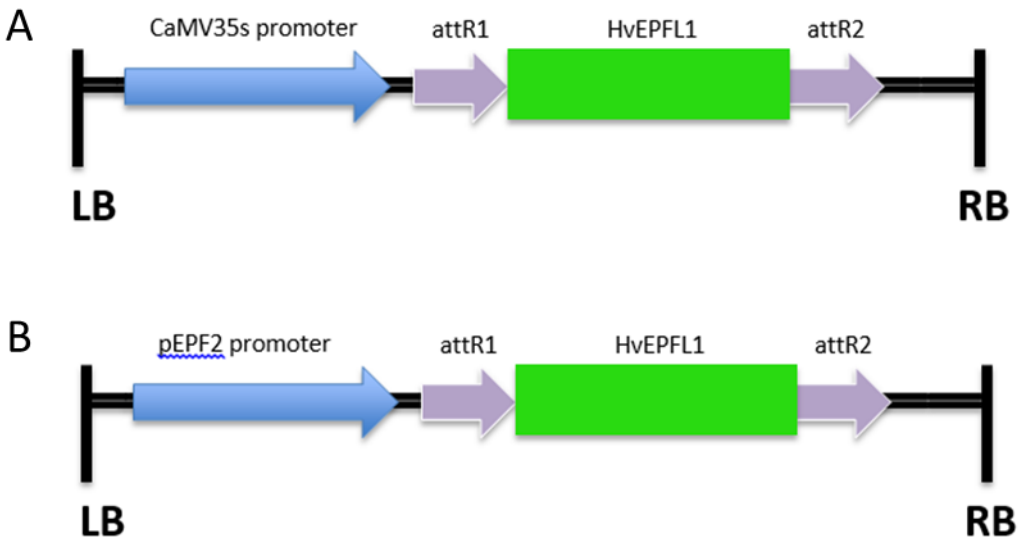

Figure 3.4- Schematic showing construct design for HvEPFL1 overexpression and complementation in an Arabidopsis thaliana background. (A) Construct for overexpressing *HvEPFL1* in Arabidopsis thaliana Col-0 ecotype. (B) Construct for complementation of the *epf2* mutant in Arabidopsis thaliana. Both constructs were produced using the cTAPi plasmid (Rohila et al., 2004). Blue arrows indicate promoters, lilac arrows represent the attR sites used for LR clonase recombination and the green box shows the location of the *HvEPFL1* gene. LB and RB label the left and right borders of the insert respectively.

3.5.2 – Ectopic expression of HvEPFL1 in Arabidopsis produces a stomatal phenotype consistent with that found in ectopic overexpression lines of native EPFLs involved in the negative regulation of stomatal density

When ectopically overexpressed both HvEPFL1 and HvEPFL2 caused a significant reduction in stomatal density compared to Col-0 controls (figure 3.5 A). This ranged from a reduction to 61.29% of mean wild type density in line *35s::HvEPFL1-A* to a reduction to 47.61% of mean wild type density in line *35s::HvEPFL1B*.

Similarly, stomatal index also significantly decreased in all lines investigated (Figure 3.5 B). Stomatal index fell between approximately a third and a half, from a mean of 21% in

Col-0 controls to means ranging from 12.1% in line *35s::HvEPFL1-A* to 14.0% in line *35s::HvEPFL2-B*. This drop in stomatal index occurred as a result of the significant drop in stomatal density as the density of epidermal pavement cells also dropping slightly, likely due to a reduction in amplifying divisions as a consequence of either the reduced number of stomatal lineage cells in total or as a consequence of meristemoid arrest (see figure 3.6 and discussion thereof below).

These findings are consistent with those seen when Arabidopsis EPFLs are overexpressed in their native background, wherein overexpressing *EPF1* reduces stomatal density and increases the prevalence of arrested stomatal precursors (Hara et al., 2007; Hara et al., 2009) whilst the EPF2 overexpressor also reduces stomatal density (Hunt and Gray, 2009; Hara et al., 2009). These findings therefore suggested that the two HvEPFLs are, like EPF1 and EPF2, negative regulators of stomatal density. Owing to a lack of expression data available for *HvEPFL2* a decision was taken at this point to focus on *HvEPFL1* for the subsequent work in both *Arabidopsis thaliana* and in barley.

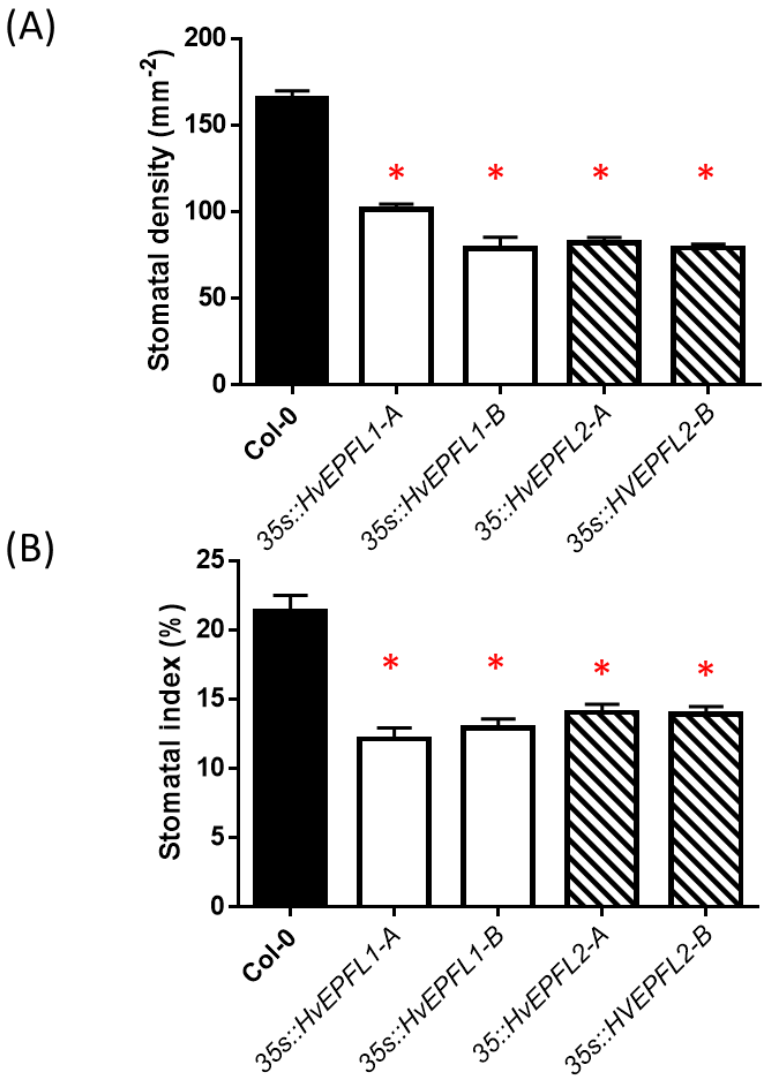

Figure 3.5- Overexpressing HvEPFL1 and HvEPFL2 in Arabidopsis thaliana significantly reduces stomatal density and stomatal index. (A) Comparison of the mean stomatal densities of HvEPFL1 and HvEPFL2 transgenic lines with Col-0 mean stomatal density. (B) Comparison of the mean stomatal index of HvEPFL1 and HvEPFL2 transgenic lines with Col-0 mean stomatal index. The stomatal densities and indices of two independent T2 transgenic lines reported for each construct. N=5. Error bars signify SE. Asterisk indicates significant reduction in the relevant stomatal trait compared to col-0 control values (Dunnett's multiple comparisons test after one-way ANOVA, $p<0.05$).

Further analysis of the epidermis of the HvEPFL1 ectopic overexpression lines revealed an interesting phenotype for further evaluating its effect in the context of the *Arabidopsis thaliana* EPFLs. As can be seen in figure 3.6, whilst stomatal density decreases there is an increased prevalence of small triangular cells consistent in morphology with meristemoids. The ectopic expression of the native *EPF1* gene leads to a similar phenotype of arrested meristemoids, which are not seen when Arabidopsis thaliana *EPF2* is ectopically expressed (Hara et al., 2007; Hunt and Gray., 2009; Hara et al., 2009).

This similarity between *EPF1* and *HvEPFL1* ectopic overexpression phenotypes in the Arabidopsis thaliana background suggested that the function of HvEPFL1 could be most similar to that of EPF1 i.e. a role primarily in the orientation of the asymmetric divisions in the lineage (Hara et al., 2007). This seems a reasonable hypothesis, given that the arrangement of the stomata in monocots requires only a single, correctly orientated asymmetric division to achieve the pattern within the file, namely two sequential stomata spaced apart by a single epidermal cell, with stomatal file identity having been specified in an earlier stage of development at the base of the leaf (Stebbins and Jain, 1960; Liu et al., 2009; Vaten and Bergmann, 2012). The absence of amplifying divisions and secondary acquisition of MMC fate in grasses, which are regulated by EPF2 in *Arabidopsis thaliana,* would also suggest that HvEPFL function in barley is most likely to be similar to EPF1 (Hara et al., 2009; Han and Torii, 2016).

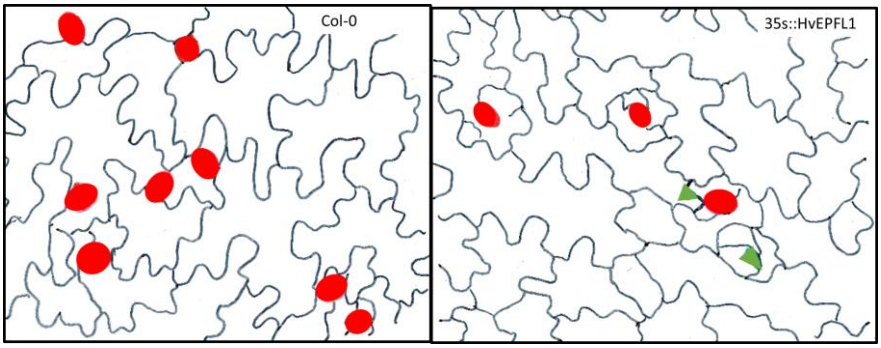

Figure 3.6- Tracings of epidermal micrographs of the epidermis of col-0 and the HvEPFL1 overexpressor Representative images of the epidermis taken from Hughes et al., 2017. Red ovals identify stomata, green triangles identify meristemoids.

3.5.3 – Complementing the *epf2* mutant with *HvEPFL1* results in only partial rescue of the phenotype

The complementation of the *epf2* mutant with the *pEPF2::HvEPFL1* construct did result in an alteration to stomatal development (see figure 3.7), albeit not consistent with any known outcome in similar experiments in the literature. Unlike EPF1 (Hara et al., 2009), HvEPFL1 does partially rescue the *epf2* mutant, with the stomatal density in complementation lines being comparable to the stomatal density of Col-0 controls. The mean stomatal density of the pooled (see section 3.5.1 for explanation*) pEPF2::HvEPFL1* lines was 99.6mm^{-2}, which was 42.3% of the mean stomatal density of the *epf2* mutant (236mm^{-2}) and 65.7% of the mean stomatal density of the control (151mm^{-2}), with only the former being statistically significant (see figure 3.7 A). This is consistent with the complementation of the epf2 mutant with the native EPF2 gene, which restored wild type stomatal density (Hara et al., 2009).

However, the stomatal index (the ratio of the number of stomata divided the number of stomata and other epidermal cells in a given area) of the complementation line remains similar to the *epf2* mutant. The stomatal index of *pEPF2::HvEPFL1* is 8.07% compared to 21.3% in the control and 12.2% in the *epf2* mutant, with the difference between the control and complementation being statistically significant (see figure 3.7 B).

The reason for this low stomatal index is very much apparent when observing the epidermis of the relevant genotypes. In *epf2* mutants there is a proliferation of small cells due to the loss of the inhibitory effect EPF2 has on the amplifying divisions that produce additional SLGCs during the stomatal development pathway, as well as the increase in stomatal density due to the loss of EPF2-mediated suppression of entry divisions and MMC fate acquisition (Hunt and Gray, 2009; Hara et al., 2009; Han and Torii, 2016). In the pEPF2::HvEPFL1 complementation lines the stomatal density regulation was restored, with wild type density observed, but wild type total cell density levels were not re-established, with the continued proliferation of small cells suggesting that the regulation of amplifying divisions remained aberrant. This observation suggests that the functions of EPF2 are separable and explains the stomatal index data in figure 3.7 B, with the wild type stomatal density and mutant-like epidermal cell density of the *pEPF2-HvEPFL1* complementation lines resulting in a stomatal index lower than both the *epf2* mutant and the control, although only the latter difference is significant statistically. That HvEPFL1 cannot regulate amplifying divisions in these complementation lines is notable, given that grasses only undertake a single asymmetric entry division during their stomatal patterning process and

do not carry out amplifying divisions. It could be that HvEPFL1 is derived from an EPF2-like ancestral peptide and that the ability to carry out this function has been lost as a consequence of redundancy after the transition between stomatal patterns. Alternatively, HvEPFL1 may be derived from an EPF1-like ancestral peptide which would probably, like EPF1, have lacked the ability to substitute for EPF2, as has previously been observed in promoter swapping experiments in *Arabidopsis thaliana* (Hara et al., 2009). In this latter case the gain of the ability to rescue the stomatal density phenotype would most likely have to be ascribed to chance and given that the HvEPFL1 mature peptide is most similar to EPF2 in terms of structure (see figure 3.2) it is the former rather than the latter explanation that seems most likely.

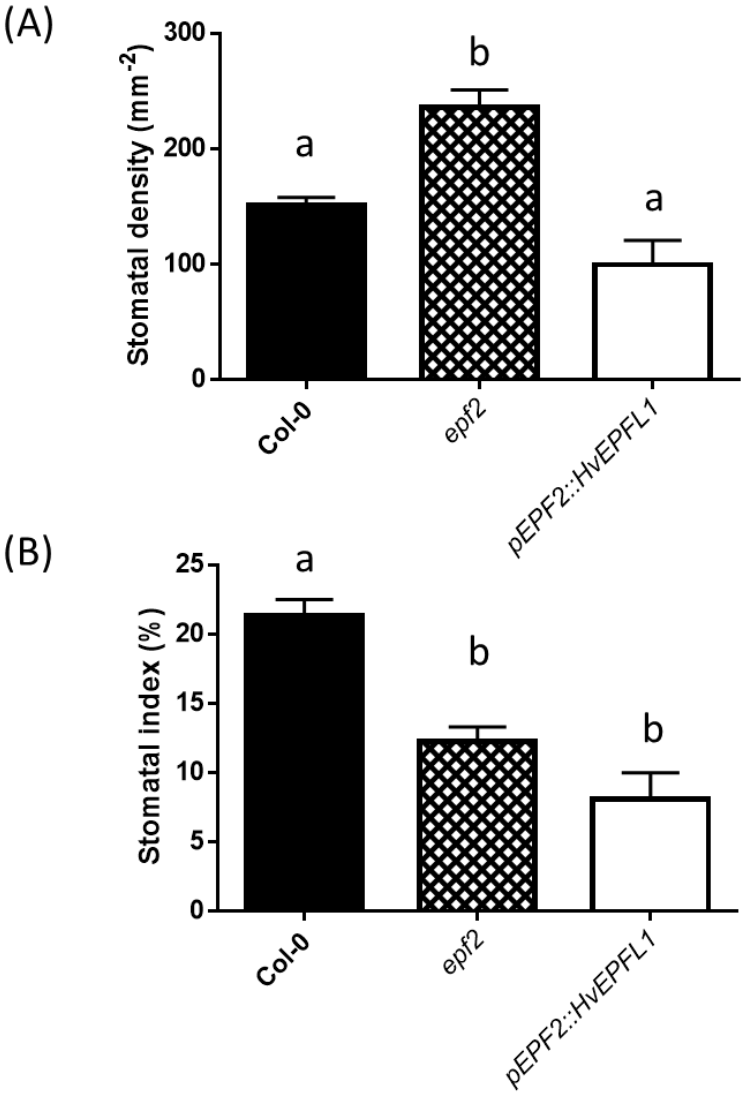

Figure 3.7- Complementation of the *Arabidopsis thaliana epf2* mutant with HvEPFL1 results in partial rescue of the phenotype. (A) Comparison of the mean stomatal density of HvEPFL1 complemented transgenic lines with the mean stomatal densities of Col-0 and the epf2 mutant. (B) Comparison of the mean stomatal index of HvEPFL1 transgenic lines with the mean stomatal index of Col-0 and the epf2 mutant. The stomatal densities and indices of three independent T1 transgenic lines were pooled to provide the reported result for HvEPFL1. N=3-5. Error bars signify SE. Different letters above the bars indicate significant differences between stomatal traits (Tukey's HSD multiple comparisons test after one-way ANOVA, $p<0.05$).

3.6 – Overexpression of HvEPFL1 in native "Golden Promise" background

3.6.1 – Introduction

Having ascertained that *HvEPFL1* functions in a similar manner to *EPF1* and *EPF2* when expressed in the *Arabidopsis thaliana* genetic background the next step was to ectopically overexpress *HvEPFL1* in its native *Hordeum vulgare* background. This provided a means to test whether the role of *EPFL*s in regulating stomatal patterning were conserved in grasses and to analyse whether these functions had diverged as the patterning transitioned from the basal scattered stomatal distribution to the highly-ordered file distribution seen in grasses.

3.6.2 – Screening transgenic lines

Following receipt of the T1 seed of the *HvEPFL1* ectopic overexpression lines generated by the JHI (as described in section 2.2.1), the lines were grown up and screened (see section 3.3) in order to identify whether HvEPFL1 overexpression affected stomatal characteristics and if so to identify lines to utilise in later experiments.

Of the 19 transgenic lines generated, 13 showed a significant stomatal density reduction phenotype whilst the remaining 6 were undistinguishable from wild type. Amongst the 13 lines that possessed this reduced density phenotype there was a considerable range of mean densities exhibited, ranging from 21.9mm^{-2} to 0.2mm^{-2}, compared to a mean control density of 32.2mm^{-2} (see figure 3.8). This represents a reduction to between 67.9% and 0.621% of wild type stomatal density. The mean stomatal density of the HvEPFL1 ectopic overexpression lines as a whole was 10.9mm^{-2}, a reduction to 33.9% of the wild type density.

This initial finding demonstrated that HvEPFL1 functions as a negative regulator of stomatal density when ectopically overexpressed in barley. This is consistent with the finding that HvEPFL1 functioned as a negative regulator of stomatal density when expressed in *Arabidopsis thaliana* and further supports the hypothesis that there is conservation of function in stomatal development amongst the EPFLs, with HvEPFL1 being a negative regulator of stomatal density in a manner similar to either EPF1 and EPF2.

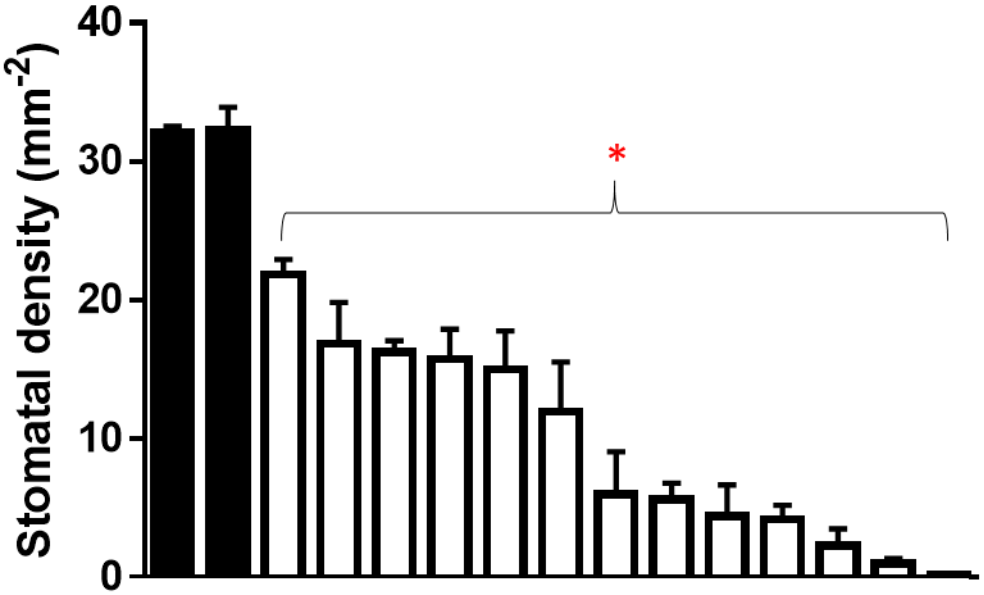

Figure 3.8-Hordeum vulgare transgenic lines, transformed to ectopically overexpress HvEPFL1, demonstrate a range of reduced stomatal density phenotypes. Independent T1 HvEPFL1 overexpressor lines represented by white bars. The black bars represent two independent T1 empty vector control lines. 8 plants per line were initially grown with the stomatal densities of null segregants, identified via genotyping, removed. Therefore, in the reported lines n=3-8, dependent upon the number of individual plants harbouring the insert. Error bars represent SE. Asterisk indicates that the means of all lines differ significantly from both the first and the second empty vector control line (Two separate Dunnett's multiple comparisons tests following one-way ANOVA, $p<0.05$).

Prior to commencing more detailed physiological analyses work was undertaken to identify suitable lines for further study, with the ideal being single insert, homozygous lines. A subset of the 13 successful transgenic lines for which there were substantial seed stocks remaining were grown to maturity to supply the T2 seed required for further investigation. The lines selected for copy number analysis mainly consisted of those lines for which the observed stomatal density in the initial screen was moderately reduced relative to controls. This decision was taken as it seemed likely that higher reductions

would be a consequence of higher gene dosage. Moreover, as stomatal conductance increases, assimilation saturates due to biochemical limitations whilst transpiration continues to increase linearly, therefore decreases in conductance in the range in which assimilation has plateaued yields similar assimilation rates for significantly reduced water loss, which results in higher WUE (Yoo et al., 2009, see section 1.3.3 for discussion). It was therefore justified to focus on moderate density reduction lines as these were more likely to have stomatal conductance drops that remained within this "sweet spot" for assimilation and WUE.

Leaf tissue samples were taken and dispatched for copy number analysis as described in section 2.18. This identified a number of lines containing a single copy of the transgene including individual plants that were homozygous for the insert (see figure 3.9).

Unfortunately, seed set from all lines was poor and so T2 seed stocks were limited. Only two lines, hereafter described as HvEPFL1OE-A and HvEPFL1OE-B, were both homozygous for the transgene and produced sufficient seed to support further study. These T2 seed were utilised for the gas exchange experiment described in chapter 4, with the T3 homozygous offspring of both lines then being utilised for further growth experiments described in chapter 5 and the detailed phenotyping described later in this chapter.

Transgenic line	Mean Stomatal Density (mm^{-2})	Copy Number
HvEPFLOE-A	5.7	1/2
HvEPFLOE-B	11.3	1/2
HvEPFLOE-C	7.83	1/2
HvEPFLOE-D	1	5

Figure 3.9- Table showing the variable insert copy number and stomatal density of the transgenic lines reported in figure 3.8. 1/2 indicates a mix of heterozygous and homozygous single copy inserts. Seed from homozygous individuals was selected for use in later experiments.

3.6.3 - Effect of HvEPFL1 OE on epidermal development

Figure 3.10 compares an epidermal micrograph of a cleared section of the second true leaf an empty vector control to one obtained from an HvEPFL1OE-A individual. The overall arrangement of the stomatal pattern remains the same in the HvEPFLOE lines, with stomata being isolated into files that border the leaf veins with no sign of disruption to this organisational motif. This would suggest that HvEPFL1 functions downstream of the specification of stomatal file initiation.

There are however a distinct number of changes between HvEPFL1 overexpressors and the control. Firstly, the stomatal density has decreased relative to controls as was previously described. Moreover, there was a significantly increased occurrence of ovoid-shaped cells that occurred only in the stomatal files in positions where a stoma would be expected to form normally. The fact that they occurred only in stomatal files, along with additional evidence presented later in this chapter, suggested that they were arrested stomatal precursors. Notably EPF1, when overexpressed in *Arabidopsis thaliana*, also produces arrested stomatal precursors, namely meristemoids, as did HvEPFL1 (Hara et al., 2007; Hara et al., 2009; see figure 3.6). This would suggest that HvEPFL1 might play a role in stomatal fate determination and maturation, in particular regulating the transition between the precursor state and the mature stoma.

One other notable difference is that occasionally in the control line and in wild type barley there is the occurrence of a double row of stomata, in which two adjacent files of cells contain stomata in an alternating pattern, as can be seen in the third row of the control micrograph in figure 3.10. These double rows have not been observed in any of the HvEPFL1 overexpression lines analysed.

The rest of this chapter, except for figure 3.15, concerns measurements various epidermal traits taken from epidermal micrographs of cleared leaves of the empty vector control, HvEPFL1OE-A and HvEPFL1OE-B, such as those seen in figure 3.10. This experiment is hereafter referred to as the epidermal phenotyping experiment.

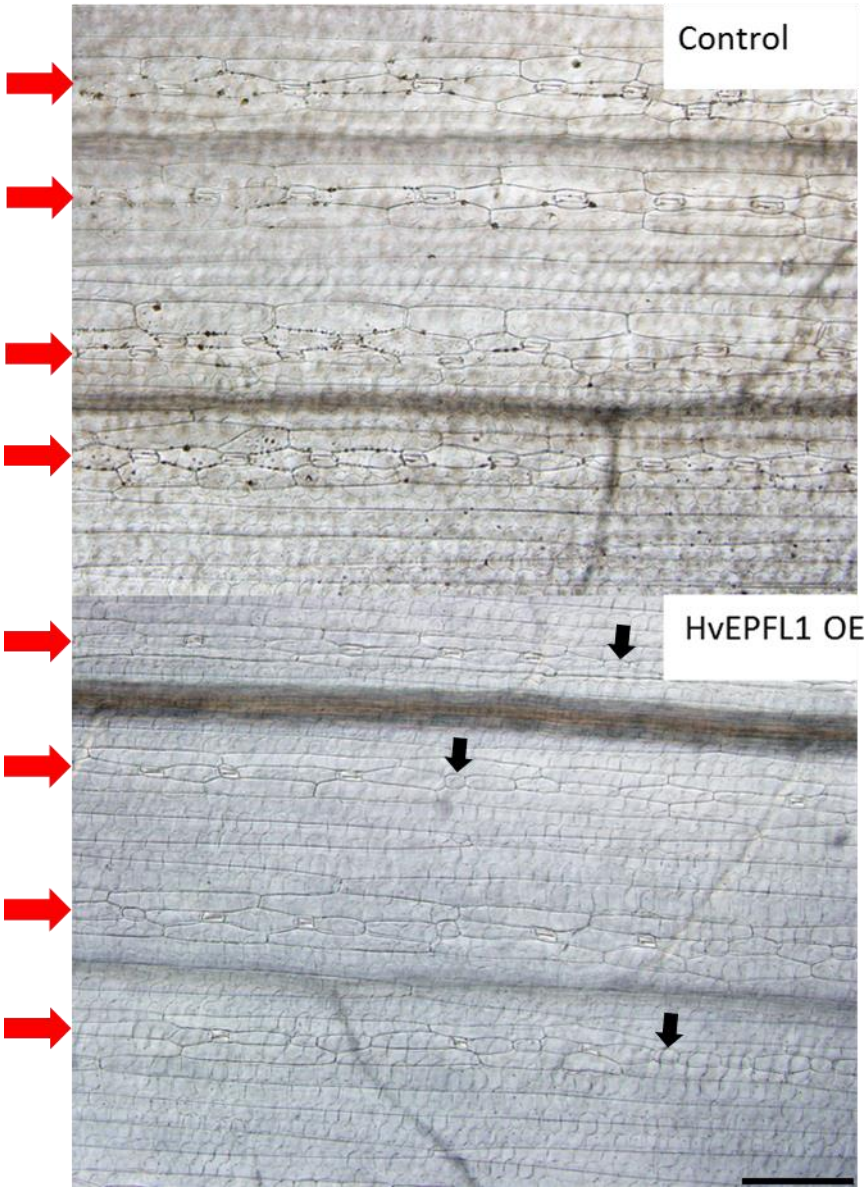

Figure 3.10- Epidermal micrographs of an empty vector control and an *HvEPFL1* overexpressor. Representative images taken from cleared leaf samples of the empty vector control and HvEPFL1OE-A. Red arrows mark stomatal rows, black arrows mark examples of arrested cells. Black scale bar represents a length of 200 µm.

As expected the stomatal densities of the HvEPFL1OE-A and HvEPFL1OE-B lines were significantly lower than that of the empty vector control in the epidermal phenotyping experiment. HvEPFL1OE-A had a mean stomatal density of 10.1mm^{-2} whilst HvEPFL1OE-B had a mean stomatal density of 12.4mm^{-2}, representing 43.8% and 53.8% of the control mean stomatal density (23mm^{-2}) respectively (see figure 3.11).

It is interesting to note here that during the course of this investigation the three lines (control and overexpressors) were grown under multiple different sets of growth conditions depending upon the experiment. Both the control and the overexpressors demonstrated different stomatal densities under different environmental conditions. Whilst these experiments were not designed with direct comparison in mind, it is possible to infer that the HvEPFL1OE lines retain the ability to alter their stomatal density in response to varying environmental conditions. Whether the degree of this responsiveness has been affected by the overexpression of a negative regulator, a potential concern if it limits the adaptability of these lines under varying environmental conditions, and which environmental conditions cause stomatal density responses in these lines, would be a good avenue of future investigation.

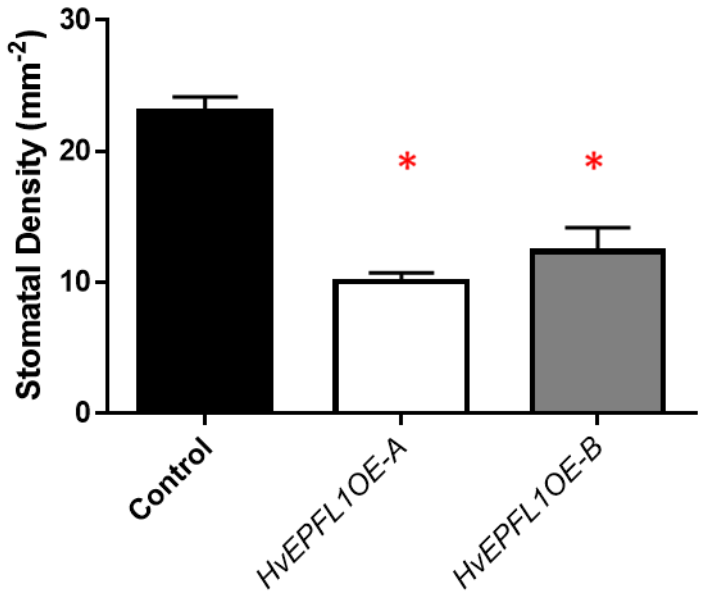

Figure 3.11- The two transgenic lines selected for characterisation of the HvEPFL1 ectopic overexpression phenotype both show reduced stomatal density. Comparison of the mean stomatal density of two independent T3 HvEPFL1 overexpressing transgenic lines with the mean stomatal density of an empty vector control line. N=4. Error bars signify SE. Asterisk indicates significant reduction in stomatal density relative to empty vector control (Dunnett's multiple comparisons test after one-way ANOVA, $p<0.05$).

As mentioned in the discussion of figure 3.10, one of the most notable phenotypes of HvEPFL1 overexpression is the proliferation of arrested stomatal precursors, which are incredibly rare in the control and in wild type plants in general, where up to around 1 to 4% of stomatal precursors have been found to arrest (Stebbins and Shah, 1960). In the epidermal phenotyping experiment these arrested precursors occurred at a density of $0.233mm^{-2}$ in the empty vector control compared to $7.03mm^{-2}$ in line *HvEPFL1OE-A* and $5.1mm^{-2}$ in line *HvEPFL1OE-B*, a percentage increase of 2910% and 2090% respectively (see figure 3.12 A).

An epidermal micrograph of an arrested precursor is shown in figure 3.12 B. These distinctive ovoid-shaped cells were only found in the stomatal files in both controls and *HvEPFL1* overexpressors.

The relative infrequency of these arrested precursors in controls suggests that the regulation of the transition between the precursor state and mature stomata is not the role of HvEPFL1. Indeed, cell fate arrest clearly isn't the means by which stomatal density is regulated in either barley or *Arabidopsis thaliana,* occurring as a side effect of overexpression in the case of EPFL manipulation.

However, the positioning of arrested cells in controls does suggest that there may be some role for this phenomenon and potentially a functional role for HvEPFL1. In general, those few arrested precursors that arose in controls did so in a distinct location. They occurred almost exclusively in the satellite file of a double row of stomata which, as mentioned above, did not form in the overexpression lines. This, coupled to the known ability of HvEPFL1 to generate arrested precursors, would seemingly suggest that HvEPFL1, or another HvEPFL, could play a role in regulating the occurrence of double rows and coordinating the spacing of stomata between adjacent rows such that they don't cluster, although without observations from a knockout mutant this remains speculative.

(A)

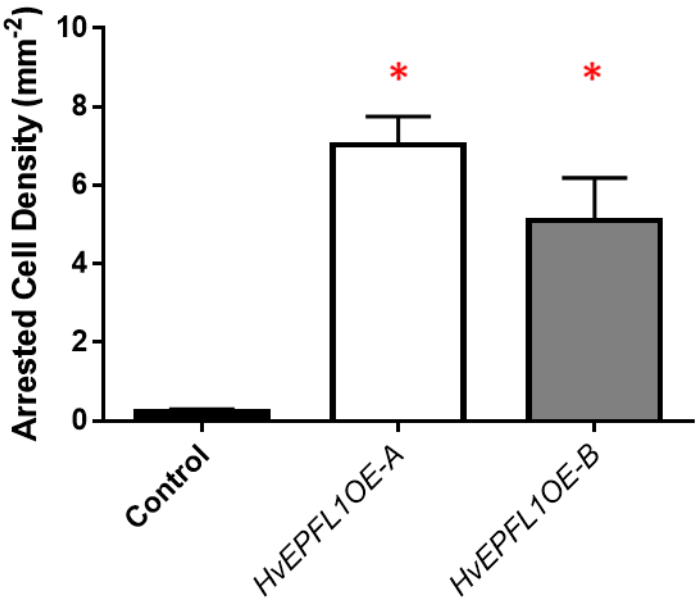

(B)

Figure 3.12- Arrested stomatal precursor frequency increases dramatically in the HvEPFL1 ectopic overexpression transgenic lines. (A) Comparison of the arrested stomatal precursor density of two independent T3 HvEPFL1 overexpressing transgenic lines with the arrested stomatal precursor density of an empty vector control line. N=4. Error bars signify SE. Asterisk indicates significant increase in arrested stomatal precursor presence relative to the empty vector control**.** (Dunnett's multiple comparisons test after one-way ANOVA, $p<0.05$). (B) Epidermal micrograph of a section of cleared, HvEPFL1OE-A leaf showing a representative arrested stomatal precursor cell (scale bar beneath = 50µm).

In terms of epidermal development there was no significant effect on the density of epidermal cells typically found on the epidermis of wild type individuals, i.e. stomatal row

spacing cells and non-stomatal row cells (figure 3.13 A). Indeed, the range of the means of the genotypes was just 2.4mm^{-2}. Even when the arrested stomatal precursors are factored in, there is no significant change to epidermal cell density, with a range of 7.2mm^{-2} between the means (figure 3.13 B). In *Arabidopsis thaliana* there are differences in epidermal development when the EPFs are overexpressed, namely differences in the density of epidermal cells of different sizes (Hara et al., 2009). EPF1 overexpressors possess more small pavement cells as a consequence of meristemoid arrest whilst EPF2 overexpressors are devoid of small pavement cells as a result of EPF2 blocking stomatal lineage entry and amplifying divisions with the result that the majority of pavement cells are generated directly from protodermal cells and are consequently larger (Hara et al., 2009). Given the absence of amplifying divisions in grass stomatal development it was unlikely that epidermal cell development would be significantly affected by overexpression. Instead, the phenotype most closely resembles that of Arabidopsis EPF1, with a significant increase in the number of small pavement cells (figure 3.12 A), although with no significant increase in total epidermal density (figure 3.13 B) as seen in *Arabidopsis thaliana* (Hara et al., 2009).

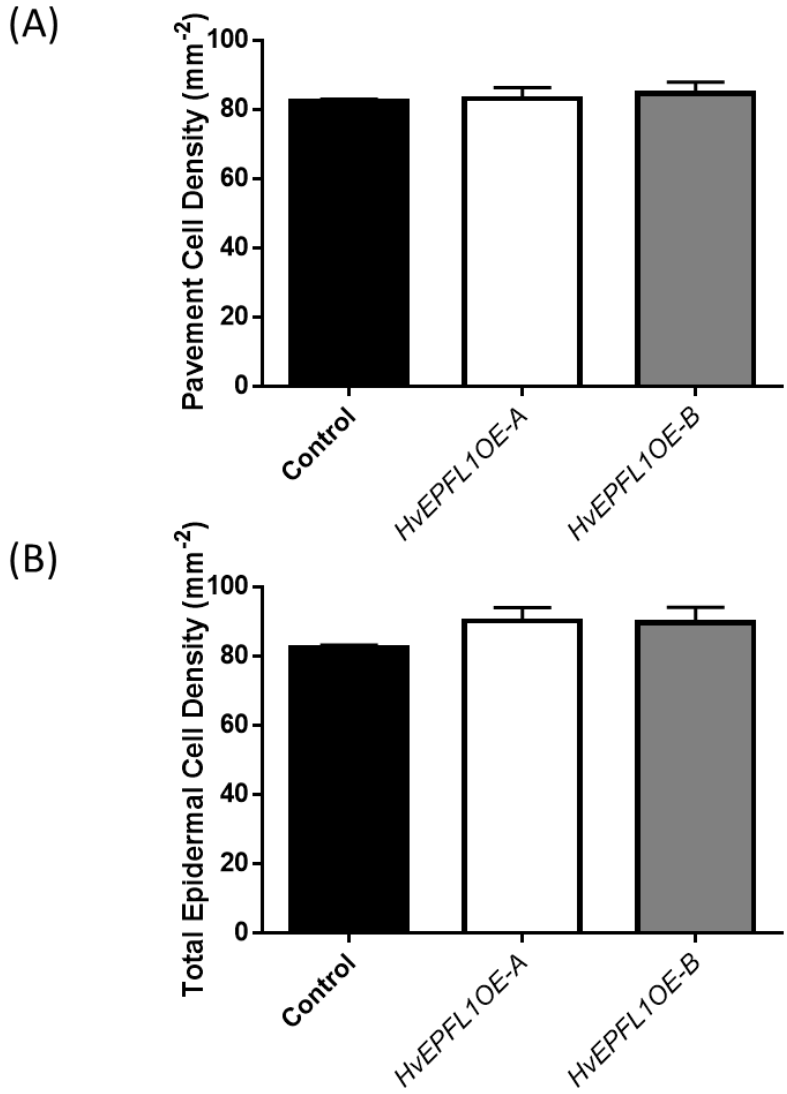

Figure 3.13- Ectopic overexpression of HvEPFL1 has no significant effect on epidermal cell numbers. (A) Comparison of the mean epidermal pavement cell density of two independent T3 HvEPFL1 overexpressing transgenic lines with the mean epidermal pavement cell density of an empty vector control line. (B) Comparison of the mean total epidermal cell density, including arrested stomatal precursors, of two independent T3 HvEPFL1 overexpressing transgenic lines with the mean total epidermal cell density of an empty vector control line. N=4. Error bars signify SE. No significant differences were found between transgenic lines and the control for both pavement cell density and total epidermal cell density (one-way ANOVA, $p>0.05$).

The stomatal index (the ratio of the number of stomata divided the number of stomata and other epidermal cells in a given area as a percentage) is unsurprisingly significantly reduced in the HvEPFL1OE lines, with a mean reduction to 46.1% and 56.25% of control values (mean 21.8%) for HvEPFL1OE-A (mean 10.0%) and HvEPFL1OE-B (mean 12.2%) respectively (Figure 3.14). This change in the ratio is driven by the significant change in the stomatal density (see figure 3.11), rather than by the negligible change in epidermal density as a consequence of stomatal lineage cell arrest (see figure 3.13 B).

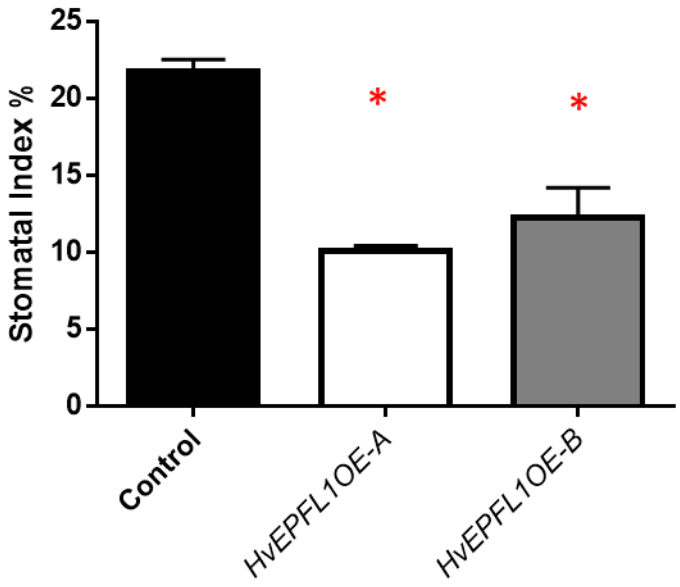

Figure 3.14- Ectopic overexpression of HvEPFL1 significantly reduces the stomatal index relative to controls. Comparison of the mean stomatal index of two independent T3 HvEPFL1 overexpressing transgenic lines with the mean stomatal index of an empty vector control line. N=4. Error bars signify SE. Asterisk indicates significant decrease in stomatal index relative to the empty vector control**.** (Dunnett's multiple comparisons test after one-way ANOVA, $p<0.05$).

3.6.4 - Effect of HvEPFL1 OE on stomatal morphology

Stomatal morphology, like stomatal density regulation, is significantly important in regulating stomatal response to environmental changes, in particular short-term fluctuations, and consequently it is important consideration when assessing the effects of the HvEPFL1OE lines in altering plant water relations.

As can be seen in the cleared leaf image in figure 3.10 and in the confocal microscopy image in figure 3.15, the default structure of mature stomata remains the same in the

HvEPFL1OE, i.e. the stomatal pore flanked by the classic dumbbell-shaped guard cells which are in turn flanked by their respective subsidiary cell. This shows that the overexpression of HvEPFL1 does not affect the stomatal development pathway in its latter stages, beyond the precursor state at which it induces lineage arrest, and so suggests that HvEPFL1 doesn't play a role in stomatal complex maturation.

Interestingly, the confocal microscopy provides some detail on where in the stomatal developmental pathway the substomatal cavity, which is important for efficient gas exchange, forms. Substomatal cavities are found beneath the mature stomatal complexes but are not found located under the arrested precursor cells (see figure 3.15). Due to the absence of substomatal cavities beneath the arrested precursors it can be inferred that the formation of the cavity occurs as a consequence of a developmental signal issued later in the developmental sequence than the precursor state at which the lineage cells arrest in the HvEPFL1 overexpressor. This would suggest that the formation of the cavity occurs either following GMC formation/maturation when the subsidiary cells form or following the formation of the guard cells i.e. in the final stages of stomatal maturation.

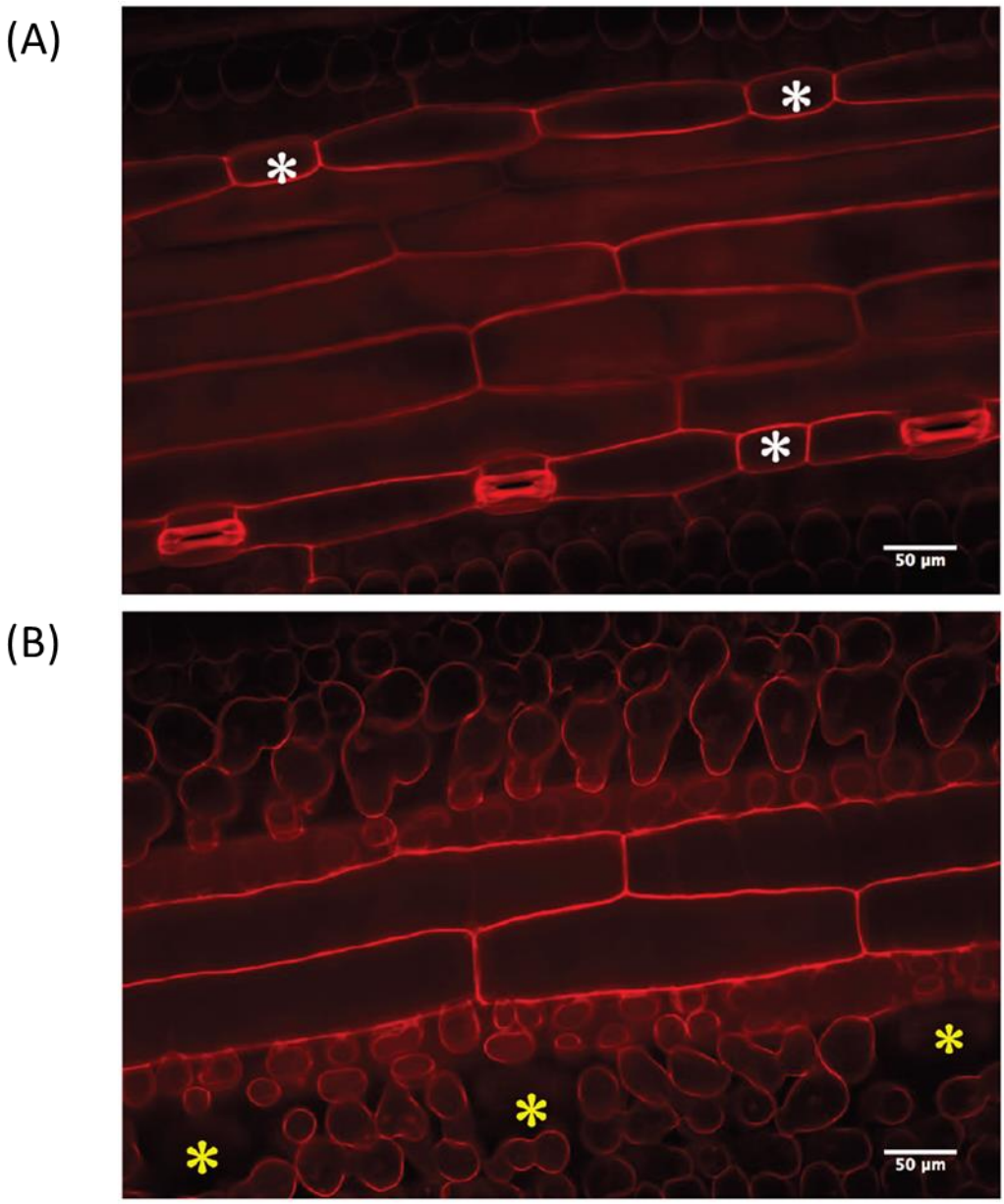

Figure 3.15- Z-plane confocal micrographs of the abaxial epidermis and below the abaxial epidermis. Image taken of the epidermis (A) and the layer underlying the same area of epidermis (B) showing the presence of substomatal cavities beneath the stomata, which are absent beneath the arrested cells**.** White asterisks mark arrested meristemoids. Yellow asterisks mark substomatal cavity. From Hughes et al., 2017.

Whilst the structure of the stomatal complex remained the same in the HvEPFL1OE lines the morphology did differ in one respect, the stomata were significantly smaller than those found in the control. As can be seen in figure 3.16, mean guard cell length declined by

approximately 20% and 25% of control mean guard cell length (56.4µm) in lines HvEPFL1OE-B (45.0µm) and HvEPFL1OE-A (41.9µm) respectively (Figure 3.16 A). Stomatal area, calculated from guard cell size as described in chapter 2, declined by approximately 35% and 45% of control mean stomatal area (398µm^2) in lines HvEPFL1OE-B (254 µm^2) and HvEPFL1OE-A (221 µm^2) respectively (Figure 3.16 B).

Possessing smaller stomata has previously been demonstrated to be advantageous for plant water relations due to smaller stomata being quicker to alter their apertures in response to fluctuations in environmental conditions such as light (Drake et al., 2013) and also possessing a smaller stomatal pore path length for diffusion (Franks and Beerling, 2009).

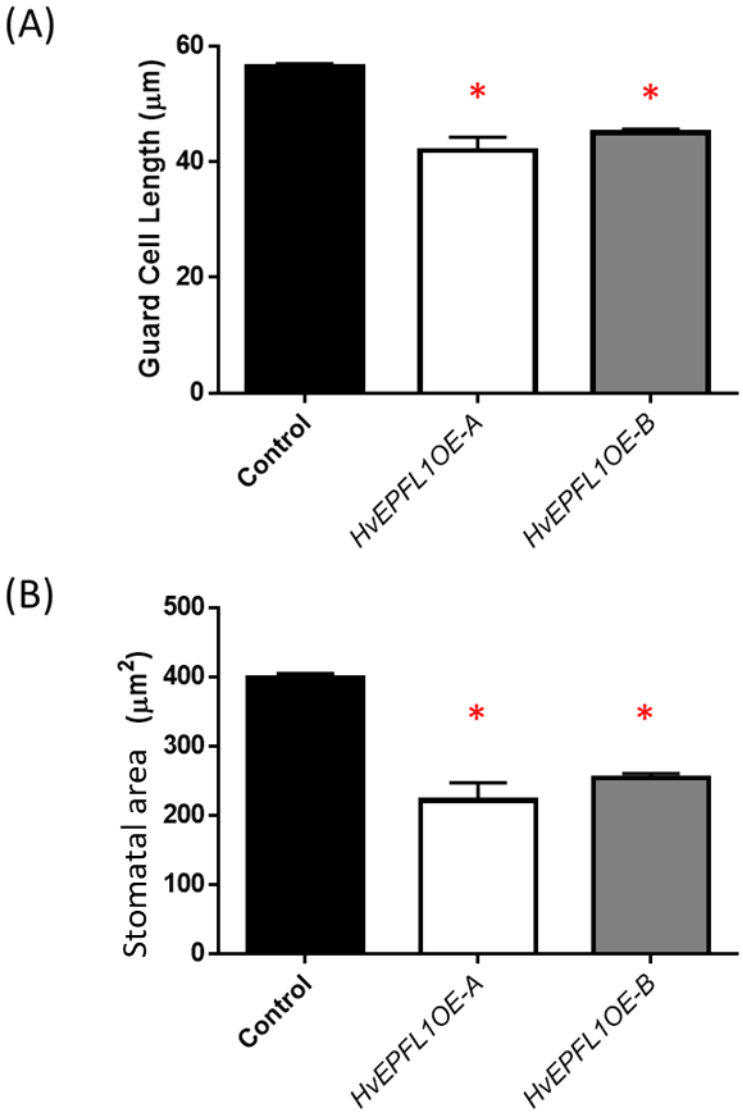

Figure 3.16- Ectopic overexpression of HvEPFL1 significantly reduces stomatal area relative to controls. (A) Comparison of the mean guard cell length of two independent T3 HvEPFL1 overexpressing transgenic lines with the mean guard cell length of an empty vector control line. (B) Comparison of the mean stomatal area of two independent T3 HvEPFL1 overexpressing transgenic lines with the mean stomatal area of an empty vector control line. The guard cell lengths of 30 stomata were measured and averaged per plant. Stomatal area was calculated using the reported raw guard cell lengths, then averaged per plant. N=4. Error bars signify SE. Asterisk indicates significant decrease in mean guard cell length or mean stomatal area relative to the empty vector control**.** (Dunnett's multiple comparisons test after one-way ANOVA, $p<0.05$).

Figure 3.17 shows that there is a strong, positive correlation (Pearson's rank correlation coefficient (r)= 0.8916) between stomatal density and stomatal area (a proxy for size). This is a relatively surprising finding given that stomatal density and stomatal size are usually found to be negatively correlated. This negative correlation has been demonstrated both within natural occuring variation (Franks and Beerling, 2009), including amongst barley cultivars (Miskin and Rasmusson, 1970), and within transgenic *Arabidopsis thaliana* modified for altered stomatal density through EPF peptide level manipulation (Doheny-Adams et al., 2012).

The discovery of a positive correlation suggests that if EPFs do influence stomatal size determination then they have the opposite effect in grass stomatal development to the effect seen in *Arabidopsis thaliana.* Whether EPFs do directly influence stomatal size has not been demonstrated. It is possible that the difference in response seen between *Arabidopsis thaliana* and barley could be a consequence of the differences in how stomatal patterning occurs, i.e. the differences in how the cells divide in order to give rise to the stomatal lineage. This positive correlation also means that unlike in *Arabidopsis thaliana,* where the reduction in stomatal conductance as a result of decreased stomatal density is partially compensated for by increased stomatal apertures, barley EPFs reduce stomatal conductance through both a density and an aperture reduction, the two traits work synergistically. Given the intention of producing low conductance plants in order to reduce water loss, this positive correlation is potentially beneficial.

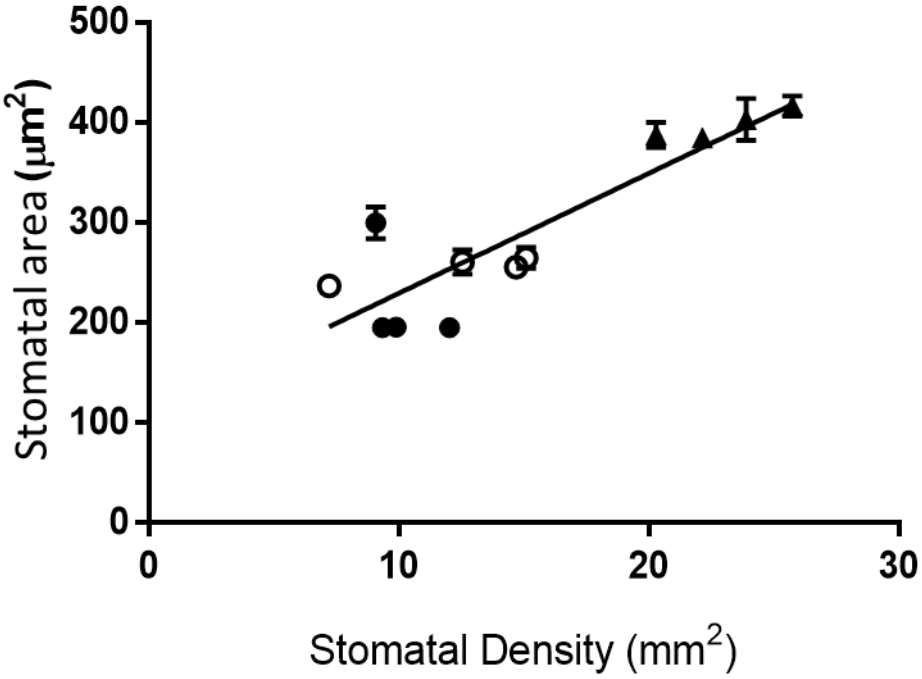

Figure 3.17- There is a positive correlation between stomatal density and stomatal area. Scatterplot of mean stomatal area against mean stomatal density for the empty vector control and 2 ectopic overexpression lines. N=4. Black triangles represent controls, closed circles represent HvEPFL1OE-A and open circles represent HvEPFL1OE-B. For each individual plant N=5. Error bars represent SE. For linear regression and correlation N=12. There is a strong correlation between stomatal area and stomatal density (Pearson's rank correlation coefficient (r)= 0.8916). This relationship is strongly supported when modelled using linear regression (modelled relationship shown by the black line, $R^2 = 0.7949$) and the slope is significantly non-zero (linear regression, $p<0.0001$).

In order to assess when the effect on stomatal size might occur within the lineage progression the mean length of the guard cells was compared to the length of the arrested stomatal precursors (see figure 3.18). This was only possible for the HvEPFL1OE lines, as arrested precursors are too rare in controls to provide a sample size sufficient for statistical analysis (see figure 3.12). The arrested precursors are the same size as the guard cells which would indicate that the process by which stomatal size is affected occurs prior to, and independent of, the precursor to mature stoma transition. This provides evidence that HvEPFL1 can influence stomatal development upstream of the transition which suggests

that there are multiple stages within the stomatal development pathway where HvEPFL1 could function, i.e. it is not restricted to simply repressing stomatal maturation at the precursor to mature stoma transition.

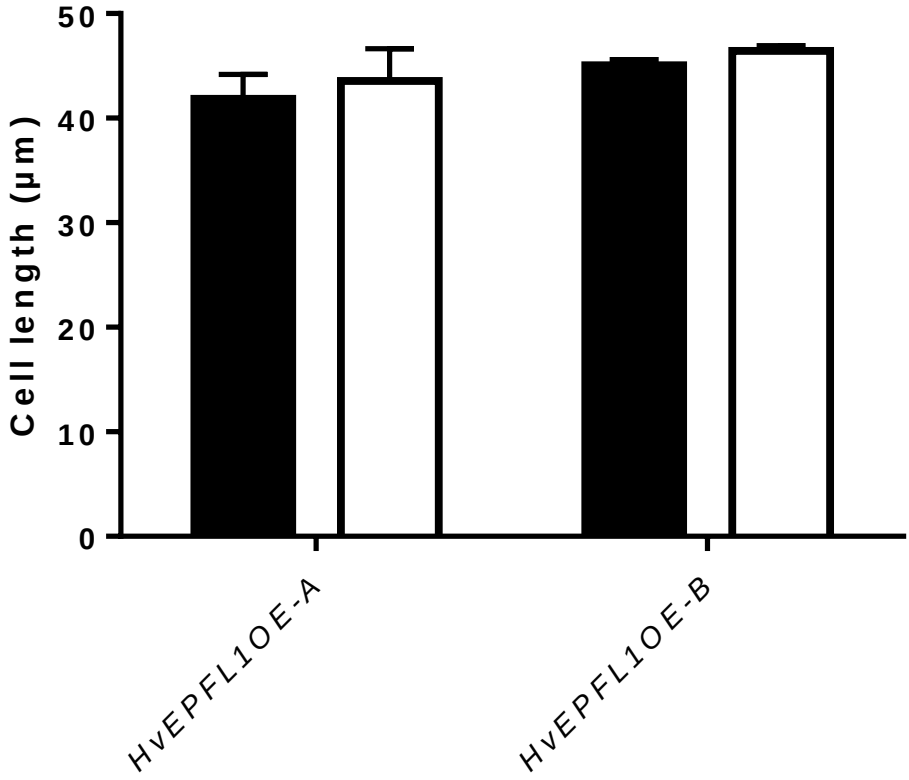

Figure 3.18- Arrested stomatal precursor cells are the same length as mature stomatal complex guard cells in HvEPFL1 ectopic overexpression lines. Comparison between the mean guard cell lengths and mean arrested stomatal precursor cell lengths of the independent T3 ectopic overexpression lines, HvEPFL1OE-A and HvEPFL1OE-B. Black bars display guard cell length data whilst white bars represent arrested stomatal precursor cell lengths. N=4. Error bars signify SE. There was no significant difference between the mean length of guard cells and the mean length of arrested stomatal precursors in either of the ectopic HvEPFL1 overexpression lines. (Two-way ANOVA, $p>0.05$).

Further evidence for an upstream role for HvEPFL1OE is supplied by Figure 3.19, a scatterplot comparing the arrested cell length and guard cell length of 20 FOV obtained from across 5 plants for each HvEPFLOE line. There was a strong correlation between

arrested cell length and guard cell length (Pearson's rank correlation coefficient (r)= 0.84) with the length of the precursors in a given FOV being roughly equal to the length of the stomata. Indeed, a simple linear regression of the data supplies the regression equation y= 1.053x + 0.8082, i.e. the equation of the line describing the data is not far removed from Y=X. This shows that final stomatal size is dependent upon and equal to the size of the precursor cell and that the size is effected irrespective of whether the lineage arrests, as a consequence of HvEPFL1 repressing the transition, or progresses to a mature stomatal complex. If HvEPFL1 only functioned at the transition between the precursor and the mature stoma then it would be expected that the arrested precursors, which are formed upstream of the transition, and consequently the mature stomata would have a wildtype size phenotype. The observation that size is effected by *HvEPFL1* ectopic overexpression, coupled with the observation that the final size of the mature stoma is set prior to the precursor to stoma transition, demonstrates that HvEPFL1 effects the progression of the stomatal lineage at an additional, upstream point.

Theoretically this reduction in precursor and hence stomatal size could be the result of either the alteration of the plane of division during the entry division that gives rise to the precursor or due to the suppression of precursor cell expansion, which occurs after the entry division (Stebbins and Shah, 1960, Raissig et al., 2016).

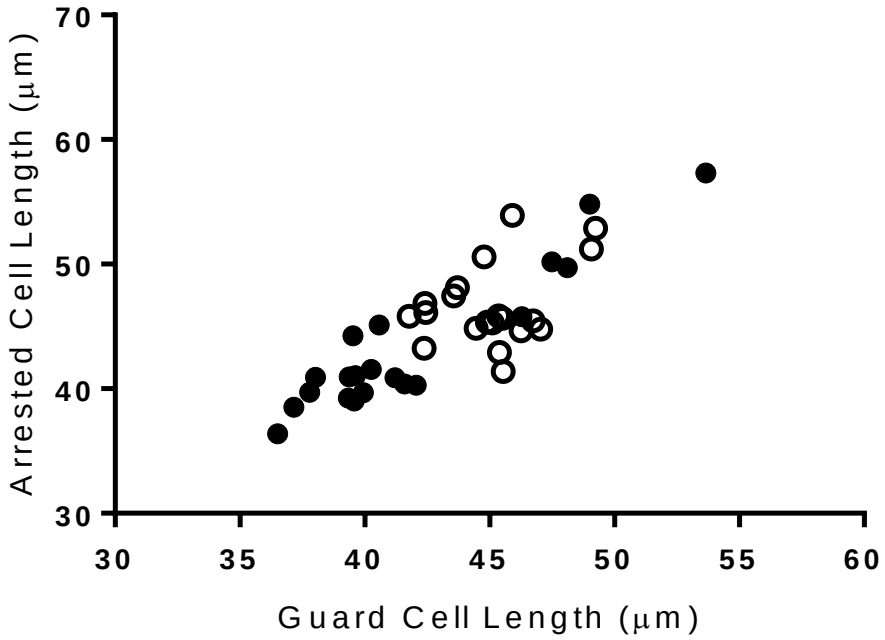

Figure 3.19- There is a positive correlation between arrested stomatal precursor cell lengths and guard cell lengths in HvEPFL1 ectopic overexpression lines. Scatterplot of mean stomatal precursor cell lengths against mean guard cell lengths. 20 FOV averages for each HvEPFL1OE line, closed circles represent HvEPFL1OE-A and open circles represent HvEPFL1OE-B. For each individual mean N=5. For linear regression and correlation n=40. There is a strong correlation between stomatal precursor cell length and guard cell length (Pearson's rank correlation coefficient (r)= 0.84). This relationship is strongly supported when modelled using linear regression (R^2 = 0.7055) and the slope is significantly non-zero (linear regression, p<0.0001).

3.6.5 - Effect of HvEPFL1 OE on stomatal lineage identity

As discussed above the stomatal index is significantly reduced in the HvEPFL1OE lines as a consequence of the significant change in the stomatal density (see figure 3.11), rather than the negligible change in epidermal cell density (see figure 3.13 B). In order to determine whether the cell arrest phenotype could entirely account for the differences observed in the stomatal density and stomatal index the stomatal lineage density and index were determined (see figure 3.20). The stomatal lineage density is the density of stomata and

arrested precursors combined whilst the stomatal lineage index is the percentage of all epidermal cells that are either stomata or arrested precursors.

The stomatal lineage densities of the HvEPFL1OE-A and HvEPFL1OE-B lines were significantly lower than that of the empty vector control. HvEPFL1OE-A had a mean stomatal lineage density of 17.1mm^{-2} whilst HvEPFL1OE-B had a mean stomatal lineage density of 17.5mm^{-2}, representing 73.6% and 75.2% of the control mean stomatal lineage density (23.2mm^{-2}) respectively (see figure 3.20 A).

Similarly, the stomatal lineage indices of the HvEPFL1OE-A and HvEPFL1OE-B lines were significantly lower than that of the empty vector control. HvEPFL1OE-A had a mean stomatal lineage index of 17.0% whilst HvEPFL1OE-B had a mean stomatal lineage index of 17.2%, representing 77.4% and 78.1% of the control mean stomatal lineage index (22.0%) respectively (see figure 3.20 B).

These results demonstrate that even if all the arrested precursors transitioned into mature stomatal complexes the stomatal density and stomatal index would still be significantly reduced in HvEPFL1 ectopic overexpression lines. This means that HvEPFL1 must influence stomatal density through another interaction in addition to causing precursor arrest. There are 3 principal ways in which reduced density of stomatal lineage cells could occur within the confines of the file pattern of stomata in barley.

1. Within the stomatal files the spacing cells, i.e. the epidermal cells between consecutive stomatal lineage cells, could be longer.
2. The stomatal files could be further apart.
3. Fewer entry divisions could occur.

The rest of section 3.6.5 analyses these potential causes of reduced stomatal lineage density in sequence. Section 2.19 contains details of the terms used, how the distance between rows was measured and illustrates what is meant by spacing cell.

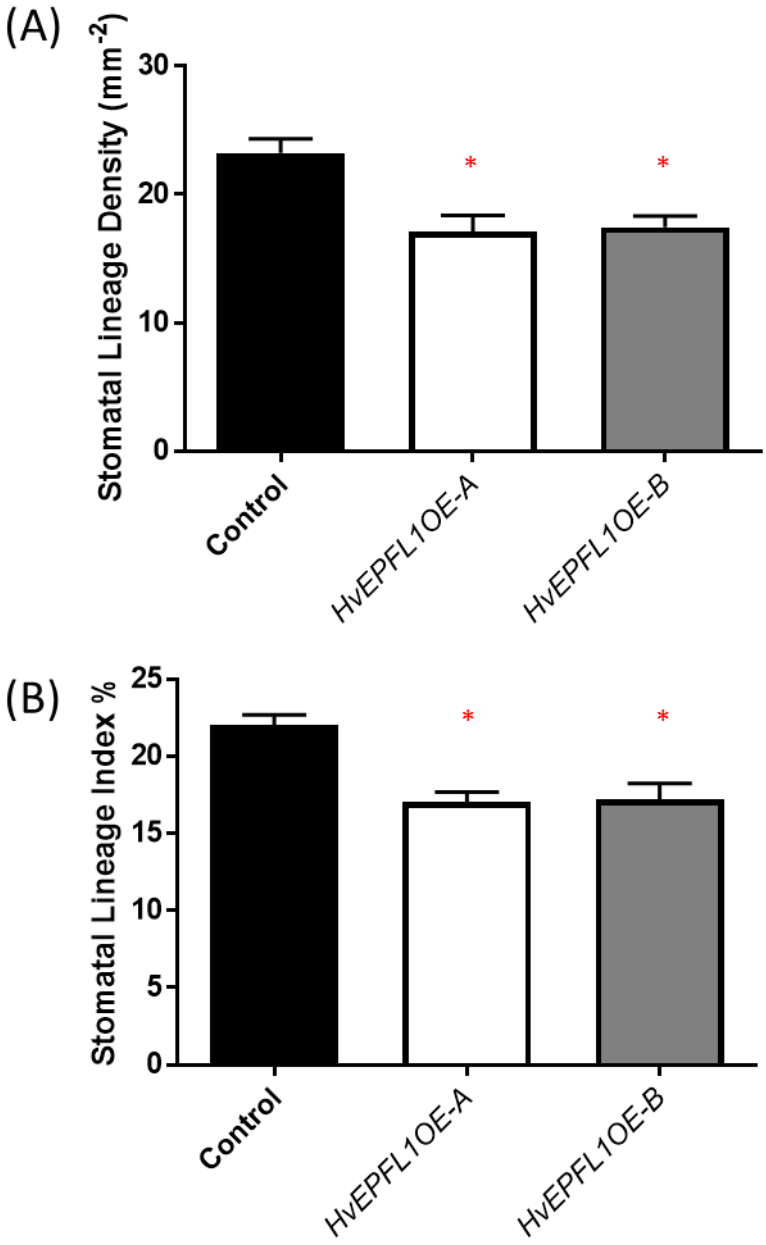

Figure 3.20- Ectopic overexpression of HvEPFL1 significantly reduces the stomatal lineage density and index relative to controls. Comparison of the mean stomatal lineage density (A) and stomatal lineage index (B) of two independent T3 HvEPFL1 overexpressing transgenic lines with the mean stomatal lineage density (A) and stomatal lineage index (B) of an empty vector control line. N=4. Error bars signify SE. Asterisk indicates significant decrease in stomatal lineage index relative to the empty vector control**.** (Dunnett's multiple comparisons test after one-way ANOVA, $p<0.05$).

The mean spacing cell length of the HvEPFL1OE-A and HvEPFL1OE-B lines were not significantly different to that of the empty vector control. HvEPFL1OE-A had a mean spacing cell length of 128µm whilst HvEPFL1OE-B had a mean spacing cell length of 123µm, compared to a control mean spacing cell length of 123µm (see figure 3.21). This result demonstrates that *HvEPFL1* ectopic overexpression does not influence the expansion of spacing cells.

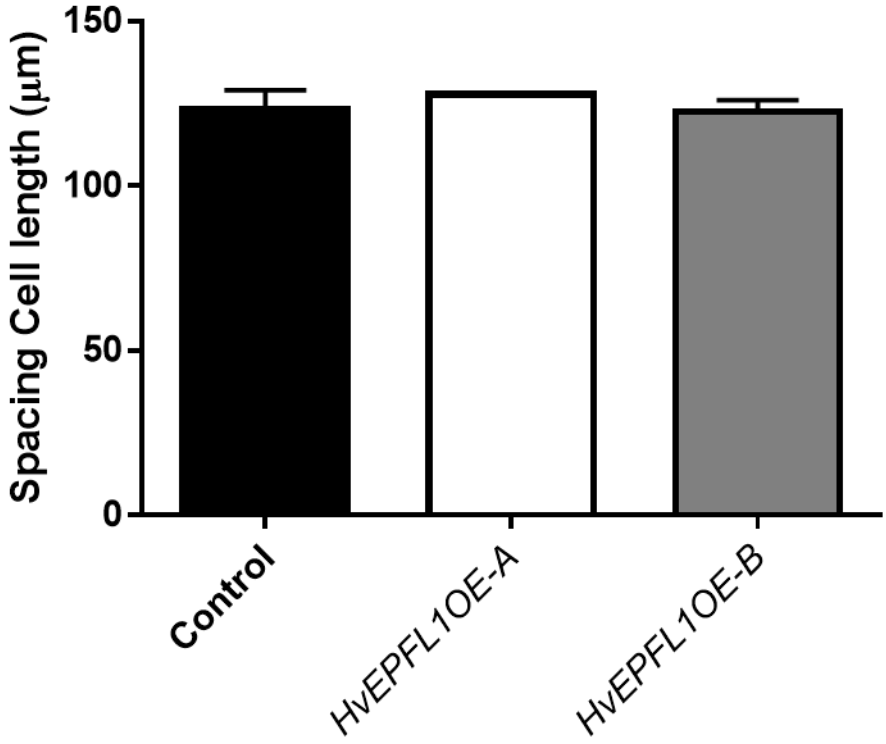

Figure 3.21- Ectopic overexpression of HvEPFL1 does not affect the length of stomatal row spacing cells relative to controls. Comparison of the mean length of spacing cells between stomata and/or arrested stomatal precursors of two independent T3 HvEPFL1 overexpressing transgenic lines with the mean length of spacing cells between stomata of an empty vector control line. Only spacing cells where both within row neighbours were stomatal lineage cells were used in this analysis. N=4. Error bars signify SE. There was no significant difference between the spacing cell lengths of ectopic HvEPFL1 overexpression lines and controls (One-way ANOVA, $p>0.05$).

The mean distance between adjacent stomatal rows of the HvEPFL1OE-A and HvEPFL1OE-B lines were not significantly to that of the empty vector control. HvEPFL1OE-A had a mean distance of 300µm whilst HvEPFL1OE-B had a mean distance of 313µm, compared to a control mean distance of 341µm (see figure 3.22). The distances reported in this analysis were measured between rows lacking an intervening vein. This result demonstrates that

HvEPFL1 ectopic overexpression does not affect the spacing of the stomatal rows, indeed the rows tend towards being closer together in the transgenic lines.

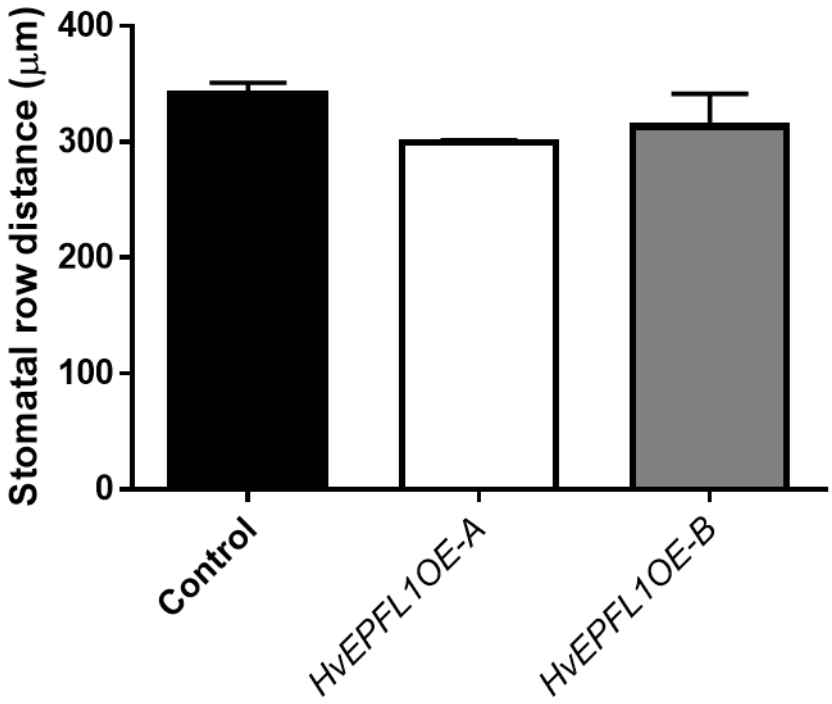

Figure 3.22- Ectopic overexpression of HvEPFL1 does not affect the distance between rows of stomata relative to controls. Comparison of the mean distance between stomatal rows of two independent T3 HvEPFL1 overexpressing transgenic lines with the mean distance between stomatal rows of an empty vector control line. The distances reported in this analysis were measured between rows lacking an intervening vein. N=4. Error bars signify SE. There was no significant difference in the distances between stomatal rows of ectopic HvEPFL1 overexpression lines and controls (One-way ANOVA, $p>0.05$).

The stomatal files in wild type barley consist of stomatal lineage cells and epidermal spacing cells with consecutive stomatal lineage being separated from one another by lone spacing cells (Stebbins and Jain, 1960; Stebbins and Shah, 1960). This pattern arises as a result of each consecutive protodermal cell within the file undergoing an asymmetric entry division (Vaten and Bergmann, 2012). It follows to reason that if HvEPFL1 were to inhibit entry divisions then some of the protodermal cells in the *HvEPFL1* ectopic overexpression

lines would not undergo an asymmetric division, becoming epidermal cells instead. This would result in consecutive stomatal lineage cells being separated by multiple spacing cells.

Figure 3.23 compares of the mean percentage of the spaces between consecutive stomatal lineage cells within rows that are comprised of a single, spacing cell in the HvEPFL1 ectopic overexpression lines and empty vector control. 96.6% of inter-stomatal spaces in the control contain only a single spacing cell, compared with 53.4% in HvEPFL1OE-A and 68.7% in HvEPFL1OE-B. From this it can be concluded that in addition to repressing the transition from precursor to stoma HvEPFL1 also represses entry into the stomatal lineage and that it is this additional regulatory interaction that causes differences in the stomatal lineage density and index of HvEPFL1 ectopic overexpression lines relative to the empty vector control (see figure 3.20).

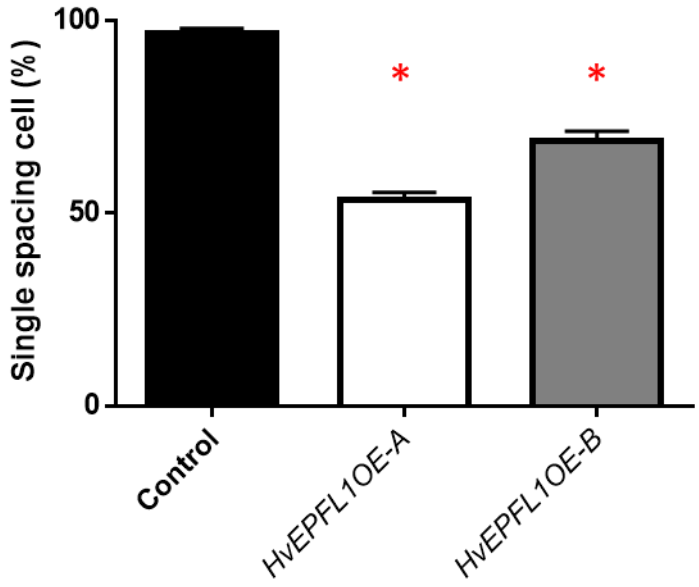

Figure 3.23- Ectopic overexpression of HvEPFL1 significantly decreases the occurrence of single spacing cell presence between successive stomatal lineage cells within stomatal rows. Comparison of the mean percentage of the spaces between successive stomatal lineage cells (both mature stomata and arrested precursor cells) within rows that comprise of a single-spacing cell in two independent T3 HvEPFL1 overexpressing transgenic lines with the mean percentage of single spacing cell occurrence in an empty vector control line. N=4. Error bars signify SE. Asterisk indicates significant decrease in HvEPFL1 overexpressing transgenic lines of the mean percentage of gaps between successive stomatal lineage cells that are comprised of a single-spacing cell relative to the empty vector control (Dunnett's multiple comparisons test after one-way ANOVA, $p<0.05$).

3.7 – Conclusions

- When ectopically overexpressed in *Arabidopsis thaliana* both *HvEPFL1* and *HvEPFL2* caused a significant reduction in both stomatal density and stomatal index compared to Col-0 controls. These findings are consistent with the phenotypes obtained when native *Arabidopsis thaliana* EPF1 and EPF2 are ectopically expressed (Hara et al., 2007; Hara et al., 2009 Hunt and Gray, 2009). Particularly notable is the increased prevalence of small triangular cells consistent

in morphology with meristemoids observed in the *HvEPFL1* ectopic overexpression lines, which are also found when *EPF1* is overexpressed, suggesting that the function of HvEPFL1 could be most similar to that of EPF1 (Hara et al., 2007; Hara et al., 2009).

- Ectopic overexpression of *HvEPFL1* in barley significantly reduces stomatal density. HvEPFL1 regulates stomatal development at two different stages. Firstly, HvEPFL1 inhibits the asymmetric entry divisions that give rise to the stomatal lineage within the stomatal files. The mechanism by which this occurs is likely similar to the process by which it occurs in Arabidopsis thaliana, namely the repression of SPCH. HvEPFL1 overexpression also causes the stomatal lineage to arrest at a precursor stage, giving rise to distinctive, ovoid, arrested precursor cells, lacking subsidiary cells, within the stomatal files. This suggests that HvEPFL1 also regulates the transition to a mature GMC capable of inducing subsidiary cell formation and dividing symmetrically to form GCs. Given that in *Brachypodium distachyon* the otholog of *Arabidopsis* MUTE is necessary and sufficient to induce subsidiary cell formation (Raissig et al., 2017) and that the transition to GMC is regulated by MUTE in *Arabidopsis thaliana*, it seems possible that HvEPFL1 regulates the transition though MUTE, possibly via phosphorylation as, unlike Arabidopsis MUTE, grass othologs possess potential MAP kinase phosphorylation sites (Liu et al., 2009).

- The ovoid cells formed can be identified as arrested precursor cells as they are only found in the stomatal files in the same pattern as stomata. Furthermore, the length of the precursor cells is also positively correlated and approximately equal to the length of the guard cells of neighbouring mature stomatal complexes.

- The absence of substomatal cavities beneath the arrested precursors infers that the formation of the cavity occurs due to a developmental signal issued later in the developmental sequence than the precursor state at which the lineage cells arrest in the *HvEPFL1* overexpressor. This would suggest that the formation of the cavity occurs in the final stages of stomatal maturation, after GMC formation/maturation.

- Contrary to the majority of the literature, including an analysis of transgenic *Arabidopsis thaliana* modified for altered stomatal density through EPF peptide level manipulation (Doheny-Adams et al., 2012), there is a positive correlation between stomatal density and stomatal size in the *HvEPFL1* ectopic overexpression lines. It is currently unknown if EPFs directly influence stomatal size as well as stomatal density but if this is the case then the discovery of a positive correlation suggests that EPFs have the opposite effect in grass stomatal development to the effect seen in *Arabidopsis thaliana* with regards to stomatal size determination.

Chapter 4 -The effect of overexpressing *HVEPFL1* on gas exchange in *Hordeum vulgare*

4.1- Introduction

This chapter focuses on the effect that overexpressing *HvEPFL1* has on gas exchange and water use efficiency. Considering that stomata are the principal means by which gas exchange is regulated the changes in stomatal density and size described in chapter 3 have obvious implications for gas exchange.

The effect of altered stomatal density on gas exchange has been analysed in a number of studies. Franks et al., 2015 found that *Arabidopsis thaliana* plants constitutively overexpressing EPF2 had reduced rates of carbon assimilation and stomatal conductance relative to Col-0, as well as improved instantaneous and long-term water use efficiency. The reduction in stomatal density in *Arabidopsis thaliana gtl1* mutants resulted in reduced stomatal conductance and increased instantaneous water use efficiency (Yoo et al., 2010; Yoo et al., 2011) whilst overexpressing *ZmSDD1* in maize, which resulted in reduced stomatal density, also resulted in reduced stomatal conductance and improved water use efficiency (Liu et al., 2015). In the case of the last two studies the rate of CO_2 assimilation was not significantly reduced despite the decline in stomatal density.

Given the reduction in the number of stomata and the reduction in individual pore apertures seen in the ectopic overexpressors of *HvEPFL1* it was fair to assume that gas exchange in these transgenics would be affected in a similar manner to what was observed in the studies highlighted. This chapter tests that hypothesis.

4.2- Method summary

The gas exchange characteristics and stomatal conductance of control and transgenic barley plants were measured using an infra-red gas exchange analyser (IRGA) system, a Licor li6400 with a li6400-40 leaf chamber fluorimeter sensor head attached (Licor, Licoln, NE).

Steady state measurements were taken to determine gas exchange parameters and stomatal conductance in ambient conditions. CO2 levels were set at 500ppm, PAR set at 200µmol m^{-2} s^{-1} and leaf temperature at 20 ^{o}C.

Light curves and A-Ci curves were generated using the flag leaf of the primary tiller. For the light curves the CO2 level was set at 500ppm, PAR initially set at 1900µmol m^{-2} s^{-1} and leaf temperature at 23oC. Readings were taken at 1900, 1800, 1700, 1600, 1200, 800, 600, 400, 200, 100, 50 and 0µmol m^{-2} s^{-1}. For the A-Ci curves the CO2 level was initially set at 500ppm, PAR set at 1900µmol m^{-2} s^{-1} and leaf temperature at 23^{o}C. Readings were taken at 500, 300, 200,100, 50, 500, 800, 1000, 1200, 1400, 1600, 1800 and 2000ppm.

For all experiments plants were left to acclimate to leaf chamber conditions for at least 35 minutes and the reference and sample IRGAs were matched at least every 15 minutes and after every reading during curve acquisition.

A more detailed description of the gas exchange methodologies utilised is supplied in section 2.8.

The A-Ci curves were fitted using an A-Ci curve fitting tool (www.landflux.org) which fits the C3 photosynthesis model (Farqhuar et al., 1980) following the method of Either and Livingston, 2004. Values for the maximum rate of rubisco carboxylation (Vmax), maximum rate of electron transport (Jmax) and maximum rate of assimilation (Amax), were obtained from the fitted data. The stomatal limitation on photosynthesis was described using the graphical method (Long and Bernacchi, 2003). The light curves were fitted using an excel spreadsheet utilising the model of Ye, 2007 obtained from Lobo et al., 2013.

4.3- Steady-state gas exchange

In order to ascertain how the reduction in stomatal density affected stomatal conductance, carbon assimilation rate, transpiration and water use efficiency of barley under natural

growth conditions, infra-red gas exchange analysis was carried out using ambient conditions as described in sections 2.8.4 and 4.2.

The rate of carbon assimilation of the HvEPFL1OE-A and HvEPFL1OE-B lines were significantly lower than that of the empty vector control in the steady-state gas exchange experiment under well-watered conditions (Dunnett's multiple comparisons test after one-way ANOVA, $p<0.05$). HvEPFL1OE-A had a mean carbon assimilation rate of 11.9 $\mu molm^{-2}s^{-1}$ whilst HvEPFL1OE-B had a mean carbon assimilation rate of 12.4 $mmolm^{-2}s^{-1}$, representing 88.8% and 92.5% of the control mean carbon assimilation rate (13.4 $\mu molm^{-2}s^{-1}$) respectively (see figure 4.1 A). This is a rather modest decrease given the large reduction in stomatal density seen in the *HvEPFL1* ectopic overexpression lines. This reduction in assimilation as a consequence of reduced stomatal density is similar to that observed in EPF overexpressors in *Arabidopsis thaliana*, albeit the data presented here was collected at ambient rather than high light (Franks et al., 2015).

The stomatal conductance of the HvEPFL1OE-A and HvEPFL1OE-B lines was also significantly lower than that of the empty vector control in the steady-state gas exchange experiment under well-watered conditions (Dunnett's multiple comparisons test after one-way ANOVA, $p<0.05$). HvEPFL1OE-A had a mean stomatal conductance of 0.129 $molm^{-2}s^{-1}$ whilst HvEPFL1OE-B had a mean stomatal conductance of 0.155 $molm^{-2}s^{-1}$, representing 70.9% and 85.2% of the control mean stomatal conductance (0.182 $molm^{-2}s^{-1}$) respectively (see figure 4.1 B). This reduction in stomatal conductance is unsurprising considering that both stomatal density and stomatal size are significantly reduced in the *HvEPFL1* overexpression lines.

Under drought conditions neither the rate of carbon assimilation nor the stomatal conductance of the HvEPFL1OE-A and HvEPFL1OE-B lines was statistically distinct from empty vector control values (one-way ANOVA, $p>0.05$) (see figure 4.1 C and 4.1 D). This would suggest that under the severe drought imposed, stomatal closure in response to drought is equalising the exchange area through which gas exchange can occur, resulting in a similar stomatal conductance and an equally constrained rate of CO_2 assimilation in both the HvEPL1 ectopic overexpression lines and the empty vector control line.

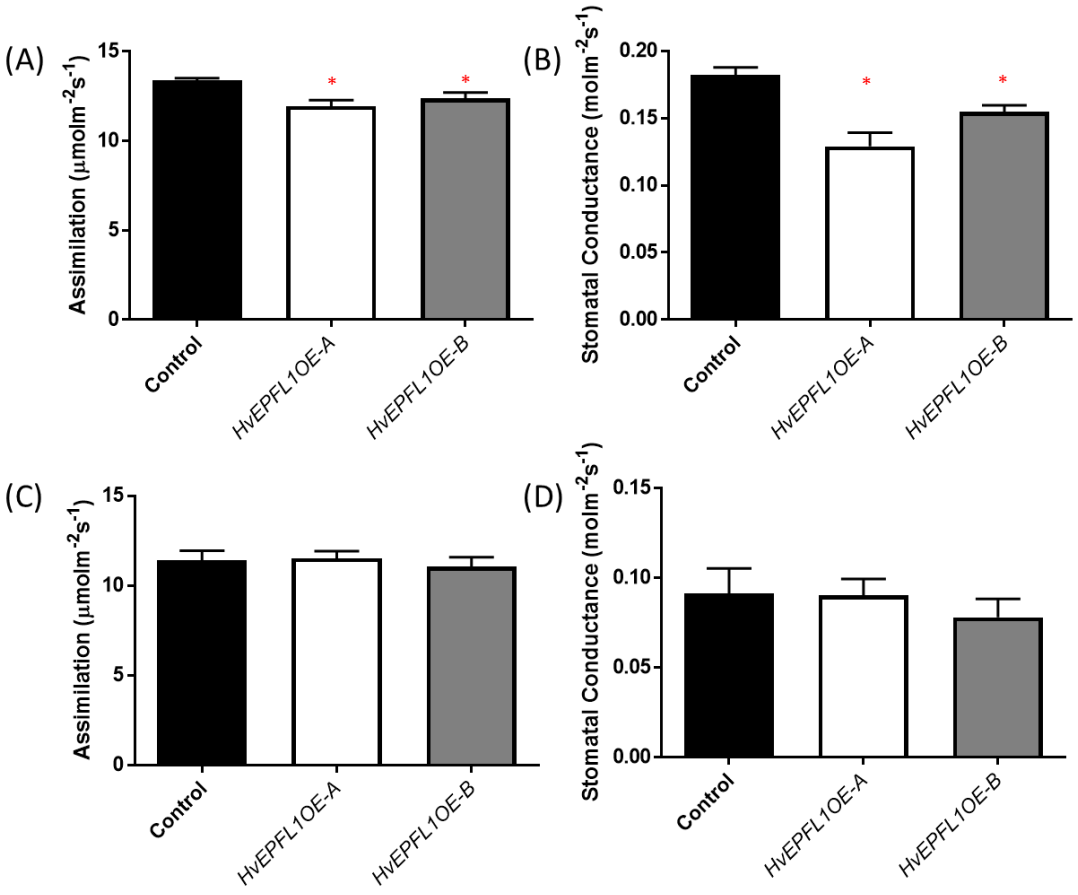

Figure 4.1- Ectopic overexpression of *HvEPFL1* significantly decreases carbon assimilation rate and stomatal conductance under well-watered conditions but not under drought conditions. Comparison of the mean rate of carbon assimilation and mean stomatal conductance in two independent T2 HvEPFL1 overexpressing transgenic lines with those of an empty vector control line using steady state gas exchange analysis. (A) and (B) are under well-watered conditions whilst (C) and (D) are under drought. N=5. Error bars signify SE. Asterisk indicates significant decrease in HvEPFL1 overexpressing transgenic lines of the mean rate of carbon assimilation or stomatal conductance relative to the empty vector control (Dunnett's multiple comparisons test after one-way ANOVA, $p<0.05$).

The rate of carbon assimilation can be restricted by one of two sets of limitations, stomatal and non-stomatal (Brodribb, 1996). When stomatal conductance is reduced, the supply rate of CO_2 is reduced as a consequence of the increased resistance to gas exchange. This supply limitation in turn reduces the internal CO_2 concentration of the leaf (Ci) as the Ci is depleted by assimilation (Farquhar and Sharkey, 1982). Analysis of the ratio of Ci to atmospheric CO_2 concentration can consequently be used to assess stomatal limitation, with a lower ratio suggesting that CO_2 supply to the leaf is relatively constrained (Brodribb, 1996).

The ratio of Ci/Ca of the HvEPFL1OE-A line was significantly lower than that of the empty vector control under well-watered conditions (Dunnett's multiple comparisons test after one-way ANOVA, $p<0.05$). HvEPFL1OE-A had a mean Ci/Ca ratio of 0.67 in comparison to a ratio of 0.735 for the control mean Ci/Ca ratio (see figure 4.2 A). This suggests that the drop in assimilation rate seen in the HvEPFL1 overexpression lines, in particular the severe density reduction line HvEPFL1OE-A, is as a consequence of stomatal limitation arising from the significantly reduced stomatal conductance.

Under drought conditions the ratio of Ci/Ca of the HvEPFL1 ectopic expression lines was not statistically distinct from empty vector control values (one-way ANOVA, $p>0.05$) (see figure 4.2 B). This again suggests that an equalisation of the exchange area due to short term stomatal aperture adjustment is resulting in equalisation of gas exchange characteristics.

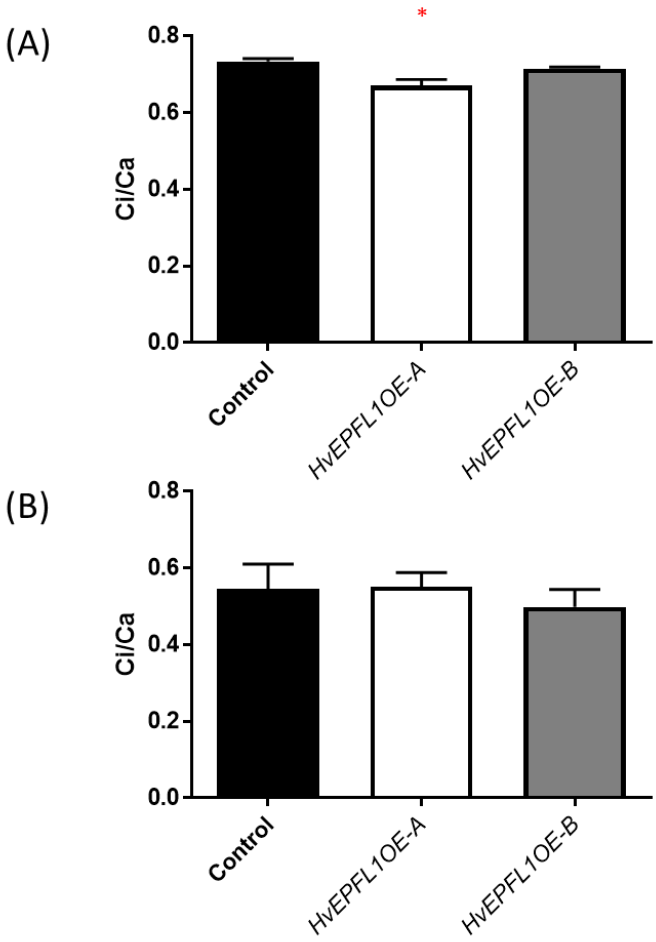

Figure 4.2- Ectopic overexpression of *HvEPFL1* significantly decreases the Ci/Ca ratio in the lowest density line under well-watered conditions. Comparison of the mean Ci/Ca ratio in two independent T2 HvEPFL1 overexpressing transgenic lines with the mean Ci/Ca ratio in an empty vector control line using steady state gas exchange analysis under well-watered (A) and droughted (B) conditions. N=5. Error bars signify SE. Asterisk indicates significant decrease in HvEPFL1 overexpressing transgenic lines of the mean Ci/Ca ratio relative to the empty vector control (Dunnett's multiple comparisons test after one-way ANOVA, $p<0.05$).

The rate of transpiration of the HvEPFL1OE-A line was significantly lower than that of the empty vector control under well-watered conditions (Dunnett's multiple comparisons test after one-way ANOVA, $p<0.05$). HvEPFL1OE-A had a mean transpiration rate of 0.839

$mmolm^{-2}s^{-1}$ representing 73% of the control mean carbon transpiration rate (1.15 $mmolm^{-2}s^{-1}$) (see figure 4.3 A). Under drought conditions the rate of transpiration of the *HvEPFL1* ectopic expression lines was not statistically distinct from empty vector control values (one-way ANOVA, $p>0.05$) (see figure 4.3 B). Again, the reduction in the rate of transpiration is to be expected given the severity of the reduction in the stomatal density and consequently the stomatal conductance of the HvEPFL1OE-A line, whilst under drought it is stomatal aperture control, rather than stomatal density, that is constraining the upper bound of gas exchange.

The principal concern of this project was to identify whether reducing stomatal density and subsequently reducing water loss could be used to produce crop plants that are more water use efficient. As discussed in section 1.3.2 there are two commonly reported WUE measures collected from gas exchange measurements, instantaneous WUE and intrinsic WUE, both of which are reported below.

Instantaneous WUE is defined as A/E where A is the rate of carbon assimilation and E is the rate of evapotranspiration (Penman and Schofield, 1951; Farquhar and Sharkey, 1982; Yoo et al., 2009; Morison et al.,2008) with instantaneous water use efficiency being improved either by increasing the rate of assimilation relative to transpiration or reducing transpiration relative to assimilation.

In contrast to the findings of Franks et al., 2015, Yoo et al., 2010 and Yoo et al., 2011 under both well-watered and drought conditions the instantaneous water use efficiency was not statistically distinct from empty vector control values in the low stomatal density lines (one-way ANOVA, $p>0.05$) (see figure 4.3 C and 4.3 D). The likely reason for this lack of improved instantaneous water use efficiency is the relatively low reduction in assimilation coupled with the error due to the variability of transpiration. There is a trend towards instantaneous WUE being higher in the HvEPFL1OE-A line, but it is not significant (see figure 4.3 C)(unpaired t-test, $p=1.163$).

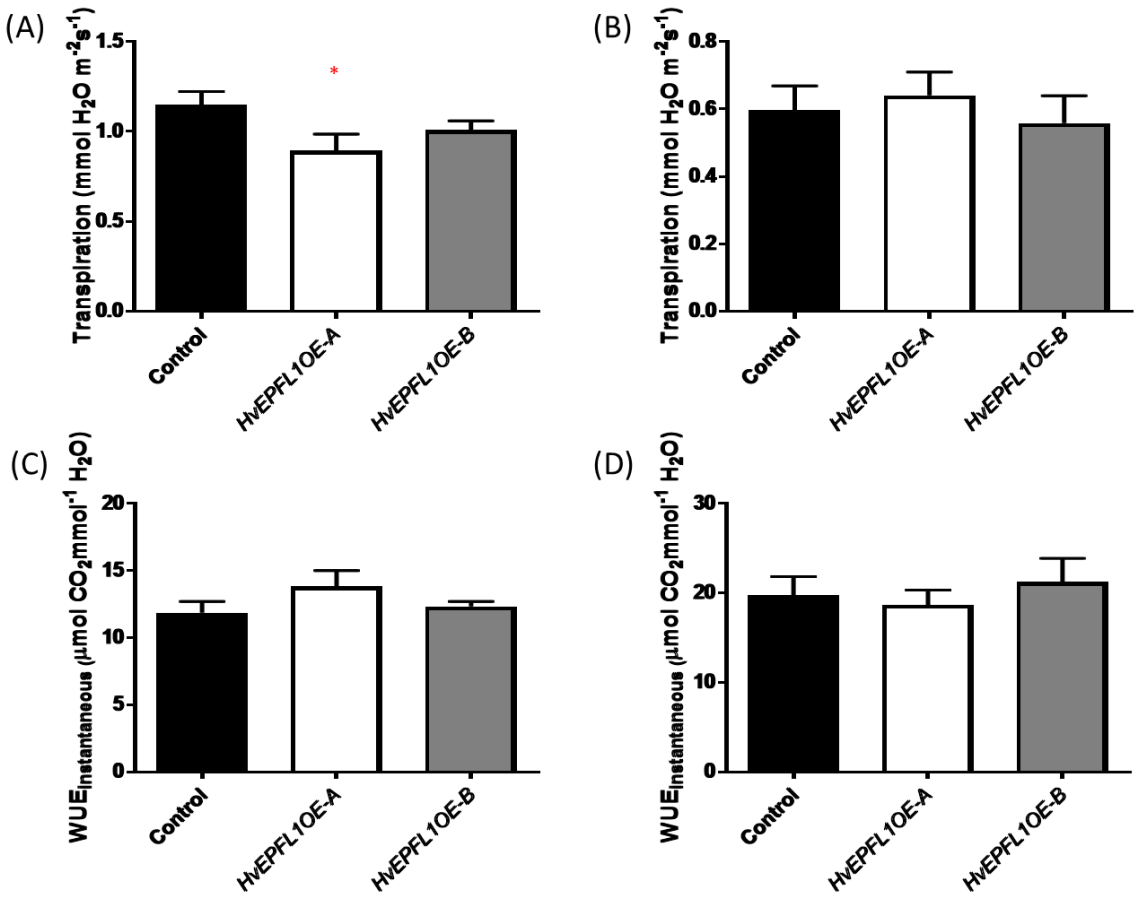

Figure 4.3- Ectopic overexpression of *HvEPFL1* significantly decreases the rate of transpiration in the HvEPFLOE-A line under well-watered conditions but otherwise does not significantly affect the rate of transpiration nor the instantaneous water use efficiency. Comparison of the mean rate of transpiration and mean instantaneous WUE in two independent T2 HvEPFL1 overexpressing transgenic lines with those of an empty vector control line using steady state gas exchange analysis. (A) and (C) are under well-watered conditions whilst (B) and (D) are under drought. N=5. Error bars signify SE. There was no significant difference between the overexpressors and the controls (one-way ANOVA, $p>0.05$) except in the case of the rate of transpiration of HvEPFL1OE-A under well-watered conditions (Dunnett's multiple comparisons test after one-way ANOVA, $p<0.05$).

The intrinsic WUE is defined as A/Gs where Gs is the stomatal conductance (Morison et al., 2008). This is a more conservative measure of WUE as it removes some of the influence and hence variability introduced by the environment by comparing photosynthetic parameters independent of evaporative demand (Seibt et al., 2008).

The intrinsic water use efficiency of the HvEPFL1OE-A line was significantly higher than that of the empty vector control under well-watered conditions (Dunnett's multiple comparisons test after one-way ANOVA, $p<0.05$). HvEPFL1OE-A had a mean intrinsic water use efficiency of 94.3 mmol $CO_2 mol^{-1} H_2O$, representing a percentage increase of 27.8% of the control mean intrinsic water use efficiency (73.8 mmol $CO_2 mol^{-1} H_2O$) (see figure 4.4 A). Under drought conditions the intrinsic water use efficiency of the *HvEPFL1* ectopic expression lines was not statistically distinct from empty vector control values (one-way ANOVA, $p>0.05$) (see figure 4.4 B). The improvement in intrinsic water use efficiency in HvEPFL1OE-A occurs as a consequence of the small drop in assimilation in contrast to the larger drop in stomatal conductance. Assimilation initially increases in a linear manner as stomatal conductance before saturating at higher conductance values when CO_2 availability for assimilation (Ci) is no longer the limiting factor in photosynthesis. Consequently, any drop in stomatal conductance within the range of conductance values where Ci is not limiting and hence assimilation is saturated can yield significant WUE improvements without a large drop in assimilation (section 1.3.3, Yoo et al., 2009).

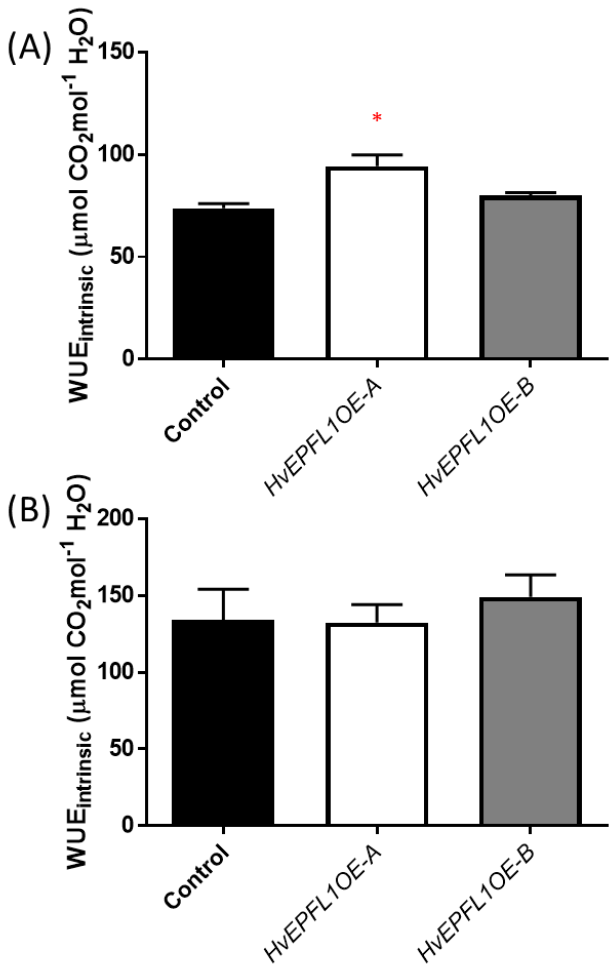

Figure 4.4- Ectopic overexpression of *HvEPFL1* significantly increases the intrinsic WUE (WUEi) of the HvEPFLOE-A line under well-watered conditions. Comparison of the mean WUEi in two independent T2 HvEPFL1 overexpressing transgenic lines with the mean WUEi in an empty vector control line using steady state gas exchange analysis under well-watered (A) and droughted (B) conditions. N=5. Error bars signify SE. Asterisk indicates significant decrease in HvEPFL1 overexpressing transgenic lines of the mean WUEi relative to the empty vector control (Dunnett's multiple comparisons test after one-way ANOVA, $p<0.05$).

4.4- Light response curves

In order to identify the light intensity required to achieve light saturation (the light saturation point) for A-Ci curves and to identify whether *HvEPFL1* ectopic overexpression has an effect on photosynthetic rate under varying light intensity light response curves were generated as described in section 2.8.5. The resulting unfitted data is plotted in figure 4.5. For the light intensities from 1600µmolm^{-2}s^{-1} upwards HvEPFL1OE-A exhibited significantly reduced assimilation relative to the empty vector control (Dunnett's multiple comparisons test following two-way ANOVA, $p<0.05$). Beneath 1600µmolm^{-2}s^{-1} there was no significant difference in the rate of assimilation between the HvEPFL1 ectopic overexpressors and the empty vector control (Dunnett's multiple comparisons test after two-way ANOVA, $p<0.05$). This would suggest that the effect of stomatal density on assimilation rate is dependent on light intensity. The assimilation rate at 200 µmolm^{-2}s^{-1} is not significantly different here, in contrast to the previous finding in the steady state gas exchange experiment (see figure 4.1 A). This is likely due to the increased error as a consequence of single readings at each light intensity being used to form the light curve for each plant, instead of the averaged readings taken over 5 minutes for the steady state readings. Moreover each light intensity, with the exception of 1900 µmolm^{-2}s^{-1} intensity at which the plants were initially acclimated, was only maintained for 2-4 minutes. This is insufficient time for the stomatal conductance to adapt fully to the diminishing light intensity, resulting stomata that are more open than they would be if they were allowed to completely adjust to the new light intensity.

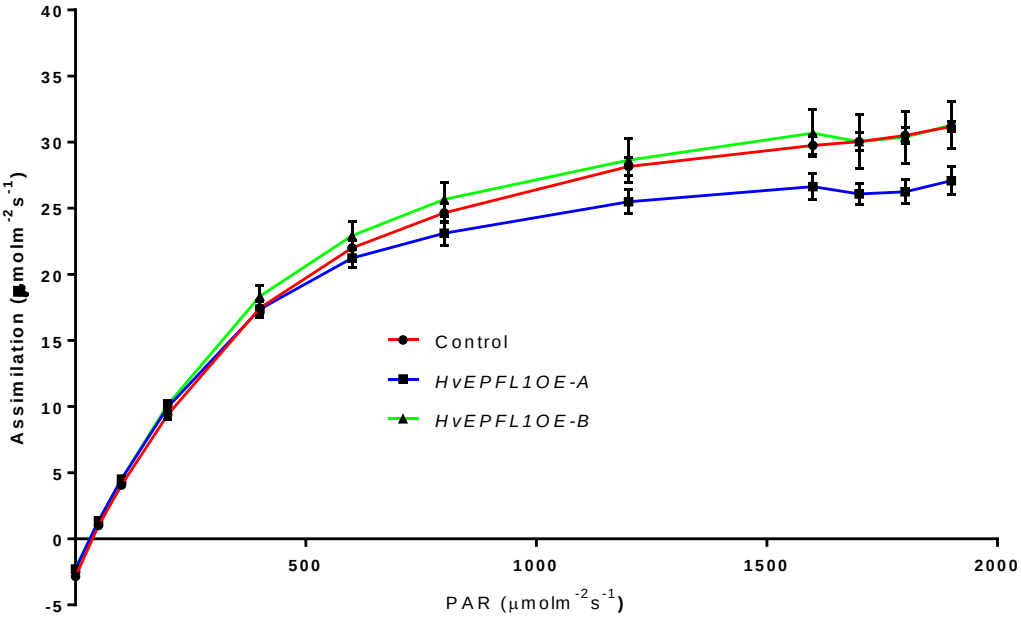

Figure 4.5- Light curves demonstrating the positive correlation between PAR and the rate of assimilation. Control (black circle, red line), HvEPFL1OE-A (black square, blue line) and HvEPFL1OE-B (black triangle, green line) leaves were exposed to a descending series of light intensities at ambient CO_2. N=5. Error bars signify SE.

The light curves were fitted using an excel spreadsheet utilising the model of Ye, 2007 obtained from Lobo et al., 2013 to identify a selection of parameters to further characterise the effect of *HvEPFL1* overexpression on the light response.
Neither the light compensation point nor the quantum yield of the HvEPFL1OE-A and HvEPFL1OE-B lines was statistically distinct from empty vector control values (one-way ANOVA, $p>0.05$) (see figure 4.6 A and 4.6 B). This suggests that the light-dependent processes are not disrupted as a consequence of *HvEPFL1* ectopic overexpression.

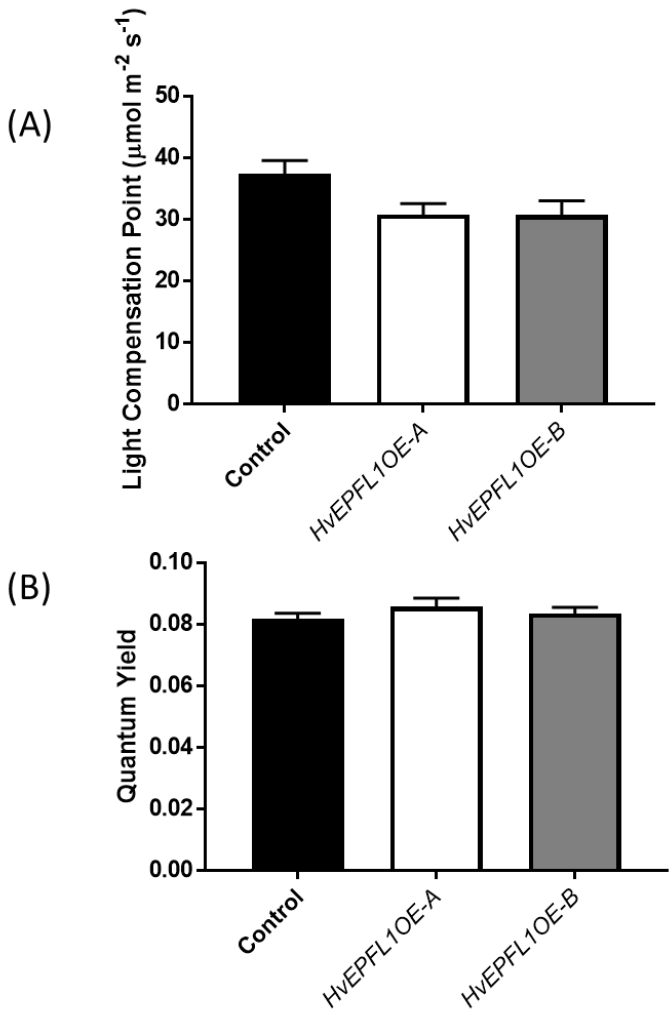

Figure 4.6- Ectopic overexpression of *HvEPFL1* does not significantly affect the light compensation point (LCP) nor the quantum yield. Comparison of the LCP (A) and quantum yield (B) of two independent T2 HvEPFL1 overexpressing transgenic lines with the LCP (A) and quantum yield (B) of an empty vector control line from fitted light curves. N=5. Error bars signify SE. There was no significant difference between the overexpressors and the controls (Dunnett's multiple comparisons test after one-way ANOVA, $p>0.05$).

The light saturation point of the HvEPFL1OE-A and HvEPFL1OE-B lines was not different from empty vector control values. (one-way ANOVA, $p>0.05$) (see figure 4.7 A). The light saturation point for the lines varied between 2009 $\mu molm^{-2}s^{-1}$ in the control to 1830 $\mu molm^{-2}s^{-1}$ in the HvEPFL1OE-A line. As a consequence of this the light level for the A-Ci

curves was set at 1900 µmolm^{-2}s^{-1}, the closest achievable light intensity to the light saturation point for the li6400 unit being utilised.

The theoretical maximum gross photosynthetic rate (P_{gmax}) at saturating light of the HvEPFL1OE-A line was significantly lower than that of the empty vector control (Dunnett's multiple comparisons test after one-way ANOVA, $p<0.05$). HvEPFL1OE-A had a mean P_{gmax} of 29.5 mmolm^{-2}s^{-1} representing 85.5% of the control mean P_{gmax} (34.5 mmolm^{-2}s^{-1}) (see figure 4.7 B). This confirms that the effect of stomatal density on assimilation is dependent on light intensity.

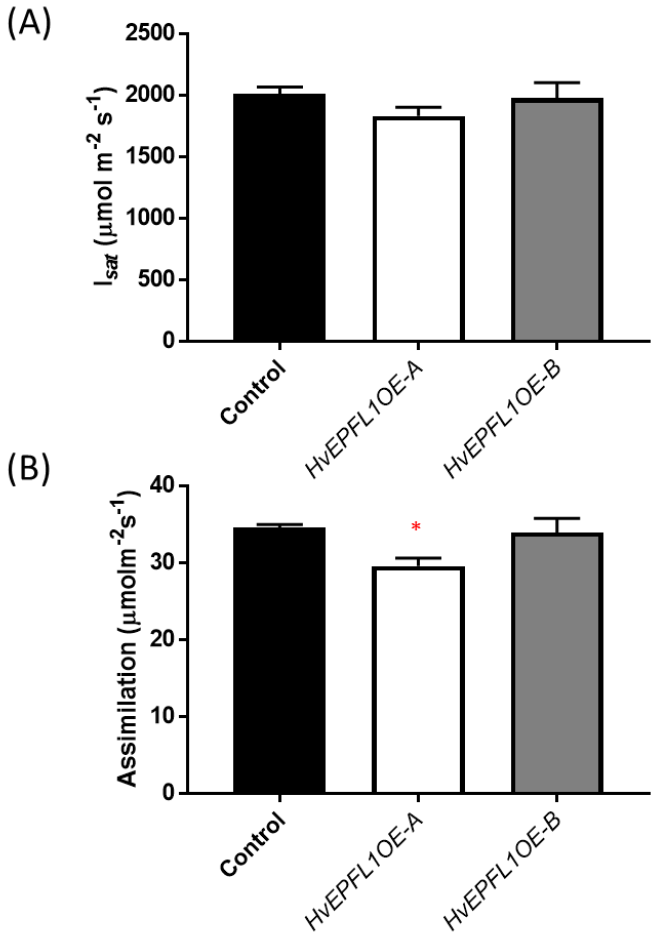

Figure 4.7- There is no significant effect of *HvEPFL1* ectopic overexpression on the light saturation point (I_{sat}), but the theoretical maximum gross photosynthetic rate (P_{gmax}) is significantly decreased in the HvEPFL1OE-A line. Comparison of the I_{sat} (A) and P_{gmax} (B) of two independent T2 HvEPFL1 overexpressing transgenic lines with the corresponding I_{sat} (A) and P_{gmax} (B) of an empty vector control line from fitted light curves. N=5. Error bars signify SE. Asterisk indicates significant decrease in HvEPFL1 overexpressing transgenic lines of the P_{gmax} relative to the empty vector control (Dunnett's multiple comparisons test after one-way ANOVA, $p<0.05$).

The stomata of the HvEPFL1 ectopic expression lines respond to light in the manner expected, with a positive correlation between stomatal conductance and PAR (see figure 4.8). The maximum stomatal conductance of HvEPFL1OE-A line was significantly lower than that of the empty vector control (Dunnett's multiple comparisons test after one-way ANOVA, $p<0.05$). HvEPFL1OE-A had a mean maximum stomatal conductance of 0.189 $molm^{-2}s^{-1}$ representing 63.9% of the control mean maximum stomatal conductance (0.296 $molm^{-2}s^{-1}$) (see figure 4.7 B). Also, the total range of stomatal conductance values was lower in the HvEPFL1 ectopic overexpression lines, 0.0664 $molm^{-2}s^{-1}$ for HvEPFL1OE-A and 0.125 $molm^{-2}s^{-1}$ for HvEPFL1OE-B in contrast to a stomatal conductance range of 0.194 $molm^{-2}s^{-1}$ for the empty vector control. The lower maximum conductance and reduced range are a consequence of the reduction in stomatal density and size observed in the *HvEPFL1* ectopic expression lines, which reduces the maximum total leaf pore area over which gas exchange can occur.

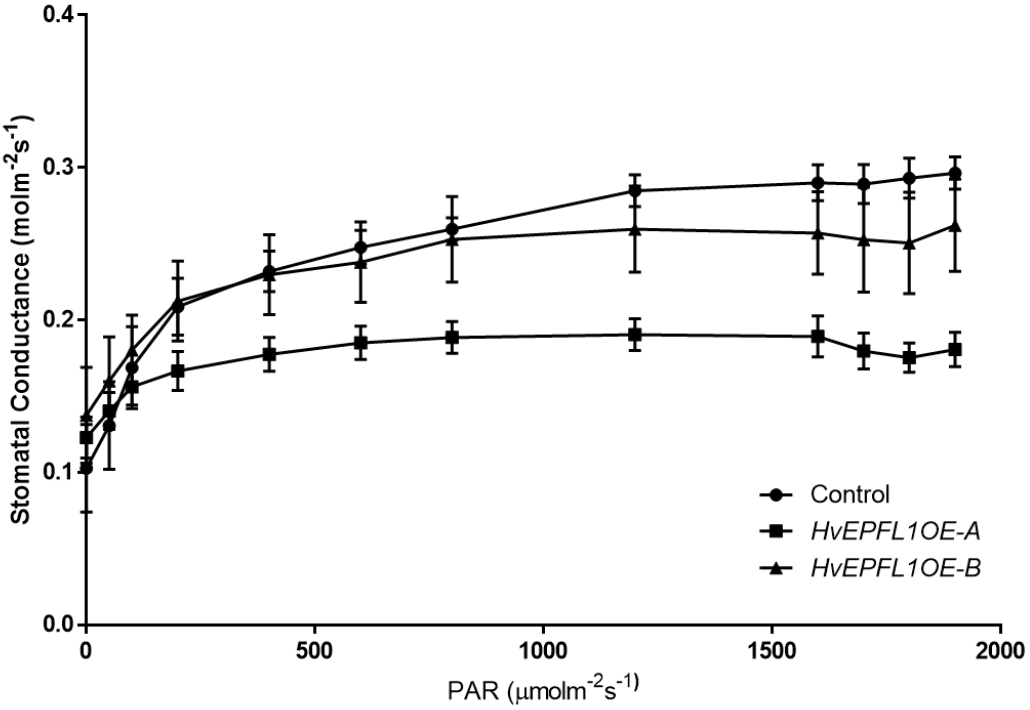

Figure 4.8- Graph demonstrating the positive correlation between PAR and the stomatal conductance. Control (black circle), HvEPFL1OE-A (black square) and HvEPFL1OE-B (black triangle) leaves were exposed to a descending series of light intensities at ambient CO_2. N=5. Error bars signify SE.

4.5- A-Ci curves

Next the response to CO_2 was assessed by subjecting the plants to a range of CO_2 levels at 1900µmol m^{-2} s^{-1} PAR and otherwise ambient conditions and recording the rate of assimilation. The method by which this was done is described in detail in section 2.8.6. The rate of assimilation is plotted against Ci in order to remove the effect of the varying stomatal conductances between the lines so that any differences observed between the lines is as a consequence of variation in underlying biochemistry. The resulting unfitted data for the A-Ci relationship is plotted in figure 4.9.

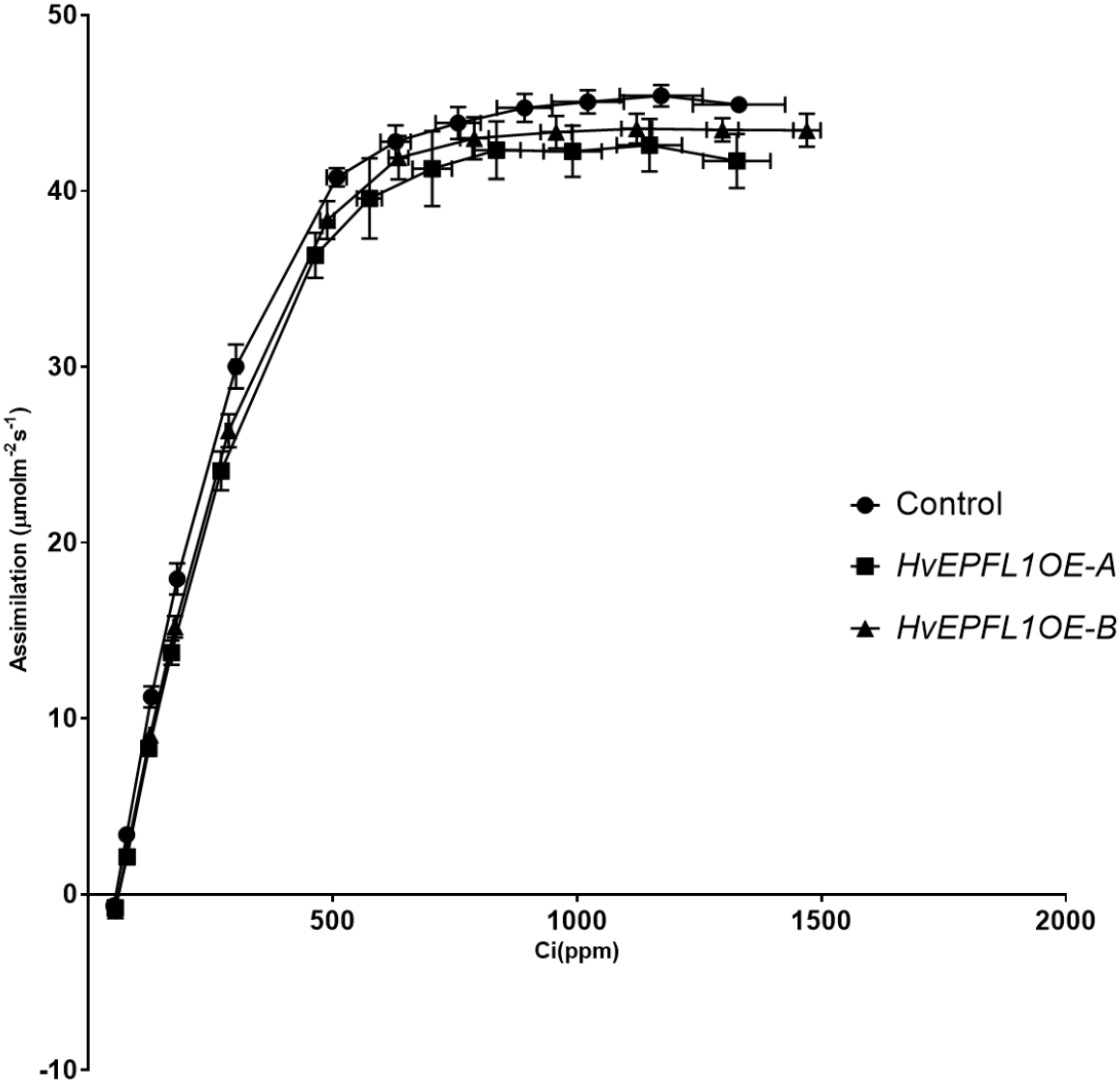

Figure 4.9- The form of the CO_2 response (A-Ci) curves does not differ between genotypes Control (black circle), HvEPFL1OE-A (black square) and HvEPFL1OE-B (black triangle) leaves were exposed to a series of CO_2 concentrations at 1900µmol$m^{-2}s^{-1}$ light intensity. N=5. Error bars signify SE.

The A-Ci curves were fitted using an A-Ci curve fitting tool (www.landflux.org) which fits the C3 photosynthesis model (Farqhuar et al., 1980) following the method of Either and Livingston, 2004. Values for the maximum rate of rubisco carboxylation (Vmax) (see figure 4.10 A), maximum rate of electron transport (Jmax) (see figure 4.10 B) and maximum rate of assimilation (Amax) (see figure 4.10 C) were obtained from the fitted data, none of which differed significantly in the HvEPFL1 ectopic overexpressor lines. Moreover, the stomatal limitation on photosynthesis was assessed using the graphical method (Long and Bernacchi, 2003) and found to be significantly higher in the HvEPFL1 ectopic overexpressor lines compared to the empty vector control (Dunnett's multiple comparisons test after one-way ANOVA, $p<0.05$) (see figure 4.10 D). Taken together these findings demonstrate that photosynthetic biochemistry has not been altered by *HvEPFL1* overexpression and that the differences in CO_2 response are as a consequence of stomatal rather than non-stomatal limitations on photosynthesis.

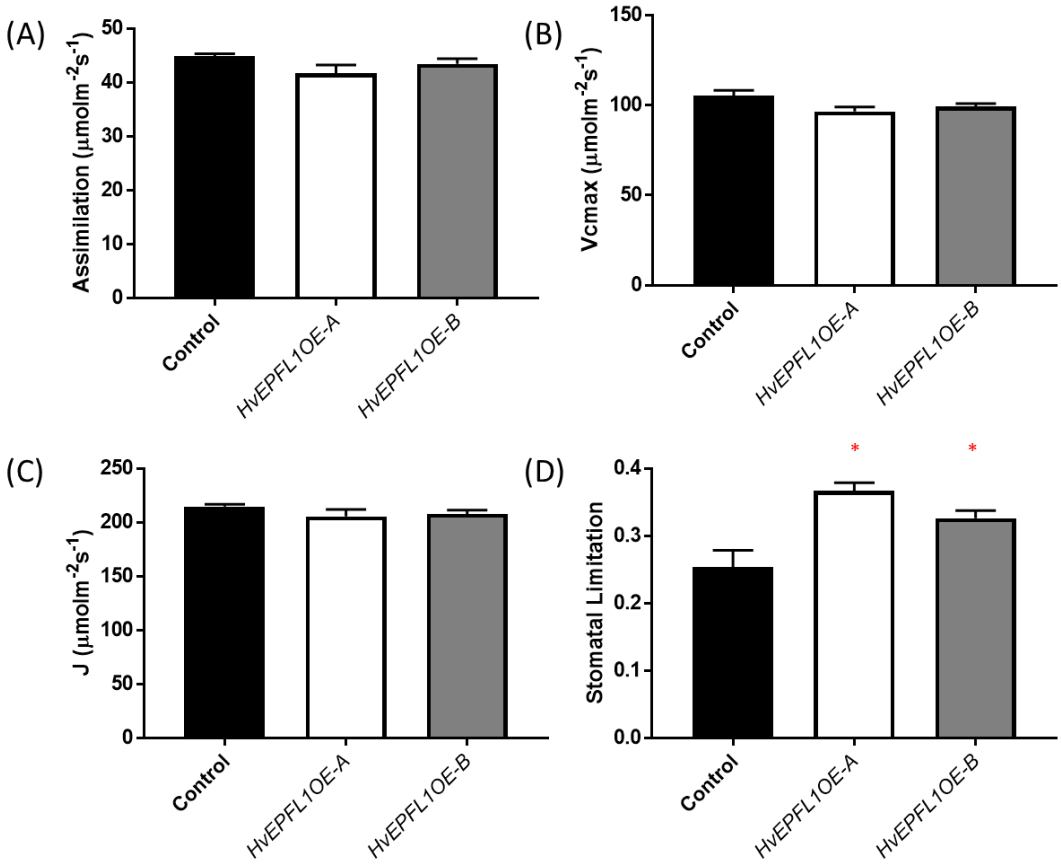

Figure 4.10- Ectopic overexpression of *HvEPFL1* does not significantly affect the underlying biochemistry of photosynthesis. Comparison of the maximum rate of carbon assimilation (A), maximum rate of ribulose-1,5-bisphosphate (RuBP) carboxylase/oxygenase (Rubisco) carboxylation Vcmax (B), maximum rate of electron transport (C) and the calculated stomatal limitation (D) of two independent T2 HvEPFL1 overexpressing transgenic lines with those of an empty vector control line. N=5. Error bars signify SE. Asterisk indicates significant increase in HvEPFL1 overexpressing transgenic lines of the stomatal limitation on photosynthesis relative to the empty vector control (Dunnett's multiple comparisons test after one-way ANOVA, $p<0.05$).

4.6- Conclusions

- HvEPFL1 overexpression significantly reduces the rate of carbon assimilation and stomatal conductance under both ambient, well-watered conditions relative to controls.
- The most severe stomatal density reduction line, HvEPFL1OE-A, shows improves intrinsic water use efficiency and reduced transpiration under ambient well-watered conditions relative to controls.
- The improvement in intrinsic water use efficiency in HvEPFL1OE-A occurs as a consequence of the small drop in assimilation in contrast to the larger drop in stomatal conductance. Assimilation initially increases in a linear manner as stomatal conductance before saturating at higher conductance values when CO_2 availability for assimilation (Ci) is no longer the limiting factor in photosynthesis. Consequently, any drop in stomatal conductance within the range of conductance values where Ci is not limiting and hence assimilation is saturated can yield significant WUE improvements without a large drop in assimilation (section 1.3.3, Yoo et al., 2009).
- There is no effect of overexpressing HvEPFL1 on the underlying biochemistry of photosynthesis, with the changes in gas exchange observed occurring as a consequence of stomatal limitations on photosynthesis, i.e. reduced Ci supply.
- There is no improvement in photosynthetic traits under drought suggesting that under the severe drought imposed, stomatal closure in response to drought is equalising the exchange area through which gas exchange can occur, resulting in a similar stomatal conductance and an equally constrained rate of CO_2 assimilation in both the HvEPL1 ectopic overexpression lines and the empty vector control line.

Chapter 5- The effect of overexpressing *HVEPFL1* on growth and drought tolerance in *Hordeum vulgare*

5.1- Introduction

In chapter 4 it was demonstrated that by reducing stomatal density in barley it is possible to produce plants with significantly increased water use efficiency. Whilst this is a useful trait in and of itself, increased water use efficiency and/or drought tolerance is often found to occur in tandem with other, less desirable traits such as slower growth rate and lower assimilation (Flexas et al., 2004; Lawson and Blatt, 2014, figure 4.1 A for assimilation) as well as reduced leaf area, reduced tillering, fewer leaves and earlier flowering with reduced yield (Blum, 2004). It is therefore necessary to assess the growth and yield in order to appraise whether or not reduced stomatal density could be used as an approach to future proof crops against climate change. A high WUE plant that yields poorly is of limited value in agricultural terms. Moreover, in terms of producing crop plants that are adapted to future, low water environments there are significant advantages to breeding for improved drought tolerance as well as improved water use efficiency. Given that the *HvEPFL1* ectopic expression lines have significantly reduced stomatal conductance and so have reduced water loss, it seemed likely they would prove to be more drought tolerant as well. In this chapter, the early growth of the HvEPFL1 ectopic expression lines is described, as is their physiology at harvest, including appraisal of the yield. It ends with an appraisal of the drought tolerance in the transgenic lines.

5.2- Methods summary

5.2.1-Early growth and development

The time taken to germinate and the germination success rate were assessed with successful germination being recorded when the individual plant reached Zadoks stage 07. Once the third leaf was fully expanded growth measurements were carried out every 3 days. This included counting the total number of leaves, both fully expanded and developing, as well as the total number of tillers in order to assess growth.

5.2.2- Harvesting

Growth and yield under 60% and 25% watering regimes was assessed at the end of the lifecycle of control and transgenic barley plants used for the gas exchange analysis discussed in chapter 4. For each plant, the total number of tillers, including the number of spike-bearing tillers and prematurely senescing tillers, as well as the total number of leaves were counted and the height of the primary tiller measured. The above ground vegetative tissue was dried down at 80^{o}C for 2 days and weighed to obtain the dry weight of the shoots and leaves. The grains were counted and weighed per ear and the sum of the number and weight of grain on all the ears of individual plants recorded as the total grain number and the yield respectively. The average weight of individual seeds for each plant was calculated as was the harvest index (see section 2.10.3). ΔC analysis was carried out to assess life time WUE (see section 2.10.4).

5.2.3- drought tolerance experiment

In order to assess drought tolerance, control and transgenic barley plants were grown until Zadoks stage 21. Half the plants of each line were then maintained at the initial watering level (60% soil water content) whilst watering was withheld from the other half. Drought tolerance was assessed by both monitoring the rate at which soil water was utilised by water restricted plants via pot weighing in order to test for drought avoidance (see section 2.12.2) and by monitoring plant stress using the light-adapted quantum yield of photosystem II (QY or Fv'/Fm') as a proxy (see section 2.12.3). Relative water content of leaves excised from both droughted and well-watered plants was measured on day 6 of the drought treatment (see section 2.12.4).

5.3- Effect of HvEPFL1 OE on early growth

During the initial screen of transgenic lines it was apparent that germination rate in the HvEPFL1 ectopic overexpression lines was diminished in contrast to the germination rate in the controls. Therefore, once the lines HvEPFL1OE-A and HvEPFL1OE- B were selected their rate of germination was determined utilising the method outlined in section 2.11. Both ectopic overexpression lines showed a delayed and slower rate of germination compared to the empty vector control (see figure 5.1). Moreover, whilst 100% of the empty vector controls successfully germinated (here defined as reaching Zadoks stage 07) only 75% and 87.5% of HvEPFL1OE-A and HvEPFL1OE-B seeds germinated respectively. *HvEPFL1* is known

to be expressed in embryonic tissue (Mayer et al., 2012), so it is possible that it possesses an unknown function in the process of germination or early growth establishment that can be fatally disrupted by its overexpression. Interestingly, referring back to the initial screen, ectopic *HvEPFL1* overexpression lines exhibiting the highest copy numbers and the lowest stomatal densities also exhibited the lowest seed viability, suggesting a connection between gene dosage and germination disruption. Alternatively, the reduced carbon assimilation in the ectopic overexpressors (see figure 4.1 A) could have reduced the supply of available photosynthate during seed development, producing grains with insufficient energy stores for germination.

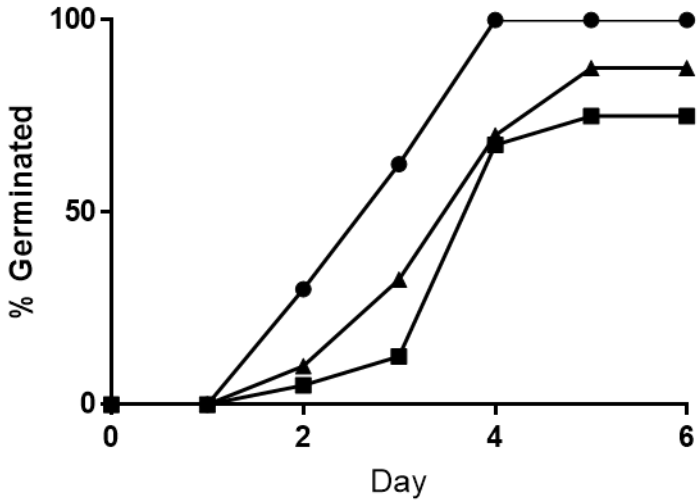

Figure 5.1- *HvEPFL1* ectopic overexpression lines display delayed germination and reduced grain viability relative to the control line. 40 T3 seeds each of the empty vector control (black circle), HvEPFL1OE-A (black square) and HvEPFL1OE-B (black triangle) lines were scored for germination.

Following germination, the ectopic *HvEPFL1* overexpression lines continue to display delayed development in comparison to the empty vector controls under well-watered and droughted conditions (60% and 25% maintained soil water content respectively). Development was assessed by monitoring two simple growth characters that are affected by plant water relations, leaf number and tiller number, as described in sections 2.11 and 5.2.1.

Under well-watered conditions leaf number tended towards being lower in the ectopic overexpressors and was statistically significantly lower than the leaf number values of the empty vector control between 18 and 21 days post germination (Dunnett's multiple comparisons test after one-way ANOVA, $p<0.05$) (see figure 5.2 A). Similarly, tiller number was initially significantly lower in the ectopic overexpressors compared to the empty vector control up until 21 days post-germination (Dunnett's multiple comparisons test after one-way ANOVA, $p<0.05$) (see figure 5.2 C). In contrast under the 25% soil water content treatment both the control and the HvEPFL1 ectopic overexpression lines showed the same initial growth rates for both tiller and leaf number. However, from 18 days post-germination the most severely reduced density line, HvEPFL1OE-A, demonstrated significantly delayed growth for both leaf number and tiller number in comparison to both the empty vector control and HvEPFL1OE-B (Tukey's HSD multiple comparisons test after one-way ANOVA, $p<0.05$) (see figure 5.2 B and D). This delay in early growth could be the result of the lower rate of CO_2 assimilation seen in the HvEPFL1OE ectopic expression lines, as demonstrated in the gas exchange experiment (see figure 4.1 A).

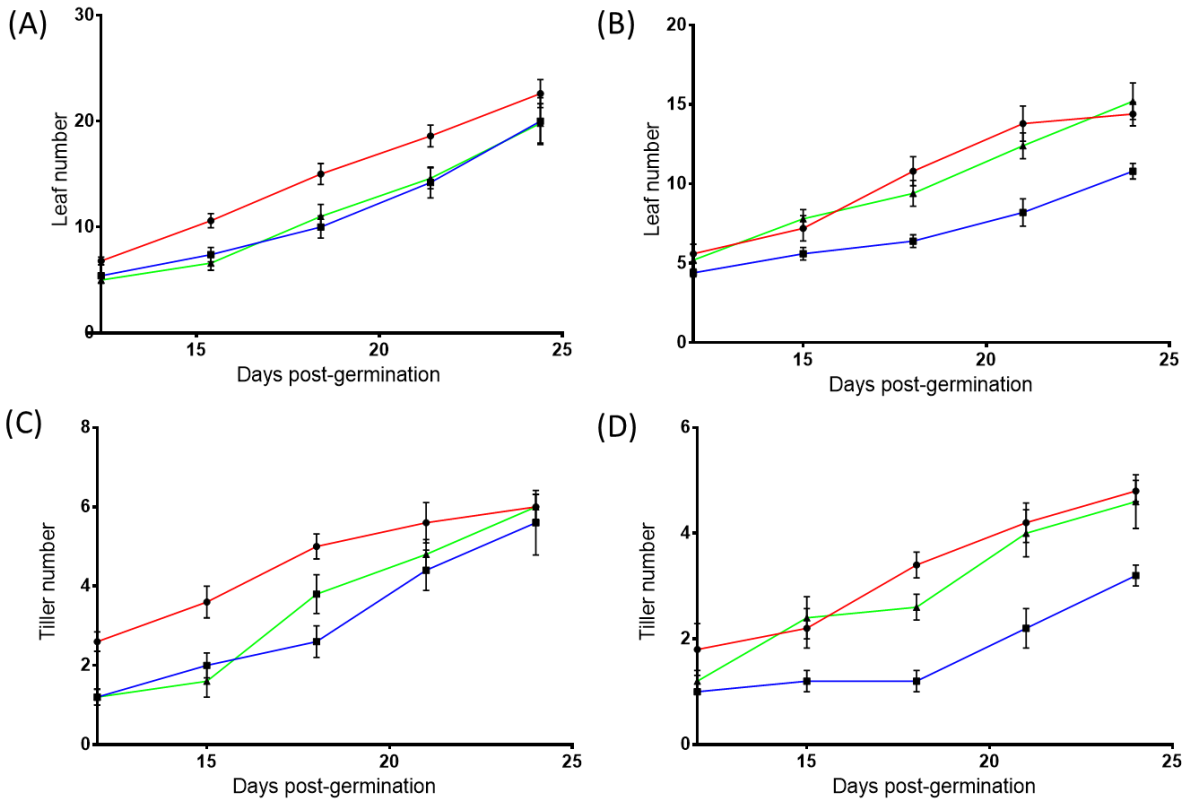

Figure 5.2- *HvEPFL1* ectopic overexpression lines display altered patterns of growth in the early stages of development under well-watered and droughted conditions. Graphs of early growth in leaf number and tiller number against days post-germination for the empty vector control (black circle, red line), HvEPFL1OE-A (black square, blue line) and HvEPFL1OE-B (black triangle, green line). A and C measured under 60% soil water content, B and D under 25% soil water content. N=5. Error bars signify SE.

5.4- Effect of HvEPFL1 OE on plant physiology and yield

In order to ascertain the effect of ectopic *HvEPFL1* overexpression on yield and total vegetative growth under both well-watered and droughted watering regimes the plants utilised for the gas exchange experiments described in chapter 3 were grown to seed set. Whilst the initial growth of the ectopic *HvEPFL1* overexpression lines was delayed relative to the empty vector control (see figure 5.2), by the end of the barley life cycle there was no significant difference in most of the basic physiological measures of growth. For example

there was no significant difference in the final leaf number between the HvEPFL1 ectopic overexpressor lines and the empty vector control under either of the watering regimes (separate one-way ANOVA for each watering regime, in both cases $p<0.05$) (see figure 5.3 A). Similarly, the maximum height of the primary tiller showed no significant change in the HvEPFL1 ectopic overexpressors in comparison to the empty vector control in either of the watering regimes (separate one-way ANOVA for each watering regime, in both cases $p<0.05$) (see figure 5.3 B). For both traits in all lines there was a significant reduction under drought conditions (individual unpaired t-tests, $p<0.05$).

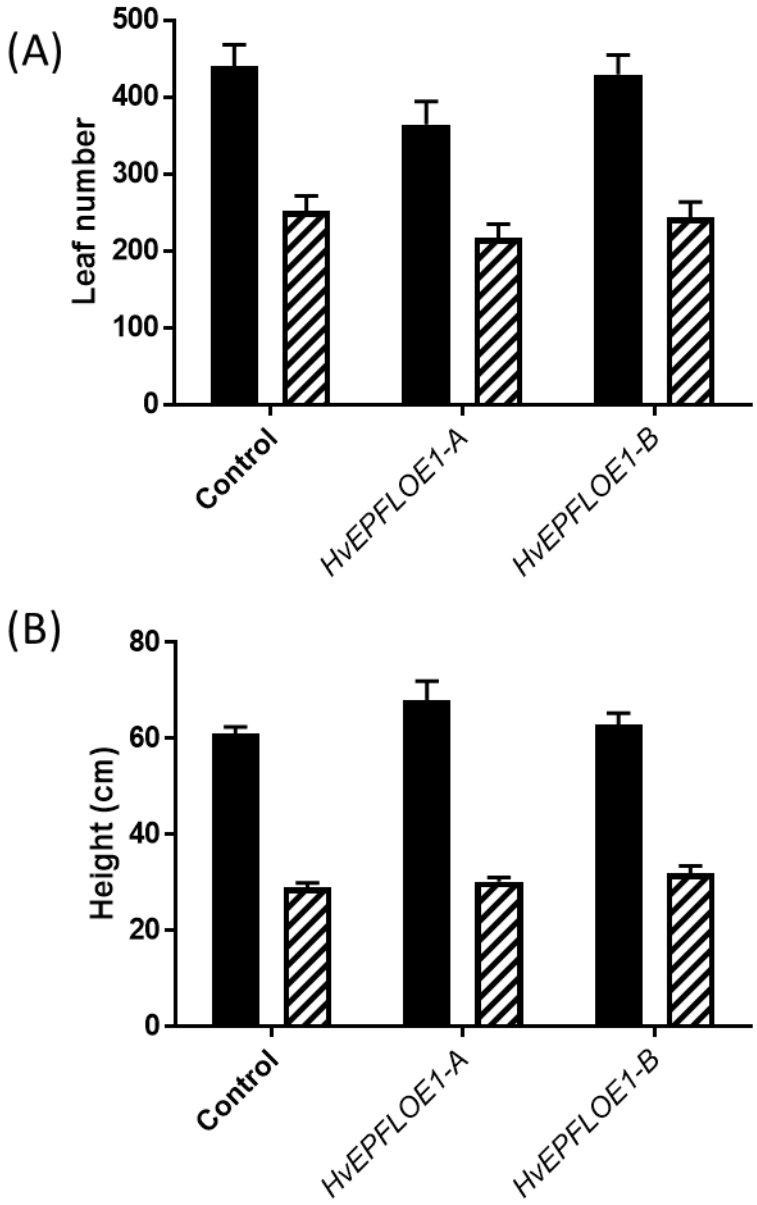

Figure 5.3- Final height and final leaf number at harvest do not significantly differ from controls in *HvEPFL1* ectopic overexpression lines under both well-watered and droughted conditions. Black bars represent 60% soil water content treatment, striped bars represent 25% soil water content. N=5. Error bars signify SE. There was no significant difference in final leaf number or final height of the primary tiller between the empty vector control and the HvEPFL1 ectopic overexpression lines within either watering regime. (one-way ANOVA, $p>0.05$).

Furthermore, there was no significant difference in total above ground biomass (the sum of the dry weight of the vegetative tissue and the grain) between the *HvEPFL1* ectopic overexpressors and the empty vector control in either of the watering regimes (separate one-way ANOVA for each watering regime, in both cases $p>0.05$) (see figure 5.4 A) with the plants appearing superficially similar within treatments (see figure 5.4 B). The absence of a significant change in biomass, as well as the lack of change in leaf numbers and tiller height (figure 5.3) suggests that the reduction in photosynthetic rate observed at ambient conditions (see figure 4.1 A) does not translate into reduced growth as one might have hypothesised. This could be due to the reduced stomatal conductance and consequent reduction in water loss allowing the allocation of resources to grain filling and development of above ground biomass at the expense of root development as seen in *Arabidopsis thaliana* EPF transgenics i.e. there is a reduced requirement for roots when water losses are low with a positive correlation between stomatal density and root size (Hepworth et al., 2016).

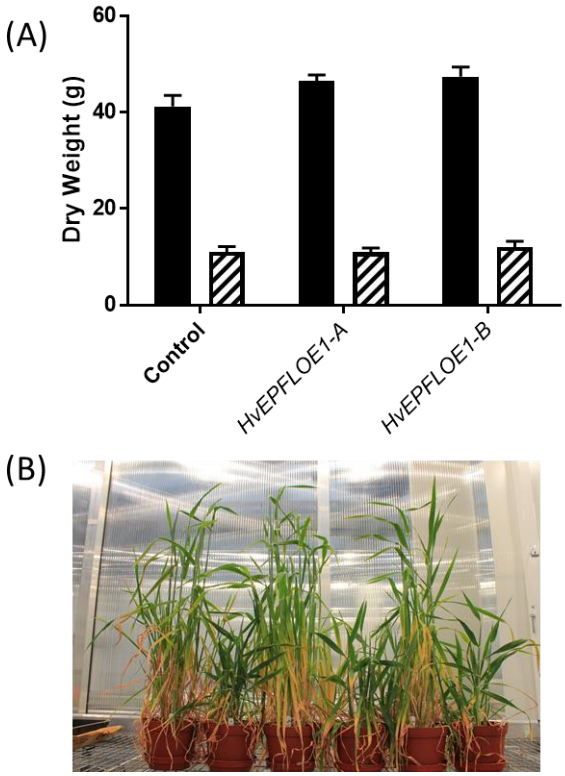

Figure 5.4- Total above ground biomass at harvest does not significantly differ from controls in *HvEPFL1* ectopic overexpression lines under both well-watered and droughted conditions. (A) Graph of above ground biomass at harvest for the empty vector control, HvEPFL1OE-A and HvEPFL1OE-B under both watering regimes. Black bars represent 60% soil water content treatment, striped bars represent 25% soil water content. N=5. Error bars signify SE. There was no significant difference in total above ground biomass at harvest between the empty vector control and the HvEPFL1 ectopic overexpression lines within either watering regime. (one-way ANOVA, $p>0.05$).

(B) digital image of plants demonstrating the similar growth habit of the different lines within each watering regime. Ordered left to right: Control 60%, Control 25%, HvEPFL1OE-A 60%, HvEPFL1OE-A 25%, HvEPFL1OE-B 60%, HvEPFL1OE-B 25%.

One aspect of vegetative growth that is different in the ectopic HvEPFL1 overexpressors is the degree to which tillering occurs. The total number of tillers formed in the HvEPFL1OE-A line was significantly lower than that of the empty vector control under well-watered conditions (Dunnett's multiple comparisons test after one-way ANOVA $p<0.05$). HvEPFL1OE-A had a mean total tiller number of 45.75 tillers, approximately a third fewer than the control mean total tiller number (68.8 tillers) (see figure 5.5 A). Under droughted conditions there was no difference between any of the lines in terms of total number of tillers formed (one-way ANOVA $p>0.05$). As expected there was a significant decline in tiller numbers between watering treatments for all lines (individual unpaired t-tests $P<0.05$)

The tillers can be grouped into two distinct sets, those that produce an ear (spike-bearing) and those that prematurely senesce without producing an ear. Interestingly the number of spike-bearing tillers does not significantly differ in either of the ectopic HvEPFL1 overexpression lines under either watering regime (one-way ANOVA $p>0.05$), despite the overall reduction in tillering seen in HvEPFL1OE-A (see figure 5.5 B). The difference in the total number of tillers is instead a consequence of the greater number of non-seed producing tillers found in the empty vector control line. The total number of non-ear bearing tillers formed in the ectopic HvEPFL1 overexpression lines was significantly lower than that of the empty vector control under well-watered conditions (Dunnett's multiple comparisons test after one-way ANOVA $p<0.05$). HvEPFL1OE-A had a mean total non-ear bearing tiller number of 23 tillers whilst HvEPFL1OE-B had a mean total non-ear bearing tiller number of 32.75 tillers, representing 45.7% and 65.2% of the control mean total non-ear bearing tiller number (50.25 tillers) (see figure 5.5 C). Unlike in the case of the total number of tillers and the spike-bearing tillers, there is no significant decrease in ear bearing tiller numbers in the ectopic HvEPFL1 overexpression lines between watering treatments, i.e. the number of non-yielding tillers does not decrease under drought.

It appears that under well-watered conditions there is increased investment in tillering in the empty vector control relative to the ectopic overexpressors but the additional tillers fail to produce ears. The maximum tiller number is important in that it is the primary determinant of maximum possible yield achievable (Garcia del Moral and Garcia del Moral, 1995) so in the absence of other limitations, such as nutrients, the maximum yield of the control could be significantly greater than the HvEPFL1 overexpressors. However it appears that, under the conditions the experiment was carried out in, there were insufficient resources for the control plants to capitalise on the additional tillers to produce additional

ears under well-watered conditions and no difference in the maximum tillering rate under drought.

An additional observation was that both the HvEPFL1 ectopic overexpression lines exhibited delayed flowering relative to the control. Flowering time was recorded as the time the primary tiller achieved Zadoks stage 59, i.e. complete ear emergence, with the flowering time of the transgenic lines being recorded relative to the mean time for control flowering. HvEPFL1OE-A flowered on average 8.6 days after the control whilst HvEPFL1OE-B flowered on average 6 days after the control. Whilst the growth cycle of barley in production is carried out in accordance to a tight schedule a delay of approximately one week does not constitute an agronomic problem. However, if the delay in flowering is greater under natural conditions than it is under the relatively controlled conditions that these plants were grown under then there could be issues in terms of field application.

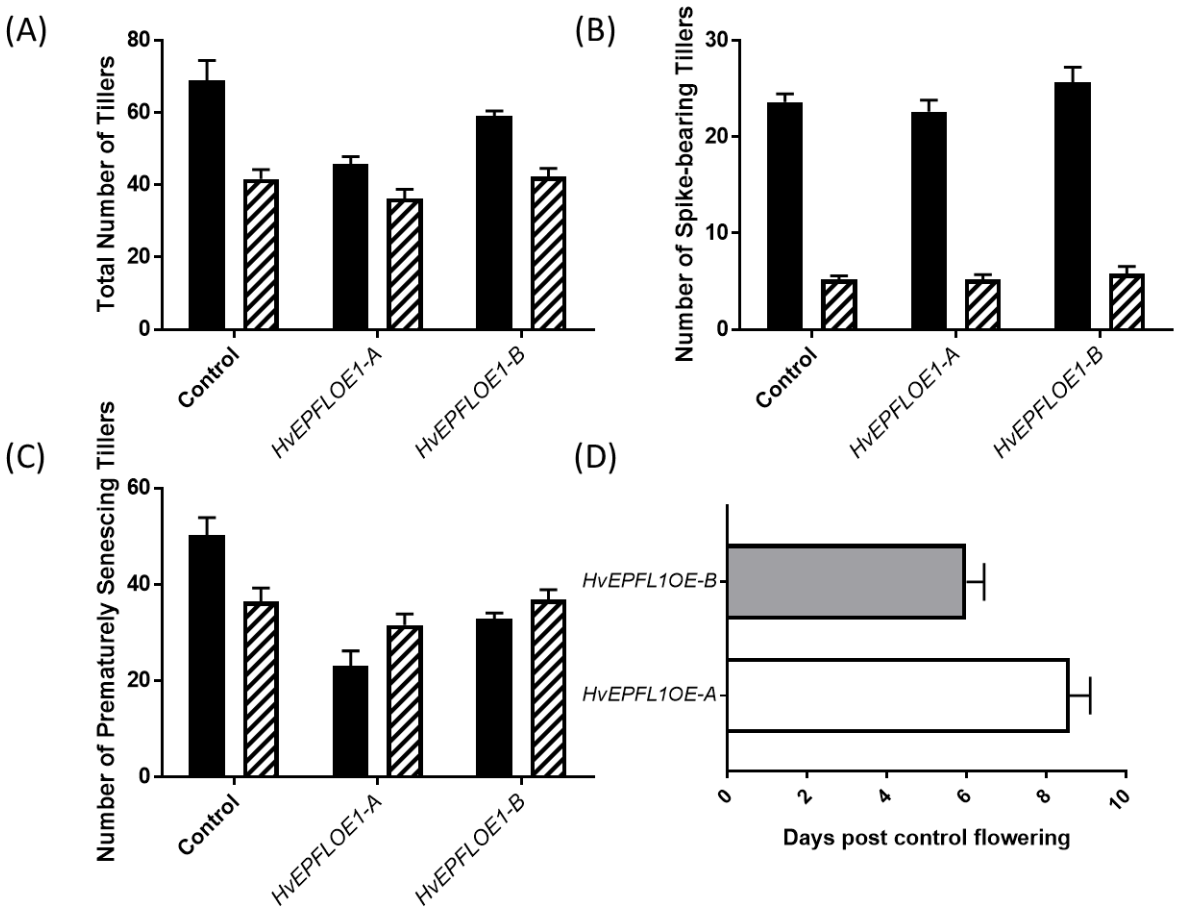

Figure 5.5- *HvEPFL1* ectopic overexpression reduces tillering and delays flowering. Comparison of the total number of tillers formed(A), the number of those tillers that give rise to an ear (B) and number of those tillers that do not (C). Black bars represent 60% soil water content treatment, striped bars represent 25% soil water content. (D) number of days after the control had flowered that the ectopic overexpressors flowered. N=5. Error bars signify SE.

The most important aspect of physiological growth in terms of agricultural applications is of course the grain, especially the yield. There was no significant difference in seed number, average weight per seed, yield or harvest index (the ratio of yield to above ground biomass) between the *HvEPFL1* ectopic overexpressors and the empty vector control in either of the watering regimes (one-way ANOVA, $p>0.05$) and as expected all traits diminished in all lines under drought in comparison to well-watered conditions (unpaired t-tests, $p<0.05$) (see figure 5.6). That improvements in intrinsic and long-term WUE (see figure 4.4 A and figure 5.7) can be achieved though stomatal density reduction without deleterious effect on yield is a significant result. Although there was no significant difference in yield between the lines under drought conditions, which was quite severe in terms of water supply, it is conceivable that under more moderate drought stress *HvEPFL1* ectopic overexpressors could achieve superior yield to the controls due to this improved WUE.

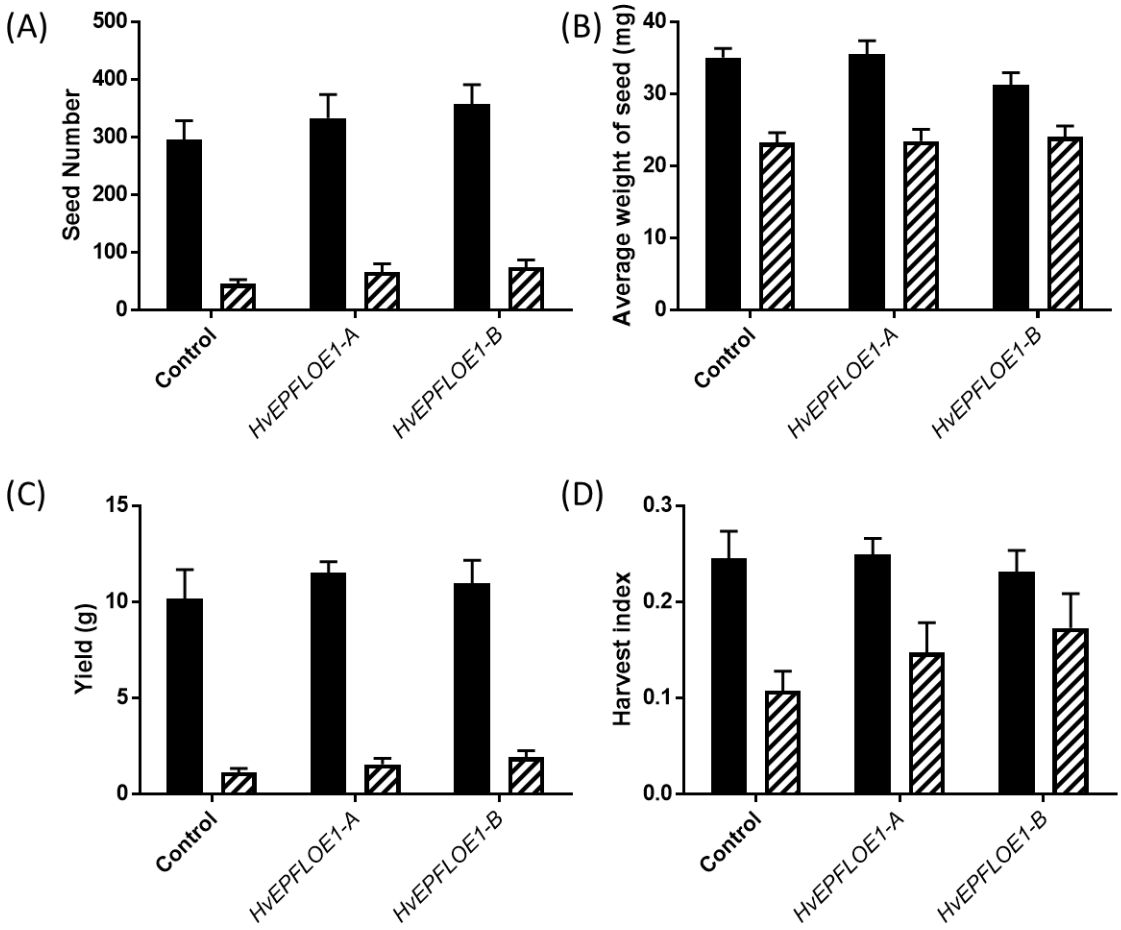

Figure 5.6- Seed number, average weight, yield and harvest index do not significantly differ from controls in *HvEPFL1* ectopic overexpression lines under both well-watered and droughted conditions. Graphs of seed number (A), average weight per seed (B), yield (C) and harvest index (D) for the empty vector control, HvEPFL1OE-A and HvEPFL1OE-B under both watering regimes. Black bars represent 60% soil water content treatment, striped bars represent 25% soil water content. N=5. Error bars signify SE. There was no significant difference between the empty vector control and the HvEPFL1 ectopic overexpression lines within either watering regime for any of the traits. (one-way ANOVA, $p>0.05$).

Carbon isotope discrimination analysis can be used as a proxy for water use efficiency in C3 plants (Farqhuar et al., 1982; Farquhar and Richards, 1984) and provides an assessment the mean water use efficiency of the analysed tissue over the course of growth and development, in contrast to the snapshot assessment obtained from gas exchange analysis. The isotope analysis demonstrated that under well-watered conditions the HvEPFL1OE-A line was more water use efficient (see figure 5.7 A) as was observed for intrinsic water use efficiency in the gas exchange analysis (see figure 4.4) whilst both HvEPFL1 ectopic expression lines were more water use efficient under drought (see figure 5.7 B). This latter finding differs from the gas exchange analysis which found no increase in water use efficiency under drought, likely due to the different natures of the two methods of assessing WUE, which can occasionally disagree, or differences in sensitivity and scale (Medrano et al., 2015).

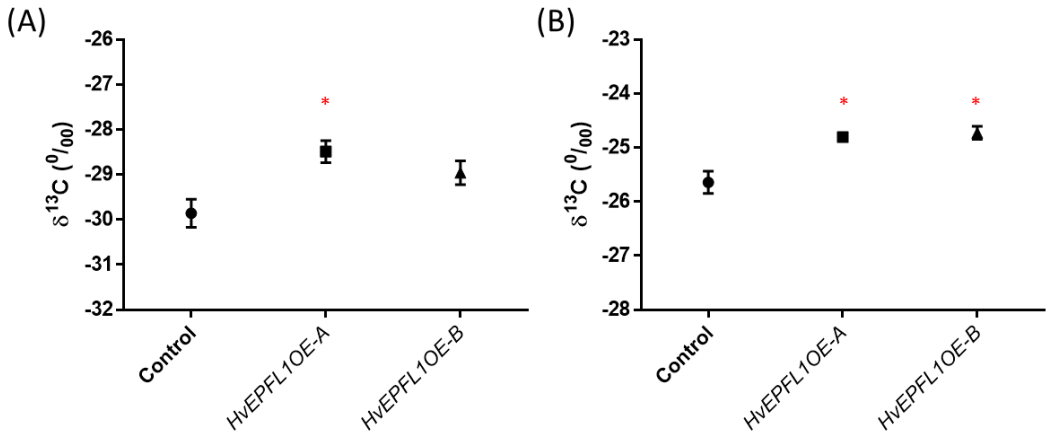

Figure 5.7- Carbon isotope discrimination demonstrated that water use efficiency was significantly improved in HvEPFL1OE-A under well-watered conditions (A) and in both HvEPFL1 ectopic overexpressors under drought (B). Empty vector control (black circle), HvEPFL1OE-A (black square) and HvEPFL1OE-B (black triangle). N=5. Error bars signify SE. Asterisk indicates significant difference in carbon isotope discrimination between HvEPFL1 overexpressing transgenic lines relative to the empty vector control (Dunnett's multiple comparisons test after one-way ANOVA, $p<0.05$).

5.5- Effect of HvEPFL1 OE on drought tolerance

As well as displaying superior long-term water use efficiency, the *HvEPFL1* ectopic expression lines also displayed improved drought tolerance in the withheld water experiment, the method for which is described in section 2.12. Following the cessation of watering both ectopic *HvEPFL1* overexpression lines retained significantly more soil water than the empty vector control from the second day after watering stopped until the 14th day (see figure 5.8). This allowed for dehydration avoidance, where the plant maintains high water status despite drought, by conserving soil water to delay the onset of drought stress relative to the environmental commencement of drought (Blum, 2005).

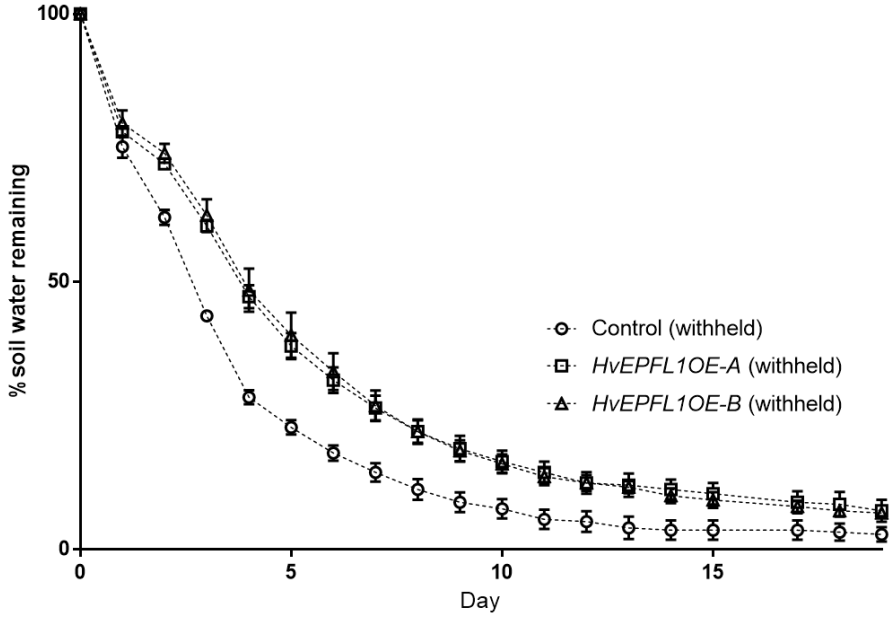

Figure 5.8- *HvEPFL1* ectopic overexpression lines display improved soil water retention relative to controls when water is withheld. Graph of percentage soil water remaining against days post-watering for the empty vector control (circle), HvEPFL1OE-A (square) and HvEPFL1OE-B (triangle). N=5. Error bars signify SE.

The light-adapted quantum yield of photosystem II (QY) declines under drought stress and consequently can be used as a proxy to monitor the onset of stress in plants exposed to drought (Genty et al., 1989; Baker and Rosenqvist, 2004). Following the cessation of watering both ectopic *HvEPFL1* overexpression lines retained QY values at well-watered levels until 13 days after watering stopped whilst the QY values of the empty vector control began to decline 4 days earlier, indicating an earlier initiation of drought stress and

subsequent reduction in photosystem II efficiency in the controls, likely due to the significantly lower soil water availability (figure 5.8). QY declined to zero after 13 days in the empty vector control, with HvEPFL1OE-A reaching zero 4 days later, suggesting that once drought stress commences, the HvEPFL1 overexpressors are as susceptible to the effects of drought stress of photosystem II efficiency as the controls, they can just avoid it for longer (see figure 5.9).

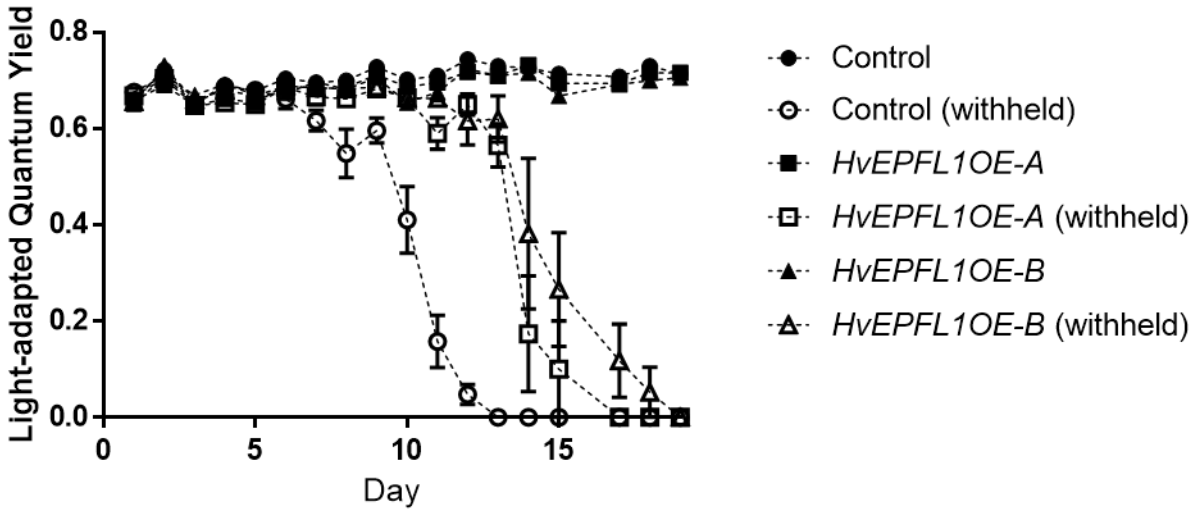

Figure 5.9- *HvEPFL1* ectopic overexpression lines display improved drought stress tolerance relative to controls when water is withheld. Graph of quantum yield (a proxy for drought stress) against days post-watering for the empty vector control (black circle), HvEPFL1OE-A (square) and HvEPFL1OE-B (triangle). Closed symbols for well-watered conditions, open symbols for water withheld. N=5. Error bars signify SE.

6 days after the cessation of watering, the relative water content of leaf samples from plants under both well-watered and water withheld treatments was obtained as described in section 2.12.4. There was no no significant difference in leaf RWC between the ectopic *HvEPFL1* overexpressors and the empty vector control under well-watered conditions (one way ANOVA, $p>0.05$). However, under water-withheld conditions, the relative water content of the leaf samples of both ectopic *HvEPFL1* overexpressors were significantly higher than the relative water content of the controls (Dunnett's multiple comparisons test following one-way ANOVA, $p<0.05$), demonstrating improved drought tolerance through maintaining a higher plant water status (see figure 5.10 A). Indeed, by day 6 the water

withheld controls were visibly wilting whilst the *HvEPFL1* ectopic overexpressors maintained turgor (see figure 5.10 B).

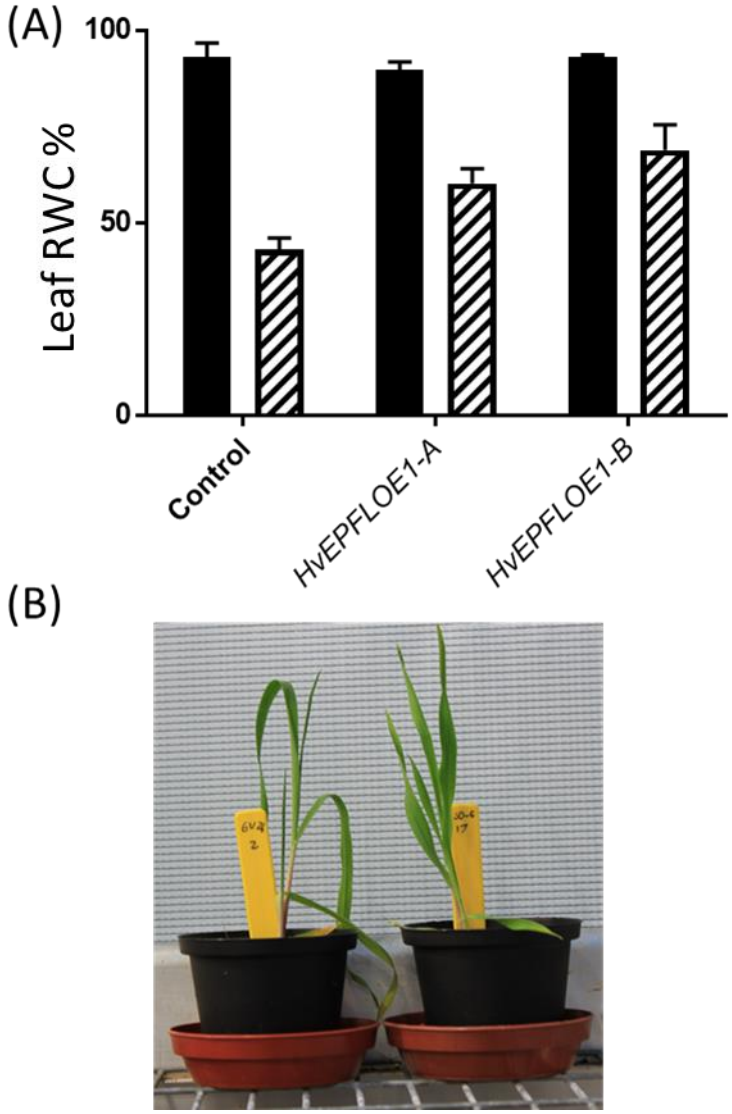

Figure 5.10- *HvEPFL1* ectopic overexpression lines maintain leaf turgor for longer when water is withheld. (A) Graph of leaf relative water content for the empty vector control, HvEPFL1OE-A and HvEPFL1OE-B under well-watered (black bars) and water withheld treatments (striped bars) after 6 days of the withheld water treatment. N=5. Error bars signify SE. There was a significant difference in RWC between the empty vector control and the *HvEPFL1* ectopic overexpression lines in the water withheld teatment. (Dunnett's multiple comparisons test after one-way ANOVA, $p<0.05$). (B) Digital image of a control and an HvEPFL1OE-B plant after water was withheld for 6 days.

5.6- Conclusions

- Overexpression of *HvEPFL1* reduces seed viability and delays germination, as well as slowing down initial vegetative development.

- There was no significant change in above ground biomass including both physiological traits (leaf number and primary tiller height) and seed yield, suggesting that the reduction in photosynthetic rate observed at ambient conditions does not translate into reduced growth or yield. This could be due to an increased availability of resources to dedicate to grain filling and shoot development as a consequence of reduced stomatal conductance and consequent reduction in water loss reducing the requirement for resource investment in roots.
- The maximum number of tillers was reduced in the most severe density line (HvEPFL1OE-A), suggesting that maximum achievable grain yield could be reduced in *HvEPFL1* ectopic overexpressors.

- Long-term water use efficiency was significantly higher in HvEPFL1OE-A under well-watered conditions and in both overexpression lines under drought.

- The *HvEPFL1* ectopic expression lines are both more drought tolerant than the empty vector control, displaying drought avoidance through retention of soil moisture with subsequent delayed onset of drought stress and turgor loss.

Chapter 6- Discussion

As has been extensively covered in chapter 1 the role of the EPIDERMAL PATTERNING FACTOR LIKE (EPFL) family in regulating the development of stomata in *Arabidopsis* has been extensively researched over the past decade. However, until the completion of this current study it was unknown whether the functions of any of the EPF signalling peptides were conserved in grasses. With the discovery that overexpressing *HvEPFL1* leads to reduced stomatal density there is now evidence that peptide function has been conserved between monocots and dicots. Added to evidence of EPF/TMM/ERECTA function in basal land plants (Caine et al., 2016) and evidence of conserved SPCH, MUTE and FAMA function in both the basal land plants (Chater et al., 2016) and in grasses (Liu et al., 2009; Raissig et al; 2016) this finding adds weight to the hypothesis that the underlying components of the EPF/TMM/ERECTA signalling module and stomatal lineage progression are truly universal. This suggests that a single molecular toolkit of ancient origins is being utilised across vast evolutionary distances. Stomata are found in a number of distinct patterns in nature, from the ring of stomata around the base of the sporophyte capsule of *Physcomitrella patens* (Caine et al., 2016) through the scattered distribution seen in dicots such as *Arabidopsis thaliana* to the highly ordered stomatal files of the grasses (Stebbins and Jain, 1960). That slight diversifications in their function can allow the same basic components to orchestrate stomatal development to such distinct outcomes is quite a surprising, if parsimonious, concept. This would also suggest that pathways that integrate into the stomatal development pathway, such as those that relay environmental signals, are likely to demonstrate high conservation of component functions as well.

The fact that reducing stomatal density can improve both water use efficiency and drought tolerance without a negative impact on yield is an exciting finding. This study is the latest to demonstrate this possible means of crop improvement, with studies of *gtl*

mutants (Yoo et al., 2010; Yoo et al., 2011), *EPF2* overexpression (Franks et al., 2015) and *PdEPF2* overexpression (Liu et al., 2016) in the model plant *Arabidopsis thaliana,* as well as *ZmSDD1* overexpression in maize (Liu et al., 2015), all showing a link between lower stomatal densities and higher water use efficiency and/or drought tolerance. This suggests that reduced stomatal density could be an ideal trait for targeted breeding for futureproofing crops against increased drought, particularly given the fact that higher atmospheric CO_2 concentration will help to mitigate the negative effects of reduced gas exchange on carbon assimilation.

The caveat to the results presented here is that they have been obtained under a particular, controlled set of environmental conditions that, whilst good for barley, do not necessarily reflect the variation and stochasticity of the natural environmental conditions to which barley is exposed when it is grown in the field. Neither can it be assumed that the improvements in water relations seen here can be replicated in other crops with distinct growth habits, such as rice. Further to this, seeing as the plants utilised for gas exchange were grown in the early part of the year (January to June), most of their early growth and development, as well as the gas exchange analysis, was done under the constant light level of supplementary lighting. This period reflects the time of year spring barley is grown in the field in England. Therefore, whilst the light levels used are relatively low, they are similar to or exceed what would be found in a typical barley growth environment, albeit lacking the natural fluctuations present in the field. Whilst it is possible that limiting light may have to some degree suppressed differences in carbon assimilation and yield between the control line and the low stomatal density lines, it is likely that any light limitation would also be present in the field.

6.1- future work

The body of work presented here is far from exhaustive, with numerous avenues for advancement.

Firstly, it is well documented that modifying stomatal density, and in so doing modifying stomatal conductance, affects the rate of evaporative cooling in the leaves (Doheny-Adams et al., 2012, see figure 6.1).

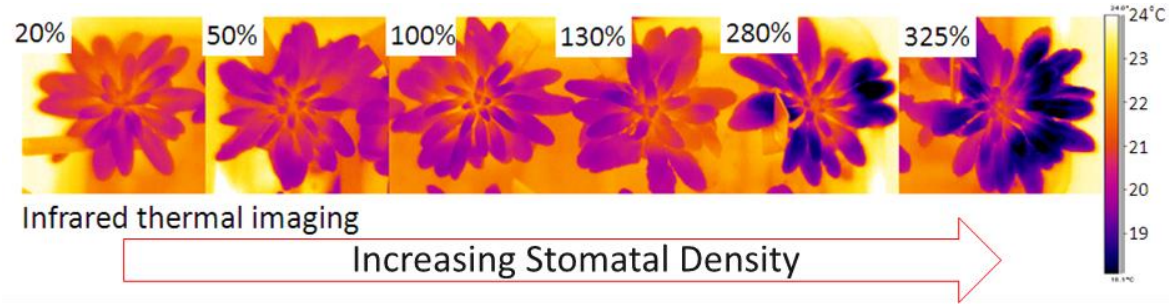

Figure 6.1- the effect of stomatal density of evaporative cooling in *Arabidopsis thaliana*. As stomatal density increases, evapotranspiration increases which leads to increased evaporative cooling of the leaves. Images taken using an Infra-red thermal imaging camera. Percentages are the proportion of stomata relative to the Col-0 control (100%). The genotypes of the plants shown in order of increasing density are: *EPF2OE*, *STOMAGEN* RNAi, Col-0, *epf2*, *epf1epf2 double mutant* and *epf1epf2STOMAGENOE*. Adapted from Doheny-Adams et al., 2012.

Temperature stress during grain filling has previously been demonstrated to result in reduced grain yield in crop plants, for example winter wheat (Gooding et al., 2003). The effects of high temperature growth conditions are likely to be exaggerated in plants with lower stomatal densities as their decreased ability to cool themselves will lead to higher plant body temperatures in comparison to plants with more normal densities. Given that

average global temperatures are on the rise, this reduction in cooling could significantly limit the benefits of using low stomatal density lines. It is therefore imperative that the growth of these low-density lines is analysed under a range of temperatures to determine whether the negative consequences of elevated plant body temperatures outweigh the benefits of reduced water loss.

Continuing on the theme of climate change, the lines should be grown under elevated CO_2 conditions to analyse whether the projected increases in atmospheric CO_2 (reviewed in chapter 1) will amplify the benefits of reduced stomatal density in terms of WUE. As WUE=A/E, and reducing stomatal density reduces E to improve WUE, conditions where assimilation is improved, i.e. high CO_2 environments, should be expected to improve WUE significantly, relative to current ambient CO_2 concentrations (Doheny-Adams et al., 2012; Franks et al., 2015).

Furthermore, evapotranspiration of water from the stomata drives the passage of water through the plant and the movement of water, and water-soluble nutrients by mass flow, through the soil towards the root (Barber, 1962). This is the transpiration stream. Evapotranspiration and nitrogen uptake have been found to correlate in studies such as Shimono and Bunce, 2009. Obviously, it would be undesirable to improve crop drought tolerance only to significantly curtail nutrient uptake. Hepworth et al., 2015 demonstrated that in *Arabidopsis thaliana* it is possible to reduce stomatal density utilising *EPF2* overexpression without negatively impacting the uptake of nitrogen but whether this result can be replicated in agronomically important plants, and whether reducing stomatal density through the manipulation of *EPFLs* effects the uptake of other nutrients, remains to be determined. In the experiments described in chapter 4 final grain yield did not differ between reduced density lines and the control which, in conjunction with the lack of difference in vegetative biomass, suggests nutrient uptake may not have been impaired. However, the rate of uptake of important nutrients wasn't analysed, nor was the nutrient

content of the grain assessed. Therefore, a suitable strand of future investigation would be to carry out experiments in the same vein as Hepworth et al., 2015 using the *HvEPFL1* lines to see whether the results of that study translate into crops. It would also be useful to analyse the nutrient content of the grains using mass spectrometry.

Finally, there is a whole suite of molecular biology experiments that could be done to further the work presented here. Whilst the effect of *HvEPF1* overexpression has been demonstrated here and the conservation of bHLH transcription factors previously described (Liu et al., 2009; Raissig et al., 2016), the biological role of the orthologues of many of the *Arabidopsis thaliana* stomatal patterning genes remains to be elucidated in grasses including the other EPFLs that were not investigated here, TMM, the ERECTA receptors and MAPK components. The creation of overexpressors and mutants in these orthologues would seem to be the next logical step in investigating how stomatal patterning occurs in grasses. Moreover, it would be very desirable to create a reporter construct for the *HvEPFL1* gene as knowing where *HvEPFL1* is expressed during stomatal development would greatly help elucidate its natural biological role.

Barley is an ideal model organism for carrying out these genetic analyses. The "Golden Promise" cultivar is relatively straight forward to transform (Harwood et al., 2009) and mutations can be generated using the CRISPR/Cas9 genome editing tool (Lawrenson et al., 2015). Barley, unlike *Bachypodium distachyon* , is a commercially important crop plant and as such the transition between theory and application in a real world context is significantly simplified. Moreover, discoveries in barley can be readily applied to other crop plants including wheat. Barley is a diploid, making it much easier to carry out investigations in barley than in hexaploid wheat. Furthermore, its epidermis is flat and smooth, making it very easy to rapidly and accurately analyse large numbers of stomatal impressions, unlike rice where the topography and the existence of abundant trichromes hinder this process. Currently stomatal research into the EPF/TMM/ERECTA signalling module and other

stomatal development regulators in grasses is been carried out in *Hordeum vulgare, Triticum aestivum (J. Dunn, Gray lab, unpublished work), Oryza sativa (R.Caine, Gray lab, unpublished work), Zea mays* (Liu et al., 2015) and *Brachypodium distachyon* (Raissig et al., 2016). It would perhaps be best to focus on a single organism to develop a complete model for the pathways controlling stomatal epidermal patterning in grasses.

References

- Abrash, E.B., and Bergmann, D.C. (2010). Regional specification of stomatal production by the putative ligand CHALLAH. Development *137*, 447–455.
- Abrash, E.B., Davies, K.A., and Bergmann, D.C. (2011). Generation of Signaling Specificity in *Arabidopsis* by Spatially Restricted Buffering of Ligand–Receptor Interactions. Plant Cell *23*, 2864–2879.
- Adrian, J., Chang, J., Ballenger, C.E., Bargmann, B.O.R., Alassimone, J., Davies, K.A., Lau, O.S., Matos, J.L., Hachez, C., Lanctot, A., et al. (2015). Transcriptome Dynamics of the Stomatal Lineage: Birth, Amplification, and Termination of a Self-Renewing Population. Dev. Cell *33*, 107–118.
- AINSWORTH, E.A., and ROGERS, A. (2007). The response of photosynthesis and stomatal conductance to rising [CO 2]: mechanisms and environmental interactions. Plant. Cell Environ. *30*, 258–270.
- Alcamo, J., Flörke, M., and Märker, M. (2007). Future long-term changes in global water resources driven by socio-economic and climatic changes. Hydrol. Sci. Sci. Hydrol. *52*, 247-275
- Alexandratos, N., and Bruinsma, J. (2012). World agriculture towards 2030/2050. Land Use Policy *20*, 375.
- Baker, N.R., and Rosenqvist, E. (2004). Applications of chlorophyll fluorescence can improve crop production strategies: an examination of future possibilities. J. Exp. Bot. *55*, 1607–1621.
- Balmford, A., Green, R.E., and Scharlemann, J.P.W. (2005). Sparing land for nature: exploring the potential impact of changes in agricultural yield on the area needed for crop production. Glob. Chang. Biol. *11*, 1594–1605.
- Barbour, M.M., Roden, J.S., Farquhar, G.D., and Ehleringer, J.R. (2004). Expressing leaf water and cellulose oxygen isotope ratios as enrichment above source water reveals evidence of a Peclet effect. Oecologia *138*, 426–435.
- Bauer, H., Ache, P., Lautner, S., Fromm, J., Hartung, W., Al-Rasheid, K.A.S., Sonnewald, S., Sonnewald, U., Kneitz, S., Lachmann, N., et al. (2013). The Stomatal Response to Reduced Relative Humidity Requires Guard Cell-Autonomous ABA Synthesis. Curr. Biol. *23*, 53–57.
- Beddington, J. (2009). Food, energy, water and the climate: a perfect storm of global events? World Development 1–9.

- BEERLING, D.J., and WOODWARD, F.I. (1997). Changes in land plant function over the Phanerozoic: reconstructions based on the fossil record. Bot. J. Linn. Soc. *124*, 137–153.
- Berger, D., and Altmann, T. (2000). A subtilisin-like serine protease involved in the regulation of stomatal density and distribution in Arabidopsis thaliana. Genes Dev. *14*, 1119–1131.
- Bergmann, D.C., and Sack, F.D. (2007). Stomatal Development. Annu. Rev. Plant Biol. *58*, 163–181.

- Bergmann, D.C., Lukowitz, W., and Somerville, C.R. (2004). Stomatal Development and Pattern Controlled by a MAPKK Kinase. Science (80-.). *304*, 1494–1497.
- Berry, J.A., Beerling, D.J., and Franks, P.J. (2010). Stomata: key players in the earth system, past and present. Curr. Opin. Plant Biol. *13*, 232–239.
- Blum, A. (2004). Sorghum physiology. In 'Physiology and biotechnology integration for plant breeding (Marcel Dekker).
- Blum, A. (2005). Drought resistance, water-use efficiency, and yield potential—are they compatible, dissonant, or mutually exclusive? Aust. J. Agric. Res. *56*, 1159–1168.
- Boccalandro, H.E., Rugnone, M.L., Moreno, J.E., Ploschuk, E.L., Serna, L., Yanovsky, M.J., and Casal, J.J. (2009). Phytochrome B enhances photosynthesis at the expense of water-use efficiency in Arabidopsis. Plant Physiol. *150*, 1083–1092.
- VAN DEN BOOGAARD, R., ALEWIJNSE, D., VENEKLAAS, E.J., and LAMBERS, H. (1997). Growth and water-use efficiency of 10 Triticum aestivum cultivars at different water availability in relation to allocation of biomass. Plant, Cell Environ. *20*, 200–210.
- Boyer, J.S. (1982). Plant Productivity and Environment. Science. *218*, 443–448.
- Brodribb, T. Dynamics of Changing lntercellular CO, Concentration (ci) during Drought and Determination of Minimum Functional ci. Plant Physiol *11*, 179–1.
- Brodribb, T.J., and McAdam, S.A.M. (2011). Passive Origins of Stomatal Control in Vascular Plants. Science (80-.). *331*, 582–585.
- Büssis, D., Von Groll B, U., Fisahn, J., and Altmann, T. (2006). Stomatal aperture can compensate altered stomatal density in Arabidopsis thaliana at growth light conditions. Funct. Plant Biol. *33*, 1037–1043.
- Caine, R., Chater, C.C., Kamisugi, Y., Cuming, A.C., Beerling, D.J., Gray, J.E., and Fleming, A.J. (2016). An ancestral stomatal patterning module revealed in the non-vascular land plant Physcomitrella patens. Development. *143*, 3306-3314
- van Campen, J., Yaapar, M.N., Narawatthana, S., Lehmeier, C., Wanchana, S., Thakur, V., Chater, C., Kelly, S., Rolfe, S.A., Quick, W.P., et al. (2016). Combined Chlorophyll Fluorescence and Transcriptomic Analysis Identifies the P3/P4 Transition as a Key stage in Rice Leaf Photosynthetic Development. Plant Physiol. *170 (3)*, 1655-1674
- Cartwright, H.N., Humphries, J.A., and Smith, L.G. (2009). A Receptor-Like Protein That Promotes Polarization of an Asymmetric Cell Division in Maize. Science. *323*, 649-651
- Casson, S.A., and Hetherington, A.M. (2010). Environmental regulation of stomatal development. Curr. Opin. Plant Biol. *13*, 90–95.
- Casson, S., and Gray, J.E. (2008). Influence of environmental factors on stomatal development. New Phytol. *178*, 9–23.
- Casson, S.A., Franklin, K.A., Gray, J.E., Grierson, C.S., Whitelam, G.C., and Hetherington, A.M. (2009). phytochrome B and PIF4 Regulate Stomatal Development in Response to Light Quantity. Curr. Biol. *19*, 229–234.

- Chater, C., Kamisugi, Y., Movahedi, M., Fleming, A., Cuming, A.C., Gray, J.E., and Beerling, D.J. (2011). Regulatory Mechanism Controlling Stomatal Behavior Conserved across 400 Million Years of Land Plant Evolution. Curr. Biol. *21*, 1025–1029.
- Chater, C., Peng, K., Movahedi, M., Hedrich, R., Gray, J.E., and Hetherington, A.M. (2015). Elevated CO 2 -Induced Responses in Stomata Require ABA and ABA Signaling. Curr. Biol. *25*, 2709–2716.
- Chater, C.C., Caine, R.S., Tomek, M., Wallace, S., Kamisugi, Y., Cuming, A.C., Lang, D., MacAlister, C.A., Casson, S., Bergmann, D.C., et al. (2016). Origin and function of stomata in the moss Physcomitrella patens. Nat. Plants *2*, 16179.
- Chater, C.C.C., Oliver, J., Casson, S., and Gray, J.E. (2014). Putting the brakes on: abscisic acid as a central environmental regulator of stomatal development. New Phytol. *202*, 376–391.
- Chen, Z.H., Chen, G., Dai, F., Wang, Y., Hills, A., Ruan, Y.L., Zhang, G., Franks, P.J., Nevo, E., and Blatt, M.R. (2017). Molecular Evolution of Grass Stomata. Trends Plant Sci. *22*, 124–139.
- Clough, S.J., and Bent, A.F. (1998). Floral dip: a simplified method for Agrobacterium-mediated transformation of Arabidopsis thaliana. Plant J. *16*, 735–743.
- Condon, A.G., Richards, R.A., Rebetzke, G.J., and Farquhar, G.D. (2004). Breeding for high water-use efficiency. J. Exp. Bot. *55*, 2447–2460.
- Cutler, S.R., Rodriguez, P.L., Finkelstein, R.R., and Abrams, S.R. (2010). Abscisic Acid: Emergence of a Core Signaling Network. Annu. Rev. Plant Biol. *61*, 651–679.
- Daszkowska-Golec, A., and Szarejko, I. (2013). Open or close the gate - stomata action under the control of phytohormones in drought stress conditions. Front. Plant Sci. *4*, 138.
- Davies, K.A., and Bergmann, D.C. (2014). Functional specialization of stomatal bHLHs through modification of DNA-binding and phosphoregulation potential. Proc. Natl. Acad. Sci. U. S. A. *111*, 15585–15590.
- DEFRA (2009). Government Response to the Committee's Fourth Report of Session 2008–09 on Securing Food Supplies up to 2050: The Challenges Faced by the UK.
- Doheny-Adams, T., Hunt, L., Franks, P.J., Beerling, D.J., and Gray, J.E. (2012). Genetic manipulation of stomatal density influences stomatal size, plant growth and tolerance to restricted water supply across a growth carbon dioxide gradient. Philos. Trans. R. Soc. B Biol. Sci. *367*, 547–555.
- Döll, P., and Siebert, S. (2002). Global modeling of irrigation water requirements. Water Resour. Res. *38*, 8-1-8–10.
- Dong, J., MacAlister, C.A., and Bergmann, D.C. (2009). BASL Controls Asymmetric Cell Division in Arabidopsis. Cell *137*, 1320–1330.
- Dow, K., Berkhout, F., and Preston, B.L. (2013). Limits to adaptation to climate change: a risk approach. Curr. Opin. Environ. Sustain. *5*, 384–391.
- Drake, P.L., Froend, R.H., and Franks, P.J. (2013). Smaller, faster stomata: Scaling of stomatal size, rate of response, and stomatal conductance. J. Exp. Bot. *64*, 495–505.

- Duckett, J.G., Pressel, S., P'ng, K.M.Y., and Renzaglia, K.S. (2009). Exploding a myth: the capsule dehiscence mechanism and the function of pseudostomata in *Sphagnum*. New Phytol. *183*, 1053–1063.
- Edwards, D., Kerp, H., and Hass, H. (1998). Stomata in early land plants: an anatomical and ecophysiological approach. J. Exp. Bot. *49*, 255–278.
- Elias, P. "Stomata density and size of apple trees growing in irrigated and non irrigated conditions." *BIOLOGIA-BRATISLAVA*- 50 (1995): 115-115.
- Engineer, C.B., Ghassemian, M., Anderson, J.C., Peck, S.C., Hu, H., and Schroeder, J.I. (2014). Carbonic anhydrases, EPF2 and a novel protease mediate CO2 control of stomatal development. Nature *513*, 246–250.
- ETHIER, G.J., and LIVINGSTON, N.J. (2004). On the need to incorporate sensitivity to CO2 transfer conductance into the Farquhar-von Caemmerer-Berry leaf photosynthesis model. Plant, Cell Environ. *27*, 137–153.
- Facette, M.R., Park, Y., Sutimantanapi, D., Luo, A., Cartwright, H.N., Yang, B., Bennett, E.J., Sylvester, A.W., Smith, L.G., Dow, G.J., et al. (2015). The SCAR/WAVE complex polarizes PAN receptors and promotes division asymmetry in maize. Nat. Plants *1*, 14024.
- FAO (Food and Agriculture Organization of the United Nations) (1996). The state of food and agriculture.
- FAO (Food and Agriculture Organization of the United Nations) (2007). The state of food and agriculture.
- FAO (Food and Agriculture Organization of the United Nations) (2009). How to Feed the World in 2050, Paper Prepared for the High Level Expert Forum.
- FAO (Food and Agriculture Organization of the United Nations) (2015). The State of food insecurity in the world.
- Farquhar, G.D., and Sharkey, T.D. (1982). Stomatal Conductance and Photosynthesis. Annu. Rev. Plant Physiol. *33*, 317–345.
- Farquhar, G., O'Leary, M., Berry, J., Farquhar, G., O'Leary, M., and Berry, J. (1982). On the Relationship Between Carbon Isotope Discrimination and the Intercellular Carbon Dioxide Concentration in Leaves. Aust. J. Plant Physiol. *9*, 121.
- Farquhar, G., Richards, R., Farquhar, G., and Richards, R. (1984). Isotopic Composition of Plant Carbon Correlates With Water-Use Efficiency of Wheat Genotypes. Aust. J. Plant Physiol. *11*, 539.
- Farquhar, G.D., von Caemmerer, S., and Berry, J.A. (1980). A biochemical model of photosynthetic CO2 assimilation in leaves of C3 species. Planta *149*, 78–90.
- Field, K.J., Duckett, J.G., Cameron, D.D., and Pressel, S. (2015). Stomatal density and aperture in non-vascular land plants are non-responsive to above-ambient atmospheric CO2 concentrations. Ann. Bot. *115*, 915–922.
- Fischer, R.A., Rees, D., Sayre, K.D., Lu, Z.-M., Condon, A.G., and Saavedra, A.L. (1998). Wheat Yield Progress Associated with Higher Stomatal Conductance and Photosynthetic Rate, and Cooler Canopies. Crop Sci. *38*, 1467.
- Fleury, D., Jefferies, S., Kuchel, H., and Langridge, P. (2010). Genetic and genomic tools to improve drought tolerance in wheat. J. Exp. Bot. *61*, 3211–3222.

- Flexas, J., Bota, J., Loreto, F., Cornic, G., and Sharkey, T.D. (2004). Diffusive and Metabolic Limitations to Photosynthesis under Drought and Salinity in C $_3$ Plants. Plant Biol. *6*, 269–279.
- Franks, P.J., and Beerling, D.J. (2009). Maximum leaf conductance driven by CO2 effects on stomatal size and density over geologic time. Proc. Natl. Acad. Sci. U. S. A. *106*, 10343–10347.
- Franks, P.J., and Farquhar, G.D. (2007). The mechanical diversity of stomata and its significance in gas-exchange control. Plant Physiol. *143*, 78–87.
- Franks, P.J., W. Doheny-Adams, T., Britton-Harper, Z.J., and Gray, J.E. (2015). Increasing water-use efficiency directly through genetic manipulation of stomatal density. New Phytol. *207*, 188–195.
- Fraser, L.H., Greenall, A., Carlyle, C., Turkington, R., and Friedman, C.R. (2009). Adaptive phenotypic plasticity of Pseudoroegneria spicata: response of stomatal density, leaf area and biomass to changes in water supply and increased temperature. Ann. Bot. *103*, 769–775.
- Gago, J., Douthe, C., Florez-Sarasa, I., Escalona, J.M., Galmes, J., Fernie, A.R., Flexas, J., and Medrano, H. (2014). Opportunities for improving leaf water use efficiency under climate change conditions. Plant Sci. *226*, 108–119.
- Garcia del Moral, M.B., and Garcia del Moral, L.F. (1995). Tiller production and survival in relation to grain yield in winter and spring barley. F. Crop. Res. *44*, 85–93.
- Geisler, M., Yang, M., and Sack, F.D. (1998). Divergent regulation of stomatal initiation and patterning in organ and suborgan regions of the Arabidopsis mutants too many mouths and four lips. Planta *205*, 522–530.
- Geisler, M., Nadeau, J., and Sack, F.D. (2000). Oriented asymmetric divisions that generate the stomatal spacing pattern in arabidopsis are disrupted by the too many mouths mutation. Plant Cell *12*, 2075–2086.
- Genty, B., Briantais, J.-M., and Baker, N.R. (1989). The relationship between the quantum yield of photosynthetic electron transport and quenching of chlorophyll fluorescence. Biochim. Biophys. Acta - Gen. Subj. *990*, 87–92.
- Godfray, H.C.J., Beddington, J.R., Crute, I.R., Haddad, L., Lawrence, D., Muir, J.F., Pretty, J., Robinson, S., Thomas, S.M., and Toulmin, C. (2010). Food Security: The Challenge of Feeding 9 Billion People. Science. *327*, 812-818
- GONZÁLEZ, C.V., IBARRA, S.E., PICCOLI, P.N., BOTTO, J.F., and BOCCALANDRO, H.E. (2012). Phytochrome B increases drought tolerance by enhancing ABA sensitivity in *Arabidopsis thaliana*. Plant. Cell Environ. *35*, 1958–1968.
- Gooding, M.J., Ellis, R.H., Shewry, P.R., and Schofield, J.D. (2003). Effects of Restricted Water Availability and Increased Temperature on the Grain Filling, Drying and Quality of Winter Wheat. J. Cereal Sci. *37*, 295–309.
- Gray, J.E. (2007). Plant Development: Three Steps for Stomata. Curr. Biol. *17*, 213–215.
- Gray, J.E., Holroyd, G.H., van der Lee, F.M., Bahrami, A.R., Sijmons, P.C., Woodward, F.I., Schuch, W., and Hetherington, A.M. (2000). The HIC signalling pathway links CO2 perception to stomatal development. Nature *408*, 713–716.

- Von Groll, U., Berger, D., and Altmann, T. (2002). The subtilisin-like serine protease SDD1 mediates cell-to-cell signaling during Arabidopsis stomatal development. Plant Cell *14*, 1527–1539.
- Hamanishi, E.T., Thomas, B.R., and Campbell, M.M. (2012). Drought induces alterations in the stomatal development program in Populus. J. Exp. Bot. *63*, 4959–4971.
- Han, S.-K., and Torii, K.U. (2016). Lineage-specific stem cells, signals and asymmetries during stomatal development. Development *143*, 1259–1270.
- Hara, K., Kajita, R., Torii, K.U., Bergmann, D.C., and Kakimoto, T. (2007). The secretory peptide gene EPF1 enforces the stomatal one-cell-spacing rule. Genes Dev. *21*, 1720–1725.
- Hara, K., Yokoo, T., Kajita, R., Onishi, T., Yahata, S., Peterson, K.M., Torii, K.U., and Kakimoto, T. (2009). Epidermal cell density is autoregulated via a secretory peptide, EPIDERMAL PATTERNING FACTOR 2 in Arabidopsis leaves. Plant Cell Physiol. *50*, 1019–1031.
- Harwood, W.A., Bartlett, J.G., Alves, S.C., Perry, M., Smedley, M.A., Leyland, N., and Snape, J.W. (2009). Barley transformation using Agrobacterium-mediated techniques. Methods Mol. Biol. *478*, 137–147.
- Hepworth, C., Doheny-Adams, T., Hunt, L., Cameron, D.D., and Gray, J.E. (2015). Manipulating stomatal density enhances drought tolerance without deleterious effect on nutrient uptake. New Phytol. *208*, 336–341.
- Hepworth, C., Turner, C., Landim, M.G., Cameron, D., Gray, J.E., and Liang, Y.-K. (2016). Balancing Water Uptake and Loss through the Coordinated Regulation of Stomatal and Root Development. PLoS One. *11*, e0156930.
- Hetherington, A.M., and Woodward, F.I. (2003). The role of stomata in sensing and driving environmental change. Nature *424*, 901–908.
- Horst, R.J., Fujita, H., Lee, J.S., Rychel, A.L., Garrick, J.M., Kawaguchi, M., Peterson, K.M., Torii, K.U., MacAlister, C., Ohashi-Ito, K., et al. (2015). Molecular Framework of a Regulatory Circuit Initiating Two-Dimensional Spatial Patterning of Stomatal Lineage. PLOS Genet. *11*, e1005374.
- Hronková, M., Wiesnerová, D., Šimková, M., Skůpa, P., Dewitte, W., Vráblová, M., Zažímalová, E., and Šantrůček, J. (2015). Light-induced STOMAGEN-mediated stomatal development in Arabidopsis leaves. J. Exp. Bot. *66*, 4621–4630.
- Hughes, J., Hepworth, C., Dutton, C., Dunn, J.A., Hunt, L., Stephens, J., Waugh, R., Cameron, D.D., and Gray, J.E. (2017). Reducing Stomatal Density in Barley Improves Drought Tolerance without Impacting on Yield. Plant Physiol. *174*, 776–787.
- Humphries, J.A., Vejlupkova, Z., Luo, A., Meeley, R.B., Sylvester, A.W., Fowler, J.E., and Smith, L.G. (2011). ROP GTPases act with the receptor-like protein PAN1 to polarize asymmetric cell division in maize. Plant Cell *23*, 2273–2284.
- Hunt, L., and Gray, J.E. (2009). The Signaling Peptide EPF2 Controls Asymmetric Cell Divisions during Stomatal Development. Curr. Biol. *19*, 864–869.
- Hunt, L., Bailey, K.J., and Gray, J.E. (2010). The signalling peptide EPFL9 is a positive regulator of stomatal development. New Phytol. *186*, 609–614.

- IFPRI (International Food Policy Research Institute) (2015). Global nutrition report 2015: Actions and accountability to advance nutrition and sustainable development.
- Impa, S.M., Nadaradjan, S., Boominathan, P., Shashidhar, G., Bindumadhava, H., and Sheshshayee, M.S. (2005). Carbon Isotope Discrimination Accurately Reflects Variability in WUE Measured at a Whole Plant Level in Rice. Crop Sci. *45*, 2517.
- IPCC (2007a). Climate Change 2007: Impacts, Adaption and Vulnerability. Contribution of Working Group II to the Fourth Assessment Report of the Intergovernmental Panel on Climate Change. Parry ML, Canziani OF, Palutikof JP, van der Linden PJ & Hanson CE (eds). Cambridge University Press, Cambridge, UK. Available online at: http://www.ipcc.ch/publications_and_data/publications_ipcc_fourth_assessment_report_wg2_report_impacts_ adaptation_and_vulnerability.htm
- IPCC (2014). Climate Change 2014: Synthesis Report. Contribution of Working Groups I, II and III to the Fifth Assessment Report of the Intergovernmental Panel on Climate Change [Core Writing Team, R.K. Pachauri and L.A. Meyer (eds.)]. IPCC, Geneva, Switzerland, 151
- IWMI (Comprehensive Assessment of Water Management in Agriculture) (2007). Water for Food, Water for Life: A Comprehensive Assessment of Water Management in Agriculture. London: Earthscan, and Colombo: International Water Management Institute.
- Joshi, R., Wani, S.H., Singh, B., Bohra, A., Dar, Z.A., Lone, A.A., Pareek, A., and Singla-Pareek, S.L. (2016). Transcription Factors and Plants Response to Drought Stress: Current Understanding and Future Directions. Front. Plant Sci. *7*, 1029.
- Kanaoka, M.M., Pillitteri, L.J., Fujii, H., Yoshida, Y., Bogenschutz, N.L., Takabayashi, J., Zhu, J.-K., and Torii, K.U. (2008). SCREAM/ICE1 and SCREAM2 Specify Three Cell-State Transitional Steps Leading to Arabidopsis Stomatal Differentiation. PLANT CELL ONLINE *20*, 1775–1785.
- Kang, C.-Y., Lian, H.-L., Wang, F.-F., Huang, J.-R., and Yang, H.-Q. (2009). Cryptochromes, phytochromes, and COP1 regulate light-controlled stomatal development in Arabidopsis. Plant Cell *21*, 2624–2641.
- Katsir, L., Davies, K.A., Bergmann, D.C., and Laux, T. (2011). Peptide Signaling in Plant Development. Curr. Biol. *21*, 356–364.
- Kenrick, P., and Crane, P.R. (1997). The origin and early evolution of plants on land. Nature *389*, 33–39.
- Kim, T.-W., and Wang, Z.-Y. (2010). Brassinosteroid Signal Transduction from Receptor Kinases to Transcription Factors. Annu. Rev. Plant Biol. *61*, 681–704.
- Kim, T.-H., Bohmer, M., Hu, H., Nishimura, N., and Schroeder, J.I. (2010). Guard Cell Signal Transduction Network: Advances in Understanding Abscisic Acid, CO 2 , and Ca 2+ Signaling. Annu. Rev. Plant Biol. *61*, 561–591.
- Kondo, T., Kajita, R., Miyazaki, A., Hokoyama, M., Nakamura-Miura, T., Mizuno, S., Masuda, Y., Irie, K., Tanaka, Y., Takada, S., et al. (2010). Stomatal Density is Controlled by a Mesophyll-Derived Signaling Molecule. Plant Cell Physiol. *51*, 1–8.

- Lake, J.A., and Woodward, F.I. (2008). Response of stomatal numbers to CO2 and humidity: Control by transpiration rate and abscisic acid. New Phytol. *179*, 397–404.
- Lake, J.A., Quick, W.P., Beerling, D.J., and Woodward, F.I. (2001). Plant development: Signals from mature to new leaves. Nature *411*, 154–154.
- Lake, J.A., Woodward, F.I., and Quick, W.P. (2002). Long-distance CO(2) signalling in plants. J. Exp. Bot. *53*, 183–193.
- Lampard, G.R., MacAlister, C.A., and Bergmann, D.C. (2008). Arabidopsis Stomatal Initiation Is Controlled by MAPK-Mediated Regulation of the bHLH SPEECHLESS. Science. *322*, 1113–1116.
- Lau, O.S., and Bergmann, D.C. (2012). Stomatal development: a plant's perspective on cell polarity, cell fate transitions and intercellular communication. Development *139*, 3683–3692.
- Lau, O., Davies, K.A., Chang, J., Adrian, J., Rowe, M.H., Ballenger, C.E., and Bergmann, D.C. (2014). Direct roles of SPEECHLESS in the specification of stomatal self-renewing cells. Science (80-.). *345*, 1605–1609.
- Lawrenson, T., Shorinola, O., Stacey, N., Li, C., Østergaard, L., Patron, N., Uauy, C., and Harwood, W. (2015). Induction of targeted, heritable mutations in barley and Brassica oleracea using RNA-guided Cas9 nuclease. Genome Biol. *16*, 258.
- Lawson, T., and Blatt, M.R. (2014). Stomatal Size, Speed, and Responsiveness Impact on Photosynthesis and Water Use Efficiency. PLANT Physiol. *164*, 1556–1570.
- Lee, E., Lucas, J.R., Goodrich, J., and Sack, F.D. (2014). Arabidopsis guard cell integrity involves the epigenetic stabilization of the *FLP* and *FAMA* transcription factor genes. Plant J. *78*, 566–577.
- Lee, J.S., Kuroha, T., Hnilova, M., Khatayevich, D., Kanaoka, M.M., McAbee, J.M., Sarikaya, M., Tamerler, C., and Torii, K.U. (2012). Direct interaction of ligand-receptor pairs specifying stomatal patterning. Genes Dev. *26*, 126–136.
- Lee, J.S., Hnilova, M., Maes, M., Lin, Y.-C.L., Putarjunan, A., Han, S.-K., Avila, J., and Torii, K.U. (2015). Competitive binding of antagonistic peptides fine-tunes stomatal patterning. Nature *522*, 439–443.
- Levitt, J. (1972). *Responses of plants to environmental stresses* (Vol. 732). Academic press New York.
- Liu, S., Wang, C., Jia, F., An, Y., Liu, C., Xia, X., and Yin, W. (2016). Secretory peptide PdEPF2 enhances drought tolerance by modulating stomatal density and regulates ABA response in transgenic Arabidopsis thaliana. Plant Cell, Tissue Organ Cult. *125*, 419–431.
- Liu, T., Ohashi-Ito, K., and Bergmann, D.C. (2009). Orthologs of Arabidopsis thaliana stomatal bHLH genes and regulation of stomatal development in grasses. Development *136*, 2265–2276.
- Liu, Y., Qin, L., Han, L., Xiang, Y., and Zhao, D. (2015). Overexpression of maize SDD1 (ZmSDD1) improves drought resistance in Zea mays L. by reducing stomatal density. Plant Cell, Tissue Organ Cult. *122*, 147–159.

- Lobo, F. de A., de Barros, M.P., Dalmagro, H.J., Dalmolin, . C., Pereira, W.E., de Souza, . C., Vourlitis, G.L., and Rodriguez Ortez, C.E. (2013). Fitting net photosynthetic light-response curves with Microsoft Excel- a critical look at the models. Photosynthetica *51*, 445–456.
- Long, S.P., and Bernacchi, C.J. (2003). Gas exchange measurements, what can they tell us about the underlying limitations to photosynthesis? Procedures and sources of error. J. Exp. Bot. *54*, 2393–2401.
- Ma, Y., Szostkiewicz, I., Korte, A., Moes, D., Yang, Y., Christmann, A., and Grill, E. (2009). Regulators of PP2C Phosphatase Activity Function as Abscisic Acid Sensors. Science (80-.). *324*, 1064–1068.
- MacAlister, C.A., and Bergmann, D.C. (2011). Sequence and function of basic helix-loop-helix proteins required for stomatal development in Arabidopsis are deeply conserved in land plants. Evol. Dev. *13*, 182–192.
- MacAlister, C.A., Ohashi-Ito, K., and Bergmann, D.C. (2007). Transcription factor control of asymmetric cell divisions that establish the stomatal lineage. Nature *445*, 537–540.
- Mahoney, A.K., Anderson, E.M., Bakker, R.A., Williams, A.F., Flood, J.J., Sullivan, K.C., and Pillitteri, L.J. (2016). Functional analysis of the Arabidopsis thaliana MUTE promoter reveals a regulatory region sufficient for stomatal-lineage expression. Planta *243*, 987–998.
- Matos, J., Lau, O.S., Hachez, C., Cruz-Ram?rez, A., Scheres, B., and Bergmann, D.C. (2014). Irreversible fate commitment in the Arabidopsis stomatal lineage requires a FAMA and RETINOBLASTOMA-RELATED module. Elife *3*, e03271
- Mayer, K.F.X., Waugh, R., Langridge, P., Close, T.J., Wise, R.P., Graner, A., Matsumoto, T., Sato, K., Schulman, A., Muehlbauer, G.J., et al. (2012). A physical, genetic and functional sequence assembly of the barley genome. Nature *491*, 711–716.
- McAdam, S.A.M., and Brodribb, T.J. (2011). Passive Origins of Stomatal Control in Vascular Plants. Science. *331*, 582–585.
- McAdam, S.A.M., and Brodribb, T.J. (2012). Stomatal innovation and the rise of seed plants. Ecol. Lett. *15*, 1–8.
- Medrano, H., Tomas, M., Martorell, S., Flexas, J., Hernandez, E., Rossello, J., Pou, A., Escalona, J.-M., and Bota, J. (2015). From leaf to whole-plant water use efficiency (WUE) in complex canopies: Limitations of leaf WUE as a selection target. Crop J. *3*, 220–228.
- Merilo, E., Jalakas, P., Kollist, H., Brosché, M., Bauer, H., Ache, P., Lautner, S., Fromm, J., Hartung, W., Al-Rasheid, K.A.S., et al. (2015). The role of ABA recycling and transporter proteins in rapid stomatal responses to reduced air humidity, elevated CO2, and exogenous ABA. Mol. Plant *8*, 657–659.
- Merlot, S., Mustilli, A.-C., Genty, B., North, H., Lefebvre, V., Sotta, B., Vavasseur, A., and Giraudat, J. (2002). Use of infrared thermal imaging to isolate Arabidopsis mutants defective in stomatal regulation. Plant J. *30*, 601–609.
- Miskin, E., and Rasmusson, D.C. (1970). Frrequency and Distribution of Stomata in Barley. Crop Sci. *10*, 575.

- Miskin, K.E., Rasmusson, D.C., and Moss, D.N. (1972). Inheritance and Physiological Effects of Stomatal Frequency in Barley. Crop Sci. *12*, 780.
- Miyazawa, S.-I., Livingston, N.J., and Turpin, D.H. (2005). Stomatal development in new leaves is related to the stomatal conductance of mature leaves in poplar (Populus trichocarpaxP. deltoides). J. Exp. Bot. *57*, 373–380.
- Monclus, R., Dreyer, E., Villar, M., Delmotte, F.M., Delay, D., Petit, J.-M., Barbaroux, C., Le Thiec, D., Brechet, C., and Brignolas, F. (2006). Impact of drought on productivity and water use efficiency in 29 genotypes of Populus deltoides x Populus nigra. New Phytol. *169*, 765–777.
- Monteith, J.L. (1993). The exchange of water and carbon by crops in a mediterranean climate. Irrig. Sci. *14*, 85–91.
- Morison, J.I.., Baker, N.., Mullineaux, P.., and Davies, W.. (2008). Improving water use in crop production. Philos. Trans. R. Soc. London B Biol. Sci. *363*. 639–658
- Mustilli, A.-C., Merlot, S., Vavasseur, A., Fenzi, F., and Giraudat, J. (2002). Arabidopsis OST1 protein kinase mediates the regulation of stomatal aperture by abscisic acid and acts upstream of reactive oxygen species production. Plant Cell *14*, 3089–3099.
- Nadeau, J.A., and Sack, F.D. (2002). Control of Stomatal Distribution on the Arabidopsis Leaf Surface. Science. *296*, 1697–1700.
- Niwa, M., Daimon, Y., Kurotani, K. -i., Higo, A., Pruneda-Paz, J.L., Breton, G., Mitsuda, N., Kay, S.A., Ohme-Takagi, M., Endo, M., et al. (2013). BRANCHED1 Interacts with FLOWERING LOCUS T to Repress the Floral Transition of the Axillary Meristems in Arabidopsis. Plant Cell *25*, 1228–1242.
- Ohashi-Ito, K., and Bergmann, D.C. (2006). Arabidopsis FAMA Controls the Final Proliferation/Differentiation Switch during Stomatal Development. PLANT CELL ONLINE *18*, 2493–2505.
- Ohki, S., Takeuchi, M., Mori, M., Hetherington, A.M., Woodward, F.I., Rowe, M.H., Bergmann, D.C., Nadeau, J.A., Sack, F.D., Shpak, E.D., et al. (2011). The NMR structure of stomagen reveals the basis of stomatal density regulation by plant peptide hormones. Nat. Commun. *2*, 512.
- Park, S.-Y., Fung, P., Nishimura, N., Jensen, D.R., Fujii, H., Zhao, Y., Lumba, S., Santiago, J., Rodrigues, A., Chow, T. -f. F., et al. (2009). Abscisic Acid Inhibits Type 2C Protein Phosphatases via the PYR/PYL Family of START Proteins. Science. *324*, 1068–1071.
- Penman, H.T., and Schofield, R.K. (1951). Some physical aspects of assimilation and transpiration. Symp. Soc. Exp. Biol *5*, 115–129.
- Peterson, K.M., Rychel, A.L., and Torii, K.U. (2010). Out of the Mouths of Plants: The Molecular Basis of the Evolution and Diversity of Stomatal Development. Plant Cell *22*, 296–306.
- Peterson, K.M., Shyu, C., Burr, C.A., Horst, R.J., Kanaoka, M.M., Omae, M., Sato, Y., and Torii, K.U. (2013). Arabidopsis homeodomain-leucine zipper IV proteins promote stomatal development and ectopically induce stomata beyond the epidermis. Development *140*, 1924–1935.

- Pillitteri, L.J., and Torii, K.U. (2012). Mechanisms of Stomatal Development. Annu. Rev. Plant Biol. *63*, 591–614.
- Pillitteri, L.J., Sloan, D.B., Bogenschutz, N.L., and Torii, K.U. (2007). Termination of asymmetric cell division and differentiation of stomata. Nature *445*, 501–505.
- Pillitteri, L.J., Bogenschutz, N.L., and Torii, K.U. (2008). The bHLH protein, MUTE, controls differentiation of stomata and the hydathode pore in Arabidopsis. Plant Cell Physiol. *49*, 934–943.
- Pillitteri, L.J., Peterson, K.M., Horst, R.J., and Torii, K.U. (2011). Molecular profiling of stomatal meristemoids reveals new component of asymmetric cell division and commonalities among stem cell populations in Arabidopsis. Plant Cell *23*, 3260–3275.
- Prasad, P.V.V., Staggenborg, S.A., and Ristic, Z. (2008). Impacts of drought and/or heat stress on physiological, developmental, growth, and yield processes of crop plants. *1*, 301–355.
- Pretty, J. (2008). Agricultural sustainability: concepts, principles and evidence. Philos. Trans. R. Soc. B Biol. Sci. *363*, 447–465.
- QUARRIE, S.A., and JONES, H.G. (1977). Effects of Abscisic Acid and Water Stress on Development and Morphology of Wheat. J. Exp. Bot. *28*, 192–203.
- Rae, A.M., Robinson, K.M., Street, N.R., and Taylor, G. (2004). Morphological and physiological traits influencing biomass productivity in short-rotation coppice poplar. Can. J. For. Res. *34*, 1488–1498.
- Raissig, M.T., Abrash, E., Bettadapur, A., Vogel, J.P., and Bergmann, D.C. (2016). Grasses use an alternatively wired bHLH transcription factor network to establish stomatal identity. Proc. Natl. Acad. Sci. U. S. A. *113*, 8326–8331.
- Raissig, M.T., Matos, J.L., Anleu Gil, M.X., Kornfeld, A., Bettadapur, A., Abrash, E., Allison, H.R., Badgley, G., Vogel, J.P., Berry, J.A., et al. (2017). Mobile MUTE specifies subsidiary cells to build physiologically improved grass stomata. Science (80-.). *355*, 1215–1218.
- Raven, J.A. (2014). Speedy small stomata? J. Exp. Bot. *65*, 1415–1424.
- Richards, R.A. (2000). Selectable traits to increase crop photosynthesis and yield of grain crops. J. Exp. Bot. *51 Spec No*, 447–458.
- Robinson, S., Barbier de Reuille, P., Chan, J., Bergmann, D., Prusinkiewicz, P., and Coen, E. (2011). Generation of Spatial Patterns Through Cell Polarity Switching. Science. *333*. 1436-1440
- Rohila, J.S., Chen, M., Cerny, R., and Fromm, M.E. (2004). Improved tandem affinity purification tag and methods for isolation of protein heterocomplexes from plants. Plant J. *38*, 172–181.
- The Royal Society (2009). Reaping the benefits. Science Policy 60
- Ruszala, E.M., Beerling, D.J., Franks, P.J., Chater, C., Casson, S.A., Gray, J.E., Hetherington, A.M., Knight, M.R., Davies, W.J., Leyser, H.M.O., et al. (2011). Land plants acquired active stomatal control early in their evolutionary history. Curr. Biol. *21*, 1030–1035.
- Sack, F.D. (1994). Structure of the Stomatal Complex of the Monocot Flagellaria indica. Am. J. Bot. *81*, 339.

- Seibt, U., Rajabi, A., Griffiths, H., and Berry, J.A. (2008). Carbon isotopes and water use efficiency: sense and sensitivity. Oecologia *155*, 441–454.
- Sekiya, N., and Yano, K. (2008). Stomatal density of cowpea correlates with carbon isotope discrimination in different phosphorus, water and CO_2 environments. New Phytol. *179*, 799–807.
- Serna, L. (2009). Cell fate transitions during stomatal development. BioEssays *31*, 865–873.
- Serna, L. (2011). Stomatal development in Arabidopsis and grasses: differences and commonalities. Int. J. Dev. Biol. *55*, 5–10.
- Shen, Y., Oki, T., Kanae, S., Hanasaki, N., Utsumi, N., and Kiguchi, M. (2014). Projection of future world water resources under SRES scenarios: an integrated assessment. Hydrol. Sci. J. *59*, 1775–1793.
- Shimono, H., and Bunce, J.A. (2009). Acclimation of nitrogen uptake capacity of rice to elevated atmospheric CO2 concentration. Ann. Bot. *103*, 87–94.
- Shpak, E.D., Lakeman, M.B., and Torii, K.U. (2003). Dominant-negative receptor uncovers redundancy in the Arabidopsis ERECTA Leucine-rich repeat receptor-like kinase signaling pathway that regulates organ shape. Plant Cell *15*, 1095–1110.
- Shpak, E.D., Berthiaume, C.T., Hill, E.J., and Torii, K.U. (2004). Synergistic interaction of three ERECTA-family receptor-like kinases controls Arabidopsis organ growth and flower development by promoting cell proliferation. Development *131*, 1491–1501.
- Shpak, E.D., McAbee, J.M., Pillitteri, L.J., and Torii, K.U. (2005). Stomatal Patterning and Differentiation by Synergistic Interactions of Receptor Kinases. Science. *309*, 290–293.
- Sirichandra, C., Gu, D., Hu, H.-C., Davanture, M., Lee, S., Djaoui, M., Valot, B., Zivy, M., Leung, J., Merlot, S., et al. (2009). Phosphorylation of the Arabidopsis AtrbohF NADPH oxidase by OST1 protein kinase. FEBS Lett. *583*, 2982–2986.
- Stebbins, G.L., and Jain, S.K. (1960). Developmental studies of cell differentiation in the epidermis of monocotyledons. Dev. Biol. *2*, 409–426.
- Stebbins, G.L., and Shah, S.S. (1960a). Developmental studies of cell differentiation in the epidermis of monocotyledons: II. Cytological features of stomatal development in the Gramineae. Dev. Biol. *2*, 477–500.
- Stebbins, G.L., and Shah, S.S. (1960b). Developmental studies of cell differentiation in the epidermis of monocotyledons. Dev. Biol. *2*, 477–500.
- Sugano, S.S., Shimada, T., Imai, Y., Okawa, K., Tamai, A., Mori, M., and Hara-Nishimura, I. (2010). Stomagen positively regulates stomatal density in Arabidopsis. Nature *463*, 241–244.
- Sutimantanapi, D., Pater, D., and Smith, L.G. (2014). Divergent roles for maize PAN1 and PAN2 receptor-like proteins in cytokinesis and cell morphogenesis. Plant Physiol. *164*, 1905–1917.
- Takada, S., Takada, N., and Yoshida, A. (2013). ATML1 promotes epidermal cell differentiation in Arabidopsis shoots. Development *140*, 1919–1923.
- Tanaka, Y., Nose, T., Jikumaru, Y., and Kamiya, Y. (2013). ABA inhibits entry into stomatal-lineage development in Arabidopsis leaves. Plant J. *74*, 448–457.

- Torii, K.U. (2004). Leucine-Rich Repeat Receptor Kinases in Plants: Structure, Function, and Signal Transduction Pathways. In International Review of Cytology, pp. 1–46.
- Tricker, P., L?pez, C., Gibbings, G., Hadley, P., and Wilkinson, M. (2013). Transgenerational, Dynamic Methylation of Stomata Genes in Response to Low Relative Humidity. Int. J. Mol. Sci. *14*, 6674–6689.
- Tricker, P.J., Gibbings, J.G., Rodríguez López, C.M., Hadley, P., and Wilkinson, M.J. (2012). Low relative humidity triggers RNA-directed de novo DNA methylation and suppression of genes controlling stomatal development. J. Exp. Bot. *63*, 3799–3813.
- Turner, N.C. (1979). Differences in response of adaxial and abaxial stomata to environmental variables. In: Structure, Function and Ecology of Stomata, D.N. Sen (ed) (Dehar Dun, India: Bishen Singh Mahendra Pal Singh) 229-250.
- Uchida, N., Lee, J.S., Horst, R.J., Lai, H.-H., Kajita, R., Kakimoto, T., Tasaka, M., and Torii, K.U. (2012). Regulation of inflorescence architecture by intertissue layer ligand-receptor communication between endodermis and phloem. Proc. Natl. Acad. Sci. U. S. A. *109*, 6337–6342.
- Umbrasaite, J., Schweighofer, A., Kazanaviciute, V., Magyar, Z., Ayatollahi, Z., Unterwurzacher, V., Choopayak, C., Boniecka, J., Murray, J.A.H., Bogre, L., et al. (2010). MAPK Phosphatase AP2C3 Induces Ectopic Proliferation of Epidermal Cells Leading to Stomata Development in Arabidopsis. PLoS One *5*, e15357.
- UN (2000). We the peoples. The role of the UN in the 21st century. United Nations: New York, NY, USA
- UNEP (2008). Vital Water Graphics: An Overview of the State of the World's Fresh and Marine Waters
- UNPD (United Nations, Department of Economic and Social Affairs, P.D. (2007). World Population Prospects: The 2006 Revision Highlights.
- UNPD (United Nations, Department of Economic and Social Affairs, P.D. (2015). World Population Prospects: The 2015 Revision, Key Findings and Advance Tables. Working Paper No. ESA/P/WP.241.
- Vatén, A., and Bergmann, D.C. (2012). Mechanisms of stomatal development: an evolutionary view. Evodevo *3*, 11.
- van Vuuren, D.P., Edmonds, J., Kainuma, M., Riahi, K., Thomson, A., Hibbard, K., Hurtt, G.C., Kram, T., Krey, V., Lamarque, J.-F., et al. (2011). The representative concentration pathways: an overview. Clim. Change *109*, 5–31.
- Wallace, J.S., and Gregory, P.J. (2002). Water resources and their use in food production systems. Aquat. Sci. *64*, 363–375.
- Wang, H., Ngwenyama, N., Liu, Y., Walker, J.C., and Zhang, S. (2007). Stomatal Development and Patterning Are Regulated by Environmentally Responsive Mitogen-Activated Protein Kinases in Arabidopsis. PLANT CELL ONLINE *19*, 63–73.
- Wong, S.C., Cowan, I.R., and Farquhar, G.D. (1979). Stomatal conductance correlates with photosynthetic capacity. Nature *282*, 424–426.
- Woodward, F.I. (1987). Stomatal numbers are sensitive to increases in CO2 from pre-industrial levels. Nature *327*, 617–618.

- WOODWARD, F.I., and KELLY, C.K. (1995). The influence of CO2 concentration on stomatal density. New Phytol. *131*, 311–327.
- World Bank (2008). Agriculture for development.
- Wuyts, N., Palauqui, J.-C., Conejero, G., Verdeil, J.-L., Granier, C., and Massonnet, C. (2010). High-contrast three-dimensional imaging of the Arabidopsis leaf enables the analysis of cell dimensions in the epidermis and mesophyll. Plant Methods *6*, 17.
- Xu, Z., and Zhou, G. (2008). Responses of leaf stomatal density to water status and its relationship with photosynthesis in a grass. J. Exp. Bot. *59*, 3317–3325.
- Yamamuro, C., Miki, D., Zheng, Z., Ma, J., Wang, J., Yang, Z., Dong, J., Zhu, J.-K., Pillitteri, L.J., Torii, K.U., et al. (2014). Overproduction of stomatal lineage cells in Arabidopsis mutants defective in active DNA demethylation. Nat. Commun. *5*, 591–614.
- Yang, M., and Sack, F.D. (1995). The too many mouths and four lips Mutations Affect Stomatal Production in Arabidopsis. PLANT CELL ONLINE *7*, 2227–2239.
- Ye, Z.-P. (2007). A new model for relationship between irradiance and the rate of photosynthesis in Oryza sativa. Photosynthetica *45*, 637–640.
- Yoo, C.Y., Pence, H.E., Hasegawa, P.M., and Mickelbart, M. V. (2009). Regulation of Transpiration to Improve Crop Water Use. CRC. Crit. Rev. Plant Sci. *28*, 410–431.
- Yoo, C.Y., Pence, H.E., Jin, J.B., Miura, K., Gosney, M.J., Hasegawa, P.M., and Mickelbart, M. V. (2010). The *Arabidopsis* GTL1 Transcription Factor Regulates Water Use Efficiency and Drought Tolerance by Modulating Stomatal Density via Transrepression of *SDD1*. Plant Cell *22*, 4128–4141.
- Yoo, C.Y., Hasegawa, P.M., and Mickelbart, M. V. (2011). Regulation of stomatal density by the GTL1 transcription factor for improving water use efficiency. Plant Signal. Behav. *6*, 1069–1071.
- van Zanten, M., Snoek, L.B., Proveniers, M.C.G., and Peeters, A.J.M. (2009). The many functions of ERECTA. Trends Plant Sci. *14*, 214–218.
- Zhang, X., Facette, M., Humphries, J.A., Shen, Z., Park, Y., Sutimantanapi, D., Sylvester, A.W., Briggs, S.P., and Smith, L.G. (2012). Identification of PAN2 by Quantitative Proteomics as a Leucine-Rich Repeat-Receptor-Like Kinase Acting Upstream of PAN1 to Polarize Cell Division in Maize. Plant Cell *24*, 4577–4589.
- Zhang, Y., Wang, P., Shao, W., Zhu, J.-K., and Dong, J. (2015). The BASL polarity protein controls a MAPK signaling feedback loop in asymmetric cell division. Dev. Cell *33*, 136–149.
- Zhang, Y., Guo, X., Dong, J., Miwa, K., Kasai, K., Fuji, K., Onouchi, H., Naito, S., Fujiwara, T., Jürgens, G., et al. (2016). Phosphorylation of the Polarity Protein BASL Differentiates Asymmetric Cell Fate through MAPKs and SPCH. Curr. Biol. *26*, 2957–2965.